One-loop phenomenology in brane models

Ben Schofield

One-loop phenomenology in brane models

A thesis presented for the degree of
Doctor of Philosophy

by

Ben Schofield

Department of Mathematical Sciences
University of Durham
England

May 2005

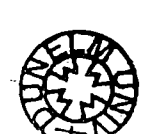

One-loop phenomenology in brane models

by

Ben Schofield

Abstract

Particular examples of one-loop string effects are explored in the context of brane-based realizations of the Standard Model. We firstly examine the consequences of a phenomenon known as Kinetic Mixing, which couples hidden $U(1)$ gauge factors to visible $U(1)$'s. The effect is shown to occur in nonsupersymmetric string set-ups between D-branes and $\overline{\mathrm{D}}$-branes, where it acts either to give millicharges (of *e.g.* hypercharge) to would-be hidden sector fermions, or to generate an enhanced communication of supersymmetry breaking that dominates over the usual gravitational suppression. In either case, the conclusion is that the string scale in these nonsupersymmetric brane configurations has a generic *upper* bound of $M_s \lesssim 10^8\,\mathrm{GeV}$.

Turning to models based on intersecting branes, Yukawa interactions at one-loop on intersecting D6 branes are calculated. The non-renormalization theorem is demonstrated in supersymmetric configurations, and it is shown how Yukawa β-functions may be extracted. In addition to the usual logarithmic running, power-law dependence on the infra-red cut-off (associated with Kaluza-Klein modes) is found. The results presented may be used to evaluate coupling renormalization in non-supersymmetric cases. Much of the discussion is applicable to one-loop calculations on intersecting branes in general.

Acknowledgements

Thanks are first and foremost due to Dr. Steven Abel for agreeing to oversee my work, suggesting interesting topics to work on and for constant support and encouragement throughout my PhD. Very few supervisors are quite so generous with their time, energy, enthusiasm and ideas.

Thanks also to all my office-mates (especially to those who also acted as drinking partners) for making the last $3 + \epsilon$ years so pleasant, to PPARC for a PhD studentship, to the Department of Mathematical Sciences for teaching opportunities, and to the IPPP for a nice office.

This thesis is dedicated to to my parents for a lifetime of support, and to Clare for putting up with me.

Declaration

The work in this thesis is based on research carried out in the Department of Mathematical Sciences and Institute for Particle Physics Phenomenology at the University of Durham, England. No part of this thesis has been previously submitted for any other degree or qualification, at this or any other university.

Chapters 1 and 2 of this thesis present a review of background material for which no claim of originality is made. Chapters 3 and 4 are original work, being the results of collaborations between Dr. Steven Abel and the author. Their content has appeared elsewhere:

- S. A. Abel and B. W. Schofield,
  Brane-Antibrane Kinetic Mixing, Millicharged Particles and SUSY Breaking,
  Nuc. Phys. **B685** (2004) 150-170, http://arXiv.org/hep-th/0311051,

- S. A. Abel and B. W. Schofield,
  One-loop Yukawas on Intersecting Branes,
  JHEP (to appear), http://arXiv.org/hep-th/0412206.

"The great book, always open and which we should make an effort to read, is that of Nature; the other books are taken from it, and in them there are the mistakes and interpretations of men."

— Antoni Gaudí

Contents

List of Figures

List of Tables

Chapter 1

Background

1.1 The Standard Model

This thesis is concerned with string phenomenology, an intermediate discipline lying somewhere between the more formal field of string theory and the more applied field of particle physics phenomenology. To understand in any detail what string phenomenology is, and why it is important, it will be useful to give a very brief survey of both areas. As particle physics is by its nature a rather speculative subject (and string theory doubly so) this could be a difficult task. Fortunately, a strong foundation exists from which to begin: the Standard Model of particle physics.

In the Standard Model (SM), one begins with a quantum field theory in which the fields transform according to an internal symmetry which depends on their position in spacetime, yet does not affect the observable physics: this is known as local gauge invariance. The gauge group is taken to be $SU(3)_C \times SU(2)_L \times U(1)_Y$, and the fields transforms in representations of this group. Table 1.1 summarizes the fields contained in the model, together with their transformation properties under the SM gauge group: gauge bosons to mediate the strong and electroweak interactions, chiral matter fields and a doublet of Higgs scalars. These latter particles give mass to the fermions by a spontaneous breaking of electroweak symmetry, $SU(2)_L \times U(1)_Y \to U(1)_Q$.

To date, experiment has found the SM lacking in only one respect; its presumption that only left-handed neutrinos exist in nature (meaning neutrinos must be massless) has been shown to be in error. However, it is possible to rectify this deficiency in a manner which leaves the rest of the model unaffected. Therefore, are there good scientific reasons to persist in constructing theories beyond the SM? In fact, there are several:

Type of particle	*spin*-0	*spin*-$\frac{1}{2}$	*spin*-1	$(SU(3)_C, SU(2)_L, U(1)_Y)$
Gluons			g	$(\mathbf{8}, \mathbf{1}, 0)$
W bosons			$W^{\pm}$, W^0	$(\mathbf{1}, \mathbf{3}, 0)$
B boson			B^0	$(\mathbf{1}, \mathbf{1}, 0)$
Quarks		(u_L, d_L)		$(\mathbf{3}, \mathbf{2}, \frac{1}{6})$
		$u_R^\dagger$		$(\bar{\mathbf{3}}, \mathbf{1}, -\frac{2}{3})$
		$d_R^\dagger$		$(\bar{\mathbf{3}}, \mathbf{1}, \frac{1}{3})$
Leptons		(ν_L, e_L)		$(\mathbf{1}, \mathbf{2}, -\frac{1}{2})$
		$e_R^\dagger$		$(\mathbf{1}, \mathbf{1}, 1)$
Higgs	(ϕ^+, ϕ^0)			$(\mathbf{1}, \mathbf{2}, \frac{1}{2})$

Table 1.1: Particle content of the Standard Model: gauge bosons, matter fermions and the Higgs (after ref. [1]).

- *Lack of gravity.* On large scales, gravitational effects are well-described by Einstein's theory of general relativity. For experimental particle physics gravity is irrelevant, as the gravitational coupling is tens of orders of magnitude smaller than the electromagnetic, weak and strong couplings: here, the Standard Model rules. Yet, it is intellectually unsatisfying for two 'correct' frameworks to exist independently. One may try to include the effects of gravity in quantum field theory by promoting the global Poincaré symmetry of Minkowski spacetime, $x^\mu \to \Lambda^\mu_{\ \nu} x^\nu + a^\mu$, to a local symmetry, $x^\mu \to x'^\mu(x)$. This step leads to theories containing a spin-2 particle known as the graviton. However, such theories are non-renormalizable, and therefore of limited use. A new approach is needed.

- *Gauge hierarchy problem.* Dimensional analysis suggests that quantum gravitational effects ought to become important at the Planck scale, $M_P = (\hbar c/G)^{\frac{1}{2}} \sim 10^{19}$ GeV, whilst the SM deals with physics at the weak scale $M_W \sim 10^2$ GeV. As we know that the SM cannot be the full story, we may treat it as an effective theory which is valid below some large cut-off Λ. Unfortunately, it may be shown that the one-loop effects shown in figure 1.1 generate corrections to the Higgs mass m_H which are sensitive to Λ; and, making the

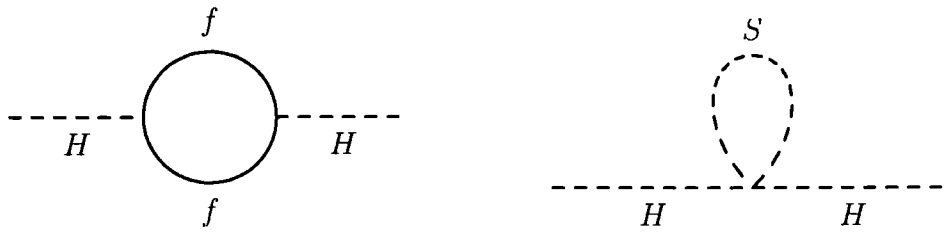

Figure 1.1: One-loop effects generating a correction Δm_H^2.

reasonable assumption that Λ is closer to the Planck scale than the weak scale, we then have a problematic hierarchy between a value of m_H of order 100 GeV and corrections to it which are potentially several orders of magnitude larger. Similar effects are caused by higher-order diagrams containing heavy fermions, and so a direct resolution to this problem – apart from engineering the mutual cancellation of all contributing diagrams by unnatural fine-tunings – appears lacking.

- *Proliferation of free parameters.* The SM contains 19 dimensionless parameters which must be inserted into the theory from experimental measurements (more if we include massive neutrinos in the theory). As reductionists, we should strive to lower this number, and as physicists to understand better the origins of any free parameters with which we are left.

- *Choice of gauge group, of three families and of four dimensions.* Along the same lines, one may equally well ask what is special about these choices.

- *Cosmological issues.* In addition, the SM fails to explain several cosmological observations, including the matter-antimatter asymmetry of the universe, the value of the cosmological constant and the origin of inflation.

This list is not exhaustive (and we will certainly not attempt to indicate solutions to all of the problems given), but should be taken as an indication that there are compelling reasons to study physics beyond the SM, even though all 'traditional' experimental data supports it.

Type of particle	*spin*-0	*spin*-$\frac{1}{2}$	*spin*-1	$(SU(3)_C, SU(2)_L, U(1)_Y)$
Gluinos, Gluons		$\tilde{g}$	g	$(\mathbf{8}, \mathbf{1}, 0)$
Winos, W bosons		$\tilde{W}^{\pm}$, $\tilde{W}^0$	$W^{\pm}$, W^0	$(\mathbf{1}, \mathbf{3}, 0)$
Bino, B boson		$\tilde{B}^0$	B^0	$(\mathbf{1}, \mathbf{1}, 0)$
Squarks, Quarks	$(\tilde{u}_L, \tilde{d}_L)$	(u_L, d_L)		$(\mathbf{3}, \mathbf{2}, \frac{1}{6})$
	$\tilde{u}_R^*$	$u_R^\dagger$		$(\bar{\mathbf{3}}, \mathbf{1}, -\frac{2}{3})$
	$\tilde{d}_R^*$	$d_R^\dagger$		$(\bar{\mathbf{3}}, \mathbf{1}, \frac{1}{3})$
Sleptons, Leptons	$(\tilde{\nu}_L, \tilde{e}_L)$	(ν_L, e_L)		$(\mathbf{1}, \mathbf{2}, -\frac{1}{2})$
	$\tilde{e}_R^*$	$e_R^\dagger$		$(\mathbf{1}, \mathbf{1}, 1)$
Higgs, Higgsinos	(H_u^+, H_u^0)	$(\tilde{H}_u^+, \tilde{H}_u^0)$		$(\mathbf{1}, \mathbf{2}, \frac{1}{2})$
	(H_u^+, H_u^0)	$(\tilde{H}_u^+, \tilde{H}_u^0)$		$(\mathbf{1}, \mathbf{2}, -\frac{1}{2})$

Table 1.2: Particle content of the Minimally Supersymmetric Standard Model: vector and chiral supermultiplets (after ref. [1]).

1.2 Beyond the Standard Model

Supersymmetry

We may repair at least one of these problems, that of gauge hierarchy destabilization, by introducing a symmetry that relates fermions and bosons: *supersymmetry*. Schematically,

$$Q\,|\text{fermion}\rangle = |\text{boson}\rangle \qquad Q\,|\text{boson}\rangle = |\text{fermion}\rangle\,.$$

Particles related in this manner are said to be in the same supermultiplet. The supersymmetry algebra is special because it mixes the internal gauge symmetry of the standard model with the Poincaré symmetry of spacetime: in fact, it is the only possible extension of the Poincaré group compatible with the symmetries of four-dimensional quantum field theory.

In principle, we may have as many supersymmetry generators Q as we wish. However, although supermultiplets of vector particles can be found for any number of generators, supermultiplets containing chiral particles only exist with one generator – $\mathcal{N} = 1$ supersymmetry. The most popular $\mathcal{N} = 1$ supersymmetric extension of

the Standard Model is the *Minimally Supersymmetric Standard Model* (MSSM). The field content of this model is shown in table 1.2, a simple extension of table 1.1 in all respects save for the enlarged Higgs sector. The gauge bosons and their gaugino superpartners are in a *vector* supermultiplet, whilst matter fields are placed in a *chiral* supermultiplet. With these additions, all of the diagrams which were previously problematic are automatically cancelled by diagrams with superpartners in the loop, avoiding the hierarchy problem without any need for fine-tuning.

In actual fact, things are not quite this simple. Since particles in a supermultiplet have identical masses, and no selectron has been discovered, supersymmetry cannot be an exact symmetry. Instead, it is assumed to be spontaneously broken at low energies to give the spectrum we observe. Fortunately, it is possible to break supersymmetry in such a way that the corrections to the Higgs mass are only of the order of the supersymmetry breaking scale; this is so-called *soft* supersymmetry breaking.

The MSSM has another attractive property, namely the unification of gauge couplings. In both the SM and MSSM, the electromagnetic, weak and strong couplings 'run' (vary) with the energy scale involved. Only in the MSSM, however, do they appear to *unify* at the same point (at an energy of around 10^{16} GeV). This theoretical observation looks like a strong hint in favour of supersymmetry. In one important area, however, the MSSM seems like something of a step backwards – without assuming any specific mechanism for supersymmetry breaking, the model contains over 100 free parameters!

Supergravity

As mentioned above, supersymmetry is the unique symmetry able to mix internal and spacetime symmetries. Therefore, we might hope to use it to tackle also the first item on our wish list for the Standard Model; the inclusion of gravity. As formulated, supersymmetry is a global symmetry. The success of local gauge theories, combined with the observation that making spacetime symmetries local leads to theories with a graviton, suggests that we should investigate the consequences of a local supersymmetry algebra.

The consequences are promising; in addition to the chiral and vector supermultiplets of global supersymmetry, gravity multiplets appear containing spin-2 gravitons $g_{\mu\nu}$ and their spin-$\frac{3}{2}$ superpartners the gravitinos Ψ^{μ}_{α}. In general, it may be shown that the four-dimensional supergravity Lagrangian depends only upon three functions of the chiral superfields: the Kähler potential, superpotential and a gauge

kinetic function. Spontaneous supersymmetry breaking in supergravity is assumed to be caused by scalars located in a 'hidden sector' which communicates with the usual visible sector only through gravitational interactions.

Unfortunately, supergravity is non-renormalizable and must therefore be viewed as an effective theory. The question remains, then, of finding the correct ultraviolet completion.

Extra dimensions

An alternative way to extend the Standard Model – often used in conjunction with the ideas above – is to increase the number of dimensions which spacetime has. There are two approaches to this; *compactification* and *brane-worlds*. In the compactification scenario the extra dimensions are 'rolled up' into a small compact space of radius R. At scales much less than the compactification scale $1/R$, spacetime appears four-dimensional, and the higher-dimensional metric decomposes. For instance, if we take spacetime to be $\mathcal{M}_4 \times S^1$, the five-dimensional metric G_{MN} decomposes as into a four-dimensional metric, a vector particle and a scalar: $G_{MN} \rightarrow \{G_{\mu\nu}, A^\mu, \phi\}$. As we increase the energy scale, extra *Kaluza-Klein modes* appear as a discrete tower of excitations in the compact space.

In the brane-world approach, the Standard Model is confined to a four-dimensional membrane embedded in some higher-dimensional 'bulk' space, and gravity allowed to propagate in the bulk. This neatly allows one to account for the relative weakness of the gravitational interaction by diluting it out into the bulk space. Furthermore, it allows one to claim that the fundamental D-dimensional Planck scale is not as large as M_P, but instead is a result of the large relative size of the bulk space – thereby deleting the hierarchy problem.

It is possible to combine both approaches; five-dimensional branes which are partially compactified, for instance. All of these extra-dimensional approaches fit in very naturally with a string scenario (indeed, the brane-world concept was inspired by string theory), and are essential ingredients for string phenomenology.

String theory

It seems very likely that one or more of the above ideas is responsible for whatever lies beyond the Standard Model. All of the above elements can be incorporated in what has come to be known as *string theory*, and moreover incorporated in a very natural way. The basic idea is simple: replace point particles with one-dimensional

Type	Open/closed in bulk?	Dp-Branes?
IIA	Closed	$p = 0, 2, 4, 6, 8$ allowed
IIB	Closed	$p = 1, 3, 5, 7, 9$ allowed
I	Open and closed	$p = 1, 5$ allowed
Heterotic $SO(32)$	Closed	No
Heterotic $E_8 \times E_8$	Closed	No

Table 1.3: The five consistent superstring theories.

strings, and claim that the various excitations of open and closed strings correspond to various particles in nature. These strings may be taken to have a characteristic length scale of $1/M_P$ (or at least, some length which is short enough to be inaccessible to current experiment), which explains why they appear one-dimensional at the weak scale.

Whilst the spectrum found in this way does not automatically and simply include the Standard Model particles, it does include a massless spin-2 particle: the graviton – string theory does not just allow gravity to be included, then, but actually *requires* it. Furthermore, the mathematical consistency of the theory requires that it exist in either twenty-six dimensions (for the bosonic string, which contains only scalars on the string worldsheet) or ten spacetime dimensions (for the superstring, which contains both fermions and bosons). It is the latter option which is most phenomenology interesting.

From anomaly cancellation, it may be shown that there are five consistent superstring theories, summarized in table 1.3. Three of these, types I, IIA and IIB, are based solely on the ten-dimensional superstring and also include objects knows as Dp-*branes*. These are $(p+1)$-dimensional membranes upon which open strings may end. Heterotic theories are a heterosis of the superstring and bosonic string in which the extra sixteen dimensions of the bosonic string are compactified on a lattice. They do not include branes. All of these theories are related by so-called duality symmetries which connect one string theory to another, leading to the conjecture that all the theories ought to come from some underlying 11-dimensional construction known as M-theory. A concrete realization of this theory is lacking, and at the time of writing it looks like this may be the situation for some time.

Even so, the string theories that we do understand make strong connections with the ideas discussed in the previous section. Firstly, as the name hints, superstring theories require supersymmetry as an essential part of their construction. Secondly, a quite remarkable discovery is that string theories have supergravity as their low-energy limit. Thirdly, the requirement of extra dimensions (which originally appeared to be a huge black mark against string theory's name) may actually turn out to provide solutions for some of the conceptual problems with the SM.

So, string theory contains lots of interesting jigsaw pieces – but how does it all fit? Often, the best thing to do with a jigsaw puzzle is to take a bottom-up approach, and build upwards from the pieces already in place. With this in mind, one may wish to explore the embedding of lower-energy physics into string theory. This endeavour is known as string phenomenology.

1.3 String phenomenology

Heterotic models

The first attempts at such an embedding came from the $E_8 \times E_8$ heterotic string. These were motivated firstly by the fact that the E_8 gauge group has rank 8 and so the $E_8 \times E_8$ heterotic string can easily incorporate a rank-four group such as $SU(3) \times SU(2) \times U(1)$ (through the embedding $SU(3) \times SU(2) \times U(1) \subset SU(5) \subset SO(10) \subset E_6 \subset E_8$, for example), whilst the other E_8 is treated as a hidden sector group.

One approach to heterotic models is to take the ten-dimensional heterotic string and compactify six of the dimensions on some manifold X. There is a problem in that in $D = 10$, the heterotic string has $\mathcal{N} = 1$ supersymmetry, but spinors are 16-dimensional. If we make the naïve choice $X = T^6$, then in $D = 4$ the four-dimensional nature of spinors leads us to $\mathcal{N} = 4$ supersymmetry. To get the phenomenologically useful $\mathcal{N} = 1$ supersymmetry, it turns out that we need to choose X to be a Ricci-flat manifold with a particular property known as $SU(3)$ holonomy – that is, spinors which are parallel-transported around the manifold transform under the group $SU(3)$. Six-dimensional manifolds with this property are known as Calabi-Yau threefolds, or CY_3 manifolds. However, in practice these manifolds are rather difficult to work with. Instead, we may choose X to be a modified toroidal compactification known as an *orbifold*. In an orbifold, points are identified under some discrete symmetry group; $T^6/\mathbb{Z}_2$ is an orbifold, for instance. The effect of the orbifolding is firstly to 'project out' certain states from the string

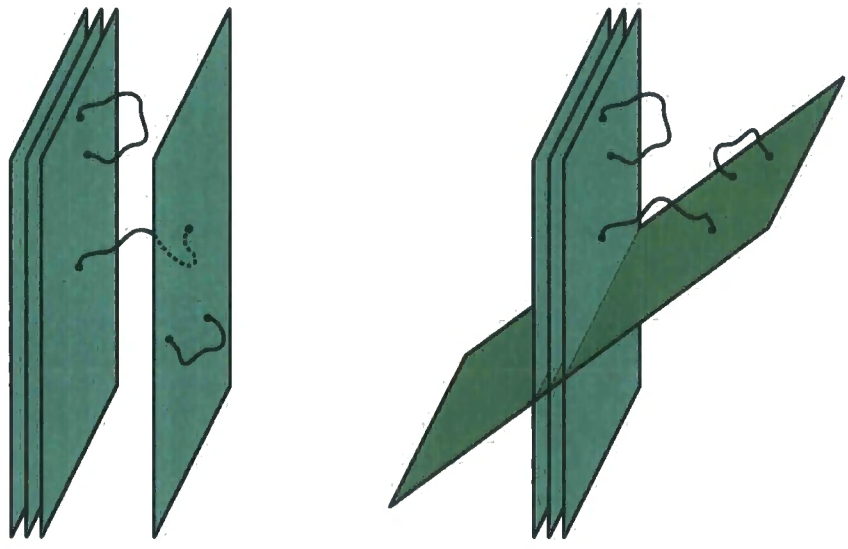

Figure 1.2: Gauge bosons and matter from brane configurations: parallel and intersecting.

spectrum, leaving behind an *untwisted sector*, and secondly to add *twisted sectors* of new states. A suitable choice of orbifold then turns out to allow the creation of models with $\mathcal{N} = 1$ supersymmetry in $D = 4$.

Brane-based models

More recently, the discovery of branes has allowed the construction of Standard-like models in type I and II theories. In brane models, one utilizes the fact that a stack of N branes generates a $U(N)$ gauge group to create the gauge group of the the Standard Model or some extension thereof. The central concept is illustrated in figure 1.2, where we see a stack of three branes and a single brane, in either a parallel or intersecting configuration. Strings with both ends on the stack of three are gauge bosons in the $\mathbf{3} \otimes \overline{\mathbf{3}}$ adjoint representation of $U(3)$, strings with both ends on the single brane are gauge bosons of $U(1)$, and strings stretching between both are matter fields in the $\mathbf{3} \otimes \overline{\mathbf{1}}$ (or $\mathbf{1} \otimes \overline{\mathbf{3}}$, depending on the orientation of the string) bifundamental of $U(3) \times U(1)$. Supplementing the configuration with a stack of two branes provides us with a $U(3) \times U(2) \times U(1)$; then, since $U(N) = SU(N) \times U(1)$, we can obtain the gauge group of the SM/MSSM.

Gravitational modes correspond to closed strings propagating in the bulk space in which the branes are embedded. If the correct four-dimensional gravity is to

be observed, it is still necessary to compactify the six extra dimensions on some manifold X.

A principal difference between the two configurations in figure 1.2 is that in the second picture, matter fields are localized at the intersection of branes and gauge states are free to move around the branes, whereas in the first both matter and gauge states are free to move around. Furthermore, in the first configuration it is necessary that the brane stacks are localized on orbifold singularities in order to obtain an $\mathcal{N} = 1$ spectrum. In the second, $\mathcal{N} = 1$ supersymmetry can be obtained by an appropriate selection of the intersection angles; the requirement that some of the branes lie on orbifold singularities is then an optional one. The first type of configuration corresponds more closely to 'bottom-up' constructions as typified by ref. [2], whereas the second corresponds to an 'intersecting brane-world' configuration – see [3–6] for recent reviews.

Configurations of branes in a compact space must obey a consistency condition known as *tadpole cancellation*, which requires that the branes' associated Ramond-Ramond charges must cancel in the compact dimensions (this is just Gauss' law). Tadpole cancellation provides a strong constraint on brane-based models. In particular, it may require that we include other branes which communicate with the SM branes only through closed-string modes: these provide a natural realization of the hidden sector discussed above.

1.4 Layout of this thesis

We will now cease to sketch outlines, and begin to fill in details. In the next chapter, we will give an introduction to string theory. We then move on to describe a particular one-loop effect known as Kinetic Mixing, which may be present in brane models containing parallel brane-antibrane pairs. This phenomenon may act either to generate particles with fractional charges or as a source of supersymmetry breaking; both effects may be used to bound the string scale. In the final chapter we move on to intersecting brane worlds, where we show how to calculate Yukawa couplings at one loop in a set-up consisting of D6-branes. We will find that the gauge coupling constants run logarithmically at low energies but switch to a power-law behaviour as Kaluza-Klein modes open up, confirming calculations performed in extra-dimensional field theories. Along the way, we will demonstrate the nonrenormalization theorem on intersecting branes.

Chapter 2

Introduction

In this chapter, we introduce the central concepts of string theory: namely, the classical theory, the quantization thereof, the perturbation theory expansion and the presence of branes. We also introduce the one-loop partition function and comment on branes at a relative angle. The main sources for this section are refs. [7–12].

2.1 Classical string theory

2.1.1 The bosonic string

A classical string may be described as a two-dimensional *worldsheet* embedded in a D-dimensional spacetime. From the worldsheet point of view, spacetime is then a set of D fields $X^\mu(\tau, \sigma)$, where τ and $\sigma \in [0, \pi]$ are worldsheet time and space respectively. The string seeks to minimize the area of its worldsheet in spacetime, leading to the Nambu-Goto action

$$S_{NG}[X] = -T \int \mathrm{d}\tau \mathrm{d}\sigma \, \sqrt{-h}\,, \tag{2.1}$$

with $h = \det h_{ab}$, where $h_{ab} = \eta_{\mu\nu} \partial_a X^\mu \partial_b X^\nu$ is the pullback of the spacetime metric $\eta_{\mu\nu} = \mathrm{diag}\,(-1, +1, \ldots, +1)$ onto the worldsheet. The constant $T = (2\pi\alpha')^{-1} = (\pi l_s^2)^{-1}$ keeps the action dimensionless. This action has two symmetries associated with it; Poincaré invariance,

$$X^\mu \longrightarrow \Lambda^\mu_{\ \nu} X^\nu + a^\mu\,, \tag{2.2}$$

and reparamaterization (diffeomorphism, or diff) invariance:

$$X^{\mu}(\tau,\sigma) \longrightarrow X'^{\mu}(\tau',\sigma') \tag{2.3}$$

for new coordinates $\tau'(\tau,\sigma)$, $\sigma'(\tau,\sigma)$.

The square root in the Nambu-Goto action makes it difficult to work with. An action which does not contain the square root may be obtained by introducing an independent world-sheet metric $\gamma_{ab}(\tau,\sigma)$ and writing

$$S_P[X,\gamma] = -\frac{T}{2}\int \mathrm{d}\tau\mathrm{d}\sigma\ \sqrt{-\gamma}\gamma^{ab}h_{ab}\,, \tag{2.4}$$

where $\gamma = \det\gamma_{ab}$. This is known as the Polyakov action. Using $\delta\gamma = -\gamma\gamma_{ab}\delta\gamma^{ab}$, the Euler-Lagrange equation for γ^{ab} reads

$$T_{ab} \equiv h_{ab} - \frac{1}{2}\gamma_{ab}\gamma^{cd}h_{cd} = 0 \tag{2.5}$$

which may be recast as

$$\frac{h_{ab}}{\sqrt{-h}} = \frac{\gamma_{ab}}{\sqrt{-\gamma}}\,, \tag{2.6}$$

allowing the Nambu-Goto action to be recovered from the Polyakov. Note that (2.6) is unchanged by a Weyl transformation,

$$\gamma_{ab}(\tau,\sigma) \to \mathrm{e}^{2\omega(\tau,\sigma)}\gamma_{ab}(\tau,\sigma)\ , \tag{2.7}$$

and so Weyl-equivalent metrics correspond to the same embedding in spacetime.

Now, the diff invariance (2.3) allows the three degrees of freedom in γ_{ab} to be replaced with with one;

$$\gamma_{ab} = \mathrm{e}^{\phi(\tau,\sigma)}\eta_{ab}\,, \tag{2.8}$$

where $\eta_{ab} = \mathrm{diag}(-1,+1)$. The Weyl invariance allows this to be further reduced to

$$\gamma_{ab} = \eta_{ab}\,.$$

In this gauge, the action reads

$$S_{PC}[X] = -\frac{T}{2}\int \mathrm{d}\sigma\mathrm{d}\tau\ \eta^{ab}\partial_a X^{\mu}\partial_b X_{\mu}\,. \tag{2.9}$$

Varying the X^μ yields

$$\delta S_{PC}[X] = T\int \mathrm{d}\sigma\mathrm{d}\tau\ (\partial^a\partial_a X_\mu)\,\delta X^\mu - T\int \mathrm{d}\tau\ (\partial_\sigma X_\mu)\,\delta X^\mu|_{\sigma=0}^{\sigma=\pi} = 0\,. \tag{2.10}$$

The first term constrains the X fields to obey the one-dimensional wave equation,

$$\partial^a\partial_a X^\mu = 0\,, \tag{2.11}$$

whereas vanishing of the second term determines the boundary conditions on the string. We may choose

- *Periodic boundary conditions*, $X^\mu(\tau,0) = X^\mu(\tau,\pi)$.

  This choice leads to closed strings. Defining $\sigma^\pm = \tau \pm \sigma$, a solution to the wave equation may be written as a superposition of right- and left-moving fields,

  $$X^\mu(\tau,\sigma) = X_-^\mu(\sigma^-) + X_+^\mu(\sigma^+)\ , \tag{2.12}$$

  where in terms of a Fourier series,

  $$\begin{aligned} X_-^\mu(\sigma^-) &= \frac{1}{2}x^\mu + \alpha' p^\mu\sigma^- + \mathrm{i}\sqrt{\frac{\alpha'}{2}}\sum_{n\neq 0}\frac{1}{n}\alpha_n^\mu \mathrm{e}^{-2\mathrm{i}n\sigma^-} \\ X_+^\mu(\sigma^+) &= \frac{1}{2}x^\mu + \alpha' p^\mu\sigma^+ + \mathrm{i}\sqrt{\frac{\alpha'}{2}}\sum_{n\neq 0}\frac{1}{n}\tilde{\alpha}_n^\mu \mathrm{e}^{-2\mathrm{i}n\sigma^+}\,. \end{aligned} \tag{2.13}$$

  Here, x^μ and p^μ are the centre of mass and momentum of the string and α_n^μ, $\tilde{\alpha}_n^\mu$ are right- and left-moving Fourier coefficients. We have defined

  $$\alpha_0^\mu = \tilde{\alpha}_0^\mu = \sqrt{\frac{\alpha'}{2}}p^\mu\,. \tag{2.14}$$

  The reality condition $X^\mu = (X^\mu)^*$ implies

  $$(\alpha_n^\mu)^* = \alpha_{-n}^\mu \qquad \text{and} \qquad (\tilde{\alpha}_n^\mu)^* = \tilde{\alpha}_{-n}^\mu\,. \tag{2.15}$$

- *Neumann boundary conditions*, $\partial_\sigma X|_{\sigma=0} = \partial_\sigma X|_{\sigma=\pi} = 0$.

  This choice of boundary conditions describes open strings, where the

left- and right-movers combine to give a standing wave:

$$X^\mu(\tau,\sigma) = x^\mu + 2\alpha' p^\mu \tau + \mathrm{i}\sqrt{2\alpha'}\sum_{n\neq 0}\frac{1}{n}\alpha_n^\mu \mathrm{e}^{-\mathrm{i}n\tau}\cos(n\sigma)\ . \tag{2.16}$$

This time,

$$\alpha_0^\mu = \sqrt{2\alpha'}p^\mu\ . \tag{2.17}$$

Again, $X^\mu = (X^\mu)^*$ implies $(\alpha_n^\mu)^* = \alpha_{-n}^\mu$.

We defer discussion of a third option, that of Dirichlet boundary conditions, until section 2.4.

2.1.2 The RNS superstring

We now proceed on to classical supersymmetric string theory. There are two approaches available; the Ramond-Neveu-Schwarz formalism, which introduces supersymmetry on the worldsheet directly and then extends it to spacetime, and the Green-Schwarz formalism which introduces spacetime supersymmetry explicitly. We work in the RNS formalism throughout this thesis. Our starting point is the ungauged Polyakov action, which we supplement with D massless Majorana spinors on the worldsheet:

$$S = -\frac{T}{2}\int \mathrm{d}\tau\mathrm{d}\sigma\ \sqrt{-\gamma}\left(\gamma^{ab}\partial_a X^\mu \partial_b X_\mu - \mathrm{i}\overline{\Psi}^\mu \rho^a \partial_a \Psi_\mu\right)\ . \tag{2.18}$$

The ρ^a are two-dimensional gamma-matrices satisfying the usual Clifford algebra $\{\rho^a,\rho^b\} = 2\eta^{ab}$,

$$\rho^0 = \begin{pmatrix} 0 & -\mathrm{i} \\ \mathrm{i} & 0 \end{pmatrix}\ , \qquad \rho^1 = \begin{pmatrix} 0 & \mathrm{i} \\ \mathrm{i} & 0 \end{pmatrix}\ , \tag{2.19}$$

and we have defined $\overline{\Psi} \equiv \Psi^T\rho^0$. This action is invariant under the global supersymmetry transformation

$$\begin{aligned} \delta X^\mu &= \bar{\xi}\Psi^\mu \\ \delta\Psi^\mu &= -\mathrm{i}\rho^a\partial_a X^\mu \xi \end{aligned} \tag{2.20}$$

for an arbitrary Majorana spinor ξ.

Promoting $\xi \to \xi(\tau, \sigma)$ requires the addition of a gravitino χ_a. Then,

$$S_L = -\frac{T}{2}\int \mathrm{d}\tau \mathrm{d}\sigma \sqrt{-\gamma}\left(\gamma^{ab}\partial_a X^\mu \partial_b X_\mu + \mathrm{i}\overline{\Psi}^\mu \rho^a \partial_a \Psi_\mu \right.$$
$$\left. +2\overline{\chi}_a \rho^b \rho^a \Psi^\mu \partial_b X_\mu + \frac{1}{2}\overline{\Psi}_\mu \psi^\mu \overline{\chi}_a \rho^b \rho^a \chi_b\right), \quad (2.21)$$

which is invariant under the local supersymmetry transformation

$$\begin{aligned}
\delta X^\mu &= \overline{\xi}\Psi^\mu \\
\delta \Psi^\mu &= -\mathrm{i}\rho^a \xi\left(\partial_a X^\mu - \overline{\Psi}^\mu \chi_a\right) \\
\delta \chi_a &= \partial_a \xi \\
\delta e_b^a &= -2\mathrm{i}\overline{\xi}\rho^a \chi_b\,,
\end{aligned} \quad (2.22)$$

where e_b^a satisfies $\gamma_{ab} = e_a^c e_b^d \eta_{cd}$. Also present is a superconformal symmetry,

$$\delta \chi_a = \mathrm{i}\rho_a \epsilon \quad (2.23)$$

for an arbitrary Majorana spinor $\epsilon(\tau, \sigma)$.

Just as for the bosonic string, (2.21) has a *diff* × *Weyl* invariance which may be used to select $\gamma_{ab} = \eta_{ab}$. Furthermore, the local super- and superconformal symmetries are enough to select a gauge with $\chi_a = 0$. Finding Euler-Lagrange equations for X^μ and Ψ^μ before selecting this *covariant gauge* recovers the one-dimensional wave equation (2.11), plus the Dirac equation

$$\mathrm{i}\rho^a \partial_a \Psi^\mu = 0\,. \quad (2.24)$$

The Euler-Lagrange equations for γ^{ab} and χ_a read, in covariant gauge,

$$T_{ab} \equiv \partial_a X^\mu \partial_b X_\mu + \frac{\mathrm{i}}{4}\overline{\Psi}^\mu(\rho_a \partial_b + \rho_b \partial_a)\Psi_\mu - \frac{1}{2}\eta_{ab}\left(\partial^c X^\mu \partial_c X_\mu + \frac{\mathrm{i}}{2}\overline{\Psi}^\mu \rho^c \partial_c \Psi_\mu\right) = 0$$
$$J^a \equiv \frac{1}{2}\rho^b \rho^a \Psi^\mu \partial_b X_\mu = 0\,. \quad (2.25)$$

These are known as super-Virasoro constraints. Note that $\partial_a J^a = 0$; the supercurrent J^a is the conserved quantity associated with the local symmetry (2.22).

As in the previous section, we have the proviso that the surface terms in the variation of S_L must vanish. For the X^μ, the requirements are identical to those of the previous section. To find boundary conditions on the fermionic fields, split Ψ^μ

into right- and left-moving fields,

$$\Psi^\mu = \begin{pmatrix} \Psi^\mu_- \\ \Psi^\mu_+ \end{pmatrix} . \tag{2.26}$$

With $\partial_\pm = \frac{1}{2}(\partial_\tau \pm \partial_\sigma)$, the Dirac equation for Ψ^μ reads

$$\partial_+ \Psi^\mu_- = 0 \qquad \text{and} \qquad \partial_- \Psi^\mu_+ = 0, \tag{2.27}$$

so that Ψ^μ_- and Ψ^μ_+describe right- and left-moving fermionic worldsheet fields respectively. The condition for surface terms to vanish is

$$[\Psi_- \cdot \delta\Psi_- - \Psi_+ \cdot \delta\Psi_+]^{\sigma=\pi}_{\sigma=0} = 0 . \tag{2.28}$$

Then,

- For closed strings, periodic (*Ramond*, or just R) and anti-periodic (*Neveu-Schwarz*, or NS) boundary conditions may be chosen independently for right- and left-movers,

$$\begin{aligned} \Psi^\mu_- (\tau, \pi) &= \pm \Psi^\mu_- (\tau, 0) \\ \Psi^\mu_+ (\tau, \pi) &= \pm \Psi^\mu_+ (\tau, 0) \end{aligned} \tag{2.29}$$

  giving four sectors in total. The mode expansions are

$$\Psi^\mu_- = \sum_r \psi^\mu_r \mathrm{e}^{-2in\sigma^-} \qquad \text{and} \qquad \Psi^\mu_+ = \sum_r \tilde{\psi}^\mu_r \mathrm{e}^{-2in\sigma^+} \tag{2.30}$$

  with r being integer moded in an R sector, and half-integer moded in an NS sector. The Majorana condition $\Psi^\mu_\pm = (\Psi^\mu_\pm)^*$ constrains the Fourier coefficients ψ^μ_r and $\tilde{\psi}^\mu_r$:

$$(\psi^\mu_r)^* = \psi^\mu_{-r} \qquad \text{and} \qquad \left(\tilde{\psi}^\mu_r\right)^* = \tilde{\psi}^\mu_{-r} . \tag{2.31}$$

- For open strings, left- and right-movers are related. Possible boundary conditions are

$$\begin{aligned} \Psi^\mu_-(\tau, \pi) &= \Psi^\mu_+(\tau, 0) \\ \Psi^\mu_-(\tau, \pi) &= \pm \Psi^\mu_+(\tau, \sigma) . \end{aligned} \tag{2.32}$$

  There are now only two sectors; Ramond and Neveu-Schwarz, with mode

expansions

$$\Psi_-^\mu = \frac{1}{\sqrt{2}} \sum_r \psi_r^\mu \mathrm{e}^{-\mathrm{i}n\sigma^-} \qquad \text{and} \qquad \Psi_+^\mu = \frac{1}{\sqrt{2}} \sum_r \psi_r^\mu \mathrm{e}^{-\mathrm{i}n\sigma^+} \tag{2.33}$$

Again, $r \in \mathbb{Z}$ in the R sector, and $r \in (\mathbb{Z} + \frac{1}{2})$ in the NS sector.

2.2 Canonical quantization

In the canonical quantization procedure, one imposes equal-time commutation relations on the X^μ and their canonical momenta $P^\mu = T\dot{X}^\mu$,

$$\left[X^\nu(\tau,\sigma'),\, P^\mu(\tau,\sigma)\right] = \mathrm{i}\pi\delta(\sigma-\sigma')\,\eta^{\mu\nu}, \tag{2.34}$$

with other commutators zero. One also imposes equal-time anticommutation relations on $\Psi_\pm^\mu$ and their canonical momenta $\frac{1}{2}\mathrm{i}T\Psi_\pm^\mu$,

$$\frac{1}{2}\mathrm{i}T\left\{\Psi_\pm^\mu(\tau,\sigma),\, \Psi_\pm^\mu(\tau,\sigma')\right\} = \mathrm{i}\delta(\sigma-\sigma')\,\eta^{\mu\nu} \tag{2.35}$$

with other anticommutators zero.

In all that follows, subscripts $\{n, m\}$ should be implicitly understood to be integer valued, whilst $\{r, s\}$ should be understood to take integer values in the R sector and half-integer values in the NS sector. Inserting the mode expansions (2.16) into (2.34) leads to

$$\begin{aligned} [x^\mu,\, p^\nu] &= \mathrm{i}\eta^{\mu\nu} \\ [\alpha_n^\mu,\, \alpha_m^\nu] = [\tilde{\alpha}_n^\mu,\, \tilde{\alpha}_m^\nu] &= m\delta_{m+n}\eta^{\mu\nu} \end{aligned} \tag{2.36}$$

with other commutators zero. Hence,

$$a_n^{\mu\dagger} = \frac{1}{\sqrt{n}}\alpha_{-n}^\mu, \qquad a_n^\mu = \frac{1}{\sqrt{n}}\alpha_n^\mu \qquad (n>0) \tag{2.37}$$

are a set of D creation/annihilation operators for right-moving modes. Similarly, inserting (2.33) into (2.35) gives

$$\{\psi_r^\mu,\, \psi_s^\nu\} = \left\{\tilde{\psi}_r^\mu,\, \tilde{\psi}_s^\nu\right\} = \delta_{r+s}\eta^{\mu\nu} \tag{2.38}$$

with other anticommutators zero.

2.2.1 The super-Virasoro algebra

Now, let us begin to examine the physical spectrum of the theory. One may write the classical constraint equations (2.25) as

$$T_{++} = T_{--} = J_+ = J_- = 0 \tag{2.39}$$

with

$$\begin{aligned} T_{\pm\pm} &\equiv \frac{1}{2}(T_{00} \pm T_{01}) = \partial_\pm X^\mu \partial_\pm X_\mu + \frac{\mathrm{i}}{2}\psi^\mu_\pm \partial_\pm \psi_{\pm\mu} \\ J_\pm &\equiv \frac{1}{2}(J_0 \pm J_1) = \Psi^\mu_\pm \partial_\pm X_\mu \,. \end{aligned} \tag{2.40}$$

It is useful to define Fourier components of T_{--} and J_-, which are

$$\begin{aligned} L_0 &\equiv \frac{1}{4\pi\alpha'}\int_0^\pi \mathrm{d}\sigma\; T_{--} + a \\ &= \frac{1}{2}\alpha_0^\mu \alpha_{0\mu} + \sum_{n>0} \alpha^\mu_{-n}\alpha_{\mu n} + \sum_{r>0} r\psi^\mu_{-r}\psi_{\mu r} + a \\ L_m &\equiv \frac{1}{4\pi\alpha'}\int_0^\pi \mathrm{d}\sigma\; \mathrm{e}^{2\mathrm{i}m\sigma^-} T_{--} \\ &= \frac{1}{2}\sum_n \alpha^\mu_{m-n}\alpha_{\mu n} + \frac{1}{2}\sum_r \left(\frac{1}{2}m - r\right)\psi^\mu_{m-r}\psi_{\mu r} \qquad (m \neq 0) \end{aligned} \tag{2.41}$$

and

$$\begin{aligned} G_r &\equiv \frac{1}{4\pi\alpha'}\int_0^\pi \mathrm{d}\sigma\; \mathrm{e}^{2\mathrm{i}r\sigma^-} J_- \\ &= \frac{1}{2}\sum_n \psi^\mu_{r-n}\alpha_{\mu n}\,. \end{aligned} \tag{2.42}$$

Notice that we have treated L_0 separately, as we have a problem in this case; the raising and lowering operators do not commute, so in which order should we write them? The convention is that the lowering operators go to the right, and the (infinite) zero-point energy a is left to be dealt with later.

Our operators obey the super-Virasoro algebra,

$$\begin{aligned} [L_m,\, L_n] &= (m-n)\, L_{m+n} + A_m \delta_{m+n} \\ [L_m,\, G_r] &= \left(\frac{1}{2}m - r\right) G_{m+r} \\ \{G_r,\, G_s\} &= 2L_{r+s} + B_r \delta_{r+s} \end{aligned} \tag{2.43}$$

with sector-dependent anomaly terms

$$\begin{aligned} A_m &= \frac{1}{8} D m^3 & B_r &= \frac{1}{8} D r^2 & \text{(R)} \\ A_m &= \frac{1}{8} D m \left(m^2 - 1\right) & B_r &= \frac{1}{8} D \left(r^2 - \frac{1}{4}\right) . & \text{(NS)} \end{aligned} \tag{2.44}$$

In terms of the *super-Virasoro operators* (2.41) and (2.42), the Virasoro constraints (2.25) applied to physical states $|\varphi\rangle$ are

$$\begin{aligned} (L_0 - a)\,|\varphi\rangle &= 0 \\ L_m|\varphi\rangle &= 0 \qquad (m > 0) \\ G_r|\varphi\rangle &= 0 \qquad (r > 0) . \end{aligned} \tag{2.45}$$

Because of the anomaly terms (2.44), it is inconsistent to impose these conditions for both positive and negative m, r. In other words, it is not possible to implement the Virasoro constraints fully at the quantum level.

For open strings, only the above algebra is present. For closed strings, the Fourier components of T_{++} give operators $\tilde{L}_m$, $\tilde{G}_r$. These are exactly similar to equations (2.42), but written in terms of the left-moving operators $\tilde{\alpha}_n$ and $\tilde{\psi}_r$. They obey an exactly similar copy of the algebra (2.43).

2.2.2 The open string spectrum

For open strings, after setting $L_0 = a$ in (2.42) and applying (2.17), the mass-shell condition reads

$$m^2 = -p^\mu p_\mu = \frac{1}{\alpha'} (N + a) , \tag{2.46}$$

where the number operator

$$N = \sum_{n>0} \alpha^\mu_{-n} \alpha_{\mu n} + \sum_{r>0} r \psi^\mu_{-r} \psi_{\mu r} \tag{2.47}$$

counts the number of states present at each level. We still have the issue of infinite zero-point energy a, which we must regularize. A convenient approach is so-called

Riemann zeta regularization, which makes use of the result

$$\begin{aligned}\sum_{n=1}^{\infty}(n-\theta) &= -\lim_{\epsilon\to 0}\frac{\mathrm{d}}{\mathrm{d}\epsilon}\left[\sum_{n}\mathrm{e}^{-\epsilon(n-\theta)}\right] \\ &= \lim_{\epsilon\to 0}\left[\frac{1}{\epsilon^2}-\frac{1}{12}-\frac{1}{2}\theta(\theta-1)+\mathcal{O}(\epsilon)\right] \\ &\equiv -\frac{1}{12}+\frac{1}{2}\theta(1-\theta)\,, \end{aligned} \tag{2.48}$$

where in the intervening steps we have summed the geometric series, expanded the result in ϵ and thrown away the leading infinity. The normal-ordering constants are then found by multiplying the usual contribution of $\frac{1}{2}$ for the harmonic oscillator by the number of states at each level and the number of contributing dimensions,

$$\begin{aligned} a_{\mathrm{X}} &= \frac{D-2}{2}\sum_{n=1}^{\infty} n = -\frac{D-2}{24} \\ a_{\psi} &= \begin{cases} -\frac{D-2}{2}\sum_{r=0}^{\infty} r = -\frac{D-2}{2}\sum_{r=1}^{\infty} r = \frac{D-2}{24} & \text{(R)} \\ -\frac{D-2}{2}\sum_{r=\frac{1}{2}}^{\infty} r = -\frac{D-2}{2}\sum_{r=1}^{\infty}(r-\frac{1}{2}) = -\frac{D-2}{48} & \text{(NS)}\,. \end{cases} \end{aligned} \tag{2.49}$$

Therefore, we have

$$a = a_{\mathrm{X}} + a_{\psi} = \begin{cases} 0 & \text{(R)} \\ -\frac{D-2}{16} & \text{(NS)}\,. \end{cases} \tag{2.50}$$

The factor of $D-2$ (rather than D) comes in because only transverse excitations of the string are possible – this may be seen explicitly by going to a light-cone gauge, in which the diff×Weyl redundancy of the action is eliminated [8]. A suitable value for D may be found by examining the two sectors of the open-string spectrum. Of particular interest to a string phenomenologist are the states which are massless at the string level.

NS sector

Here, the ground state $|0;k\rangle$ has

$$\alpha' m^2 = -\frac{D-2}{16} \tag{2.51}$$

which is tachyonic for all $D > 2$ – we will deal with this problem shortly.

The first excited state $\psi^{\mu}_{-\frac{1}{2}}|0;k\rangle$ transforms as a vector under the Lorentz group, and has $D-2$ transverse degrees of freedom. It is therefore a candidate for a

spacetime boson A^μ, transforming under $SO(D-2)$. If this is so, then it ought to be a massless state. Since

$$\alpha' m^2 = \frac{1}{2} - \frac{D-2}{16}, \tag{2.52}$$

this constrains us to the value $D = 10$, in which $\psi^\mu_{-\frac{1}{2}} |0;k\rangle$ is an $\mathbf{8_v}$ of $SO(8)$. In fact, states in the NS sector are spacetime bosons at each mass level.

R sector

In the R sector, the ground states ψ^μ_0 are massless. Furthermore, they obey a Clifford algebra

$$\left\{\sqrt{2}\psi^\mu_0, \sqrt{2}\psi^\nu_0\right\} = 2\eta^{\mu\nu}, \tag{2.53}$$

implying that $\Gamma^\mu = \sqrt{2}\psi^\mu_0$ are ten-dimensional gamma matrices. Let us define a set of raising and lowering operators by

$$\begin{aligned} d^{0\pm} &= \frac{1}{2}\left(\pm\Gamma^0 + \Gamma^1\right) \\ d^{a\pm} &= \frac{1}{2}\left(\Gamma^{2a} \pm \mathrm{i}\Gamma^{2a+1}\right), \qquad a = 1,\ldots,4 \end{aligned} \tag{2.54}$$

which obey

$$\left\{d^{a+}, d^{b-}\right\} = \delta^{ab} \tag{2.55}$$

with other anticommutators zero. Beginning from a lowest weight state satisfying $d^{a-}|\zeta\rangle = 0$, a representation of dimension $2^5 = 32$ may be created by acting on $|\zeta\rangle$ in all possible ways with the d^{a+}. These 32 states may be denoted as

$$|\mathbf{s}\rangle = \left|\pm\frac{1}{2}, \pm\frac{1}{2}, \pm\frac{1}{2}, \pm\frac{1}{2}, \pm\frac{1}{2}\right\rangle \tag{2.56}$$

where $|\zeta\rangle$ is the state with $-\frac{1}{2}$ in each position.

The utility of this definition may be seen by noting that the generators of the $SO(9,1)$ Lorentz algebra are

$$M^{\mu\nu} = -\frac{\mathrm{i}}{4}\left[\Gamma^\mu, \Gamma^\nu\right] \tag{2.57}$$

which may be written in terms of the raising and lowering operators as

$$S_a \equiv \mathrm{i}^{\delta_a} M^{2a,2a+1} = d^{a+}d^{a-} - \frac{1}{2} \tag{2.58}$$

where $|\mathbf{s}\rangle$ is an eigenvector of S_a with eigenvalues $s_a = \pm\frac{1}{2}$. Therefore, the spinors

$|\mathbf{s}\rangle$ form the so-called Dirac representation of the Lorentz algebra, and the ground states ψ_0^μ are seen to form a ten-dimensional spacetime fermion. Defining a ten-dimensional chirality operator,

$$\Gamma^{11} = \Gamma^0\Gamma^1\cdots\Gamma^9\,, \tag{2.59}$$

the Dirac representation may be reduced into two inequivalent Weyl representations of $SO(9,1)$ depending upon the value of $\Gamma^{11}|\mathbf{s}\rangle = \pm 1$:

$$\mathbf{32} = \mathbf{16} + \mathbf{16'}\,. \tag{2.60}$$

Not all possibilities for $|\mathbf{s}\rangle$ survive the physical state conditions (2.45). In particular,

$$G_0|\mathbf{s}\rangle = 0 \implies k\cdot\Gamma|\mathbf{s}\rangle = 0 \tag{2.61}$$

which is the Dirac equation. Choosing the (massless) frame $k = (-k_1, k_1, 0, \ldots, 0)$, we see that

$$k\cdot\Gamma|\mathbf{s}\rangle = 2k_1\Gamma^0\left(S_0 - \frac{1}{2}\right)|\mathbf{s}\rangle = 0 \tag{2.62}$$

so that only states with $s_0 = +\frac{1}{2}$ survive. Now, the two Weyl representations decompose under $SO(9,1) \longrightarrow SO(1,1)\times SO(8)$ as [11]

$$\begin{aligned}\mathbf{16} &\longrightarrow \left(+\frac{1}{2}, \mathbf{8_S}\right) + \left(-\frac{1}{2}, \mathbf{8_C}\right)\\ \mathbf{16'} &\longrightarrow \left(+\frac{1}{2}, \mathbf{8_C}\right) + \left(-\frac{1}{2}, \mathbf{8_S}\right)\,.\end{aligned} \tag{2.63}$$

Therefore, surviving physical ground states in the R sector fall into either an $\mathbf{8_S}$ or $\mathbf{8_C}$ of $SO(8)$.

The GSO projection

As we mentioned, the lowest-lying state in the NS sector is tachyonic. A prescription which removes the tachyon is the *Gliozzi-Scherk-Olive* (GSO) *projection*, in which physical states $|\varphi\rangle$ have a projection operator applied,

$$|\varphi\rangle \longrightarrow P_{\text{GSO}}|\varphi\rangle\,. \tag{2.64}$$

In the NS sector,

$$P_{\text{GSO}} = \frac{1}{2}\left[1 - (-1)^F\right] \tag{2.65}$$

where the fermion number operator F is defined as

$$F = \sum_{r>0} \psi^{\mu}_{-r}\psi_{\mu r} \,. \tag{2.66}$$

The GSO projection in the NS sector then acts to remove states with an even number of ψ oscillator excitations, deleting the tachyon from the spectrum.

In the R sector, the definition is modified to include the chirality operator Γ^{11}:

$$P^{\pm}_{\text{GSO}} = \frac{1}{2}\left[1 \mp \Gamma^{11}(-1)^{F}\right] . \tag{2.67}$$

The projection P^{+}_{GSO} now acts to delete states with an odd number of ψ oscillator excitations in the $\mathbf{8_S}$ of $SO(8)$, and an even number of ψ oscillator excitations in the $\mathbf{8_C}$. P^{-}_{GSO} acts in the opposite fashion, but as there is no absolute definition of chirality the choice of $P^{\pm}_{\text{GSO}}$ is irrelevant for open strings.

The true importance of the GSO projection lies in its ability to create a string spectrum which has spacetime supersymmetry. After applying the projection, there are an equal number of degrees of freedom in both the NS and R sector ground states: these form a $\mathbf{8_V} \oplus \mathbf{8_S}$ vector supermultiplet of the $D = 10$, $\mathcal{N} = 1$ supersymmetry algebra. In fact, the GSO projection ensures spacetime supersymmetry between NS sector bosons and R sector fermions at each mass level.

2.2.3 The closed string spectrum

The closed-string spectrum is obtained by taking tensor products of left- and right-moving states, each of which is very similar in form to the states found in the previous section. The physical state conditions $(L_0 - a)\,|\varphi\rangle = \left(\tilde{L}_0 - a\right)|\varphi\rangle = 0$ lead to the level-matching requirement that there be an equal number of excitations of left- and right-movers, so that we are constrained to gluing together only those states with the property

$$m_L^2 = m_R^2 \,. \tag{2.68}$$

At each mass level, there are four possible sectors, summarized in table 2.1.

When we perform the GSO projection, the relative choice of $P^{\pm}_{\text{GSO}}$ for the left- and right-movers is now important.

- Taking the opposite projection on both sides leads to a spectrum

$$(\mathbf{8_V} \oplus \mathbf{8_S}) \otimes (\mathbf{8_V} \oplus \mathbf{8_C}) \,, \tag{2.69}$$

Sector	Type	$SO(8)$ rep.	Corresponding massless fields
NS-NS	bosonic	$\mathbf{8_V} \otimes \mathbf{8_V} = \mathbf{35} \oplus \mathbf{28} \oplus \mathbf{1}$	graviton $g_{\mu\nu}$, B-field $B_{\mu\nu}$, dilaton Φ
NS-R	fermionic	$\mathbf{8_V} \otimes \mathbf{8_S} = \mathbf{8_S} \oplus \mathbf{56_S}$	gravitino Ψ_μ, dilatino λ
R-NS	fermionic	$\mathbf{8_S} \otimes \mathbf{8_V} = \mathbf{8_S} \oplus \mathbf{56_S}$	gravitino Ψ'_μ, dilatino λ'
R-R	bosonic	$\mathbf{8_S} \otimes \mathbf{8_S} = p$-forms	Ramond-Ramond fields

Table 2.1: Massless states of the closed string (after ref. [12]).

in which the spinors have opposite chiralities on either side. This is known as a *type IIA* theory. The spectrum of states is the same as that of a *non-chiral* ten-dimensional $\mathcal{N} = 2$ supergravity theory.

- Taking the same projection on both sides leads to a spectrum

$$(\mathbf{8_V} \oplus \mathbf{8_S}) \otimes (\mathbf{8_V} \oplus \mathbf{8_S}) \tag{2.70}$$

(or equivalently, $(\mathbf{8_V} \oplus \mathbf{8_C}) \otimes (\mathbf{8_V} \oplus \mathbf{8_C})$), in which the spinors have the same chirality on either side. This is a *type IIB* theory, and the resulting spectrum of states is that of a *chiral* ten-dimensional $\mathcal{N} = 2$ supergravity theory.

The ten-dimensional closed string spectrum is not directly relevant to our work in this thesis. It is included here firstly to indicate how string theory makes contact with supergravity, and secondly to introduce the concept of Ramond-Ramond fields in spacetime; we will talk more about this in section 2.4 below.

2.3 String perturbation theory

Just as in field theory, we may define a perturbation series expansion for string scattering amplitudes. Perturbation theory with strings is potentially superior to perturbation theory with particles for two reasons. Firstly, since the different elements of a string worldsheet contain a multiple of string states simultaneously, a single string diagram contains many Feynman diagrams: string theory is potentially much more efficient than field theory. Secondly, there is no unique point in spacetime at which all observers will agree that a string interaction takes place. In field theory, propagators coming together at a well-defined interaction point lead to ultraviolet divergences, but since the interaction point in string diagrams is somehow 'smeared out' over spacetime, UV divergences are avoided.

In field theory, terms in the perturbation expansion of a scattering amplitude are ordered topologically according to the number of loops in the Feynman diagram, and the expansion parameter is taken to the coupling strength of the field. In string theory, terms are also ordered topologically: we add a term $\lambda\chi$ to the action (2.18), where χ is the *Euler number*,

$$\chi = \frac{1}{4\pi}\int_M \mathrm{d}\sigma\mathrm{d}\tau\ \sqrt{-\gamma}R + \frac{1}{2\pi}\int_{\partial M} \mathrm{d}s\ k\,. \tag{2.71}$$

Here, R is the Ricci scalar for a given worldsheet M with boundary ∂M, and k is the extrinsic curvature of the worldsheet. This term is not dynamical, and does not affect the spectrum found above: instead, its effect is to weight the action by a factor which depends only on the topology of the worldsheet. The perturbation expansion parameters are taken to coupling strength of open and closed strings, g_O and g_C respectively.

The Euler number may also be expressed as

$$\chi = 2 - 2h - b - c\,, \tag{2.72}$$

where h is the number of handles a given worldsheet has, b is the number of boundaries it possesses and c is the number of cross-caps present. Some example diagrams showing worldsheets with boundaries and handles are presented in figure 2.1. In the third diagram, we see that one closed string can be replaced by two open strings. Therefore, one should expect a closed string to 'cost' approximately the same as two open strings, so that the couplings have the relation

$$g_O^2 \sim g_C\,. \tag{2.73}$$

Cross-caps occur only in unorientated theories, in which only those the states described in sec. 2.2.2 which are preserved under the worldsheet parity operator

$$\Omega: \quad \sigma \longrightarrow \pi - \sigma \tag{2.74}$$

are retained. They may be viewed as arising from a small hole which has been cut in the worldsheet, and had all diametrically opposed edges glued together.

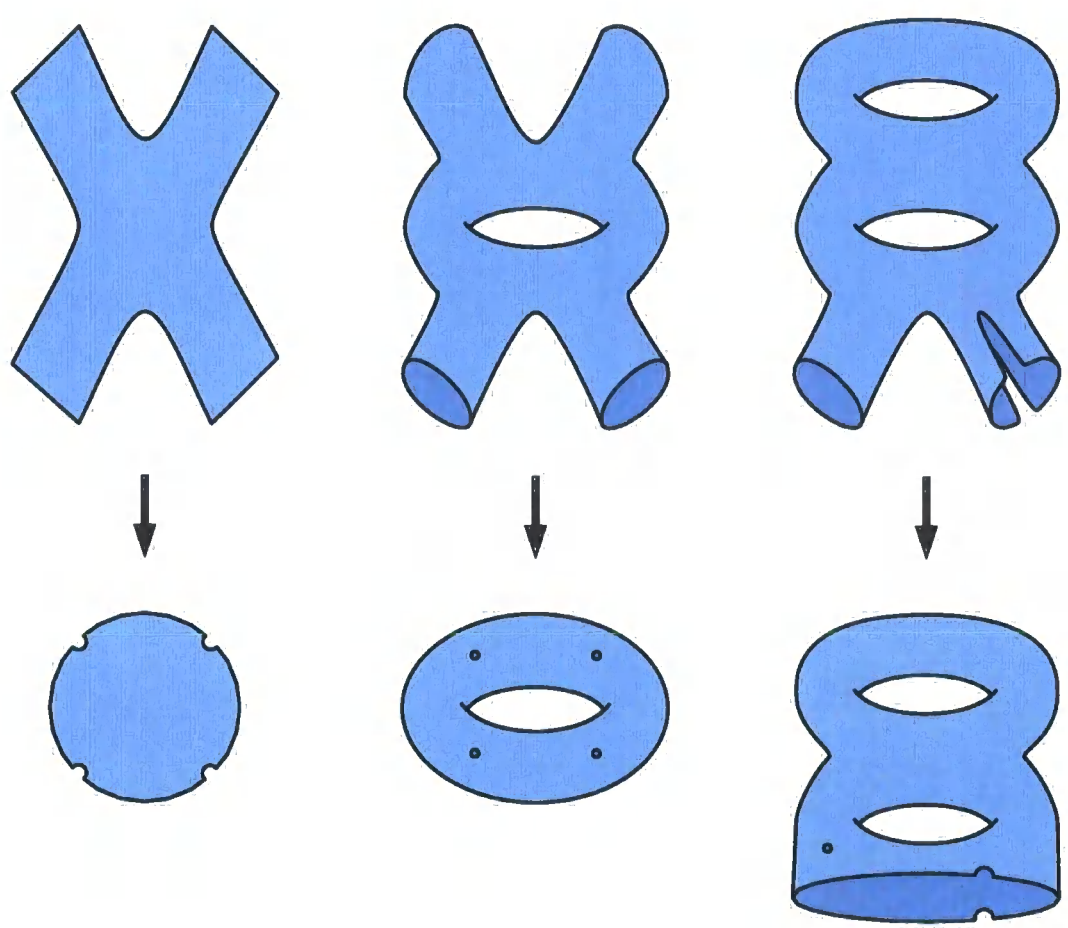

Figure 2.1: Example diagrams in string perturbation theory. In the second row, the external states have been conformally mapped to points, to be replaced by vertex operators.

2.3.1 The Polyakov path-integral

To obtain the S-matrix for string theory, one should imagine that the incoming and outgoing states are taken off to infinity, just as one does in field theory. The Weyl invariance (2.7) may then be used to map the external states to local disturbances on the worldsheet, as shown in the figure, which are then replaced by local *vertex operators* $\mathcal{V}(k,\tau,\sigma)$. The general procedure for calculating scattering amplitudes is then to consider a particular topology, insert vertex operators onto it, calculate the probability of the diagram spontaneously occurring, and sum over all physically distinct cases.

There are three complications associated with this procedure. Firstly, to avoid overcounting, we must account for the diff×Weyl gauge invariance of the action. Secondly, some of the topologies have *moduli* associated with them, describing different embeddings of the worldsheet into spacetime. For the torus, for instance, one may imagine tori of different 'fatness' and 'oval-ness' – and indeed, the torus does have a complex modulus τ. All values of the moduli associated with a particular topology must be taken into account. Thirdly, topologies may have *Conformal Killing Vectors* associated with them. These isometries lead to worldsheets which are mathematically distinct but have the same physical embedding in spacetime, and as such we should divide out by them. Taking the torus as an example again, the CKVs can be thought of as the two ways in which the (regular) torus may be rotated whilst leaving it physically unchanged. For a given topology, the number of moduli μ and CKVs κ are related to the Euler number by the Riemann-Roch theorem,

$$\mu - \kappa = -3\chi\,. \tag{2.75}$$

There are two general approaches to calculating amplitudes in a manner consistent with the above remarks: the operator approach, as typified by [7, 8], and the (Polyakov) path-integral approach, as typified by [10, 11]. The operator approach is not without its merits, but the algebra involved can be tiresome. Therefore, we generally make use of the path-integral formalism in this thesis. Here, one first Euclideanizes the worldsheet,

$$(\tau,\sigma) \longrightarrow (-\mathrm{i}y, x)\ , \tag{2.76}$$

after which one may write down a well-defined path-integral,

$$\mathcal{S} = \sum_{\chi,\alpha\beta} \int \frac{\mathcal{D}X\,\mathcal{D}\psi\,\mathcal{D}g}{V_{\text{diff}\times\text{Weyl}}} \mathrm{e}^{-S_E - \lambda\chi} \prod_{i=1}^{n} \int \mathrm{d}^2 z\, \sqrt{g}\mathcal{V}_i\left(k_i, z_i\right) , \tag{2.77}$$

where S_E is the Euclideanized version of the action (2.18) and the $z_i = x_i + \mathrm{i}y_i$ are points on the Euclideanized worldsheet. The sum is over topologies χ and also *spin-structures* $\alpha\beta$, which are all possible ways in which we may choose periodic and anti-periodic boundary conditions for the fermions Ψ on a particular topology.

A gauge in the diff×Weyl space is then fixed by a Faddeev-Popov procedure [10,11], in which one fixes the coordinates of κ of the vertex operators, and integrates over the positions of those that remain. The moduli and CKVs are accounted for by introducing anticommuting *ghost* fields b, c and on the worldsheet: one b ghost is introduced for each modulus, and one c ghost for each CKV. In practice, we will never need to worry about these ghosts, as we will absorb them into a one-loop partition function which will be found by operator methods.

We now discuss some of the specific topologies which play a role in perturbation theory, beginning with tree level where $\chi > 0$. There are three possible topologies to consider, none of which have any moduli associated with them:

- The sphere S_2, with $\chi = 2$. The Riemann-Roch result (2.75) tells us that $\kappa = 6$ CKVs are present. We may use these to completely fix the positions of three vertex operators on the worldsheet.
- The disk D_2, which has one boundary. Here, $\chi = 1$ and so $\kappa = 3$ by eq. (2.75). As the vertex operators must be on the worldsheet boundary, this is again enough to fix the positions of three vertex operators.
- The projective plane RP_2, which has one cross-cap and hence also $\chi = 1$, $\kappa = 3$.

At one-loop level, $\chi = 0$. There are four possible topologies,

- The torus T_2, with $\mu = \kappa = 2$.
- The cylinder/annulus C_2, with $\mu = \kappa = 1$.
- The Klein bottle K_2, with $\mu = \kappa = 2$.
- The Möbius strip M_2, with $\mu = \kappa = 1$.

We will be most interested in the cylinder/annulus. An important distinction between amplitudes at tree- and one-loop level comes from the so-called *partition function* contribution $\mathcal{Z}$ to (2.77). At tree-level, $\mathcal{Z}$ may be absorbed into the string coupling, but at one-loop level the moduli prevent this and so amplitudes contain explicit factors of $\mathcal{Z}$. We discuss the annulus partition function in section 2.4.1 below.

2.3.2 Vertex operators

Mathematically, the state-operator correspondence may be described using the tools of conformal field theory. After the Euclideanization (2.76), the closed-string mode expansions (2.13) may be written

$$\partial X^\mu_-(z) = -\mathrm{i}\sqrt{\frac{\alpha'}{2}}\sum_n \alpha^\mu_n z^{-n-1}\,, \qquad \overline{\partial} X^\mu_+(\overline{z}) = -\mathrm{i}\sqrt{\frac{\alpha'}{2}}\sum_n \tilde{\alpha}^\mu_n \overline{z}^{-n-1}\,, \tag{2.78}$$

where $\partial \equiv \partial_z$, $\overline{\partial} \equiv \partial_{\overline{z}}$. Notice that the left-moving (*holomorphic*) fields are written in terms of z, whilst the right-moving (*antiholomorphic*) fields are in terms of $\overline{z}$. These expressions invert to

$$\alpha^\mu_n = \sqrt{\frac{2}{\alpha'}}\oint_C \frac{\mathrm{d}z}{2\pi} z^n \partial X^\mu_-(z)\,, \qquad \tilde{\alpha}^\mu_n = -\sqrt{\frac{2}{\alpha'}}\oint_C \frac{\mathrm{d}\overline{z}}{2\pi} \overline{z}^n \overline{\partial} X^\mu_+(\overline{z})\,, \tag{2.79}$$

with the contour C taken to enclose the origin of the complex plane anti-clockwise. Applying the residue theorem gives the state-operator correspondence for the X fields,

$$\alpha^\mu_{-n} \longrightarrow \mathrm{i}\sqrt{\frac{2}{\alpha'}}\frac{1}{(n-1)!}\partial^n X^\mu(0)\,, \qquad \tilde{\alpha}^\mu_{-n} \longrightarrow \mathrm{i}\sqrt{\frac{2}{\alpha'}}\frac{1}{(n-1)!}\overline{\partial}^n X^\mu(0)\,. \tag{2.80}$$

This result is valid for operators inserted at the origin; for operators at arbitrary points z, the fields are simply translated. Now, an operator which localizes the string to a particular point X in spacetime is

$$\int \mathrm{d}^2 z\, \delta^{10}\left(X - X(z,\overline{z})\right)\,, \tag{2.81}$$

and the (tachyonic) ground state is the spacetime Fourier transform of this operator:

$$|0;k\rangle \longrightarrow \int \mathrm{d}^2 z\, \mathrm{e}^{\mathrm{i}k\cdot X}(z)\,. \tag{2.82}$$

Excited states are then constructed using eq. (2.80); for instance, the first excited state of the closed string (the graviton, $g^{\mu\nu}$) has the vertex operator

$$\alpha^{\mu}_{-1}\tilde{\alpha}^{\nu}_{-1}\left|0;k\right\rangle \longrightarrow \int \mathrm{d}^2 z\, \partial X^{\mu}\partial\overline{X}^{\nu}\mathrm{e}^{\mathrm{i}k\cdot X}\left(z\right) . \tag{2.83}$$

For the open string, the procedure is analogous, except that we only have one set of operators α^{μ}_{n}.

The fermionic oscillators ψ^{μ}_{r} may be treated in a similar fashion to the α^{μ}_{n}. Here, the mode expansions (2.30) become

$$\Psi^{\mu}\left(z\right) = \sum_{r} \psi^{\mu}_{r} z^{-r-\frac{1}{2}} \qquad \tilde{\Psi}^{\mu}\left(\overline{z}\right) = \sum_{r} \tilde{\psi}^{\mu}_{r} \overline{z}^{-r-\frac{1}{2}} . \tag{2.84}$$

And the state-operator correspondence is

$$\psi^{\mu}_{r} \longrightarrow \frac{1}{\left(r-\frac{1}{2}\right)!}\partial^{r-\frac{1}{2}}\Psi^{\mu}\left(0\right) \qquad \tilde{\psi}^{\mu}_{r} \longrightarrow \frac{1}{\left(r-\frac{1}{2}\right)!}\overline{\partial}^{r-\frac{1}{2}}\tilde{\Psi}^{\mu}\left(0\right) . \tag{2.85}$$

This is all the information required to construct vertex operators of NS-sector states. R-sector states, built up from $\left|\mathrm{s}\right\rangle$, are potentially more complicated since the expansion (2.84) has a branch-cut in that case and the state-operator correspondence is not simple. The solution lies in an equivalence known as *bosonization*, in which we group the fields Ψ^{μ} into complex pairs as

$$\Psi = \frac{1}{\sqrt{2}}\left(\Psi^{1} + \mathrm{i}\Psi^{2}\right) \qquad \overline{\Psi} = \frac{1}{\sqrt{2}}\left(\Psi^{1} - \mathrm{i}\Psi^{2}\right) . \tag{2.86}$$

The behaviour of these fields as they come together at a point on the worldsheet is determined by their *operator product expansion* (OPE):

$$\Psi\left(w\right)\overline{\Psi}\left(z\right) \sim \frac{1}{w-z} . \tag{2.87}$$

If we introduce a complex bosonic field H obeying

$$H\left(w\right)H\left(z\right) \sim -\log\left(w-z\right) \tag{2.88}$$

then the identification

$$\Psi\left(z\right) = \mathrm{e}^{\mathrm{i}H(z)} \qquad \overline{\Psi}\left(z\right) = \mathrm{e}^{-\mathrm{i}H(z)} \tag{2.89}$$

is consistent with the OPE (2.87); as such, all physics must be unchanged by the

identification. The antiholomorphic fields $\tilde{\Psi}(\bar{z})$ may be bosonized in an analogous manner. Bosonizing the ten dimensions of the string into five complex pairs of the form (2.86) and promoting H to a vector of five bosonic fields, the open string R-sector ground state is then identified as

$$|\mathrm{s}\rangle \longrightarrow \int \mathrm{d}z\, \mathrm{e}^{\mathrm{i}s\cdot H} \tag{2.90}$$

where s is the vector (2.56) and the integration is over the worldsheet boundary. For the closed string, a symmetric operator in $\tilde{H}$ is added, and the integration is taken over d^2z.

Although the ten-dimensional R-sector operator is not of direct interest to us, we will come across these *spin field* operators again when we come to vertex operators on intersecting branes in chapter 4. A state which *will* be of interest to is the open string photon, $\psi^\mu_{-\frac{1}{2}}|0;k\rangle$, with vertex operator

$$\mathcal{V}^\mu_{-1}(k,z) = g_O \lambda^a \mathrm{e}^{-\phi}\Psi^\mu \mathrm{e}^{\mathrm{i}k\cdot X}(z)\ . \tag{2.91}$$

This operator should be understood to be integrated over the worldsheet boundary, and a factor of the open string coupling g_O has been explicitly inserted. Two other points about this expression deserve further comment.

Picture-changing

Firstly, notice that the subscript -1 has been attached to (2.91), and an operator $\mathrm{e}^{-\phi}$ included. The argument for its presence goes as follows: firstly, use the Virasoro constraints (2.25) to define a stress-energy tensor for X and Ψ fields on the worldsheet. In general, the OPE of this tensor with a vertex operator $\mathcal{V}$ takes the form

$$T(w)\,\mathcal{V}(z) = \frac{h}{(w-z)^2}\mathcal{V}(z) + \ldots \tag{2.92}$$

where h is the *conformal weight* of $\mathcal{V}$. To offset the factor of $\mathrm{d}z$ which appears together with (2.91), it turns out that $\mathcal{V}$ must have a total conformal weight of one. The conformal weights of Ψ and $\mathrm{e}^{\mathrm{i}k\cdot X}$ are $-\frac{1}{2}$ and $\frac{\alpha'}{4}k^2$ respectively, and $k^2 = 0$ for the state $\psi^\mu_{-\frac{1}{2}}|0;k\rangle$, so we have a problem if we try to build a vertex operator from only these components. The solution is to add commuting *superconformal ghost* fields β, γ onto the worldsheet, which may be bosonized in terms of the field ϕ. The operator $\mathrm{e}^{a\phi}$ then has weight $-\frac{1}{2}a(a+2)$ [13], so that the composite operator (2.91) correctly has unit weight.

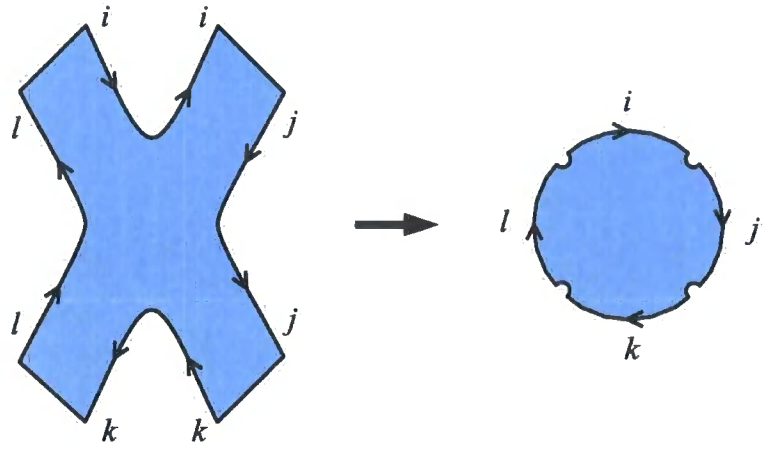

Figure 2.2: Scattering amplitudes with orientated worldsheets contain traces of Chan-Paton factors.

To avoid an anomaly in the $\beta\gamma$ CFT, it is necessary that the total superghost charge in a particular amplitude sums to the Euler number χ of the associated topology. In general then, we will need some prescription for changing the ϕ-charge, or *picture*, of our vertex operators. Such a prescription is the picture-changing operation,

$$\mathcal{V}_{i+1}(k,z) = \lim_{w\to z} \mathrm{e}^{\phi}\partial X^{\mu}\psi_{\mu}(w)\,\mathcal{V}_i(z)\ . \tag{2.93}$$

Picture-changing will play a key role in the calculations of chapter 4.

Chan-Paton factors

A *Chan-Paton* factor λ^a has been introduced into (2.91). This is a non-dynamical quantity associated with the endpoints of strings. The idea is to write the general open string state $|a;k\rangle$ in the basis

$$|a;k\rangle = \sum_{i,j} |ij;k\rangle\,\lambda^a_{ij}\ . \tag{2.94}$$

Then, as figure 2.2 demonstrates, open-string scattering amplitudes must contain a factor

$$\sum_{i,j,k,l} \lambda^1_{ij}\lambda^2_{jk}\lambda^3_{kl}\lambda^4_{li} = \mathrm{tr}\left(\lambda^1\lambda^2\lambda^3\lambda^4\right)\ . \tag{2.95}$$

Since the trace is cyclic, scattering amplitudes are invariant under the gauge symmetry

$$\lambda^a \longrightarrow U\lambda^a U^\dagger \tag{2.96}$$

where $U \in U(N)$. Under this symmetry, one end i of the string transforms in the $\mathbf{N}$ of $U(N)$, whilst the other end (due to the relative orientation reversal) transforms in the $\overline{\mathbf{N}}$. Therefore, the open string vertex operator $\mathcal{V}^\mu_{-1}$ transforms in the adjoint $\mathbf{N} \otimes \overline{\mathbf{N}}$ representation, which supports our identification of it as a gauge boson.

2.4 Branes

When we introduced strings in section 2.1, we mentioned that there was one further possible choice for the string boundary conditions: that of *Dirichlet* conditions,

$$\partial_\tau X|_{\sigma=0} = \partial_\tau X|_{\sigma=\pi} = 0\,. \tag{2.97}$$

In keeping with the principle that all which is not forbidden is compulsory, the consequences of this choice should be explored. In the p dimensions X^μ in which the boundary conditions are Neumann, the string becomes confined to a $(p+1)$-dimensional hyperplane known as a Dp-brane, whilst in the remaining $9-p$ Dirichlet dimensions the string is fixed at a point.

In classical electromagnetism, the one-dimensional electric charge is sourced by a one-form A_μ, with field strength

$$F_{\mu\nu} = \partial_{[\mu} A_{\nu]}\,. \tag{2.98}$$

If our $(p+1)$-dimensional objects also carry charge, we might expect that they be sourced by a set of $(p+1)$-forms $C^{(p+1)}$, so that

$$F_{\mu_1 \cdots \mu_{p+2}} = \partial_{[\mu_1} C^{(p+1)}_{\mu_2 \cdots \mu_{p+2}]}\,. \tag{2.99}$$

Exactly such a set of p-forms comes from the R-R sector of the closed string (c.f. table 2.1). Taking a suitable basis of gamma matrices [12], the $|\mathrm{s}\rangle \otimes |\tilde{\mathrm{s}}\rangle$ states decompose into

$$\begin{aligned}
&\text{in IIA theory:} && C^{(1)}, C^{(3)}, C^{(5)}, C^{(7)} && \Longrightarrow && \text{D0, D2, D4, D6 branes} \\
&\text{in IIB theory:} && C^{(0)}, C^{(2)}, C^{(4)}, C^{(6)}, C^{(8)} && \Longrightarrow && \text{D}(-1)\text{, D1, D3, D5 branes}\,.
\end{aligned}$$

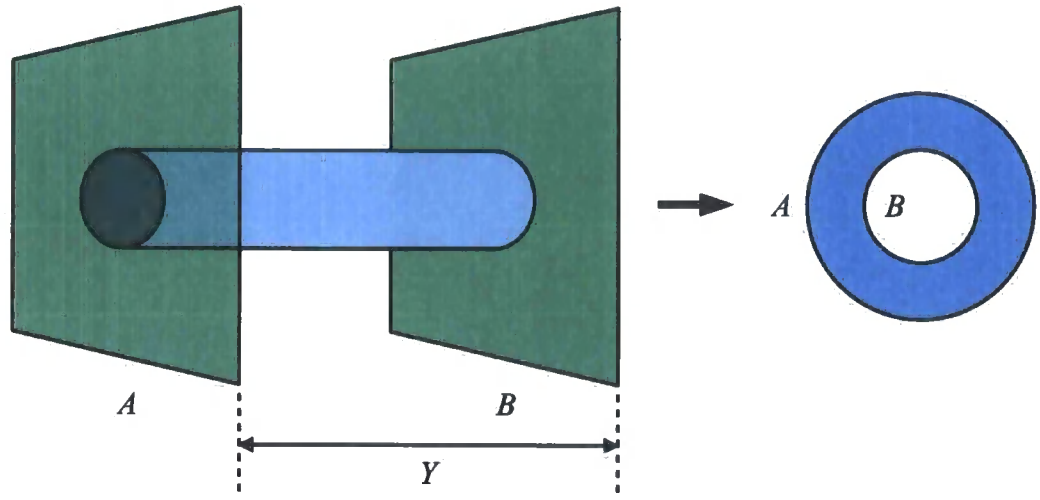

Figure 2.3: The one-loop partition function between parallel branes A and B, separated by a distance Y, is an annulus diagram with one edge of the annulus on each brane.

The charge associated with the branes is known as Ramond-Ramond charge.

D-branes provide a solid realization of the concept of Chan-Paton factors discussed above. In particular, we may re-interpret the Chan-Paton degrees of freedom as labelling the branes upon which strings end, so that a state $|ij;k\rangle$ is stretched between branes i and j. In general, if the branes are separated by distances Y_{ij}, the open-string mass formula is modified to include a contribution from the tension of the stretched string,

$$m^2 \longrightarrow m^2 + \frac{Y_{ij}^2}{(2\pi\alpha')^2}\,, \tag{2.100}$$

so that the only massless NS-sector state is $\psi^\mu_{-\frac{1}{2}}\,|ii;k\rangle$. An observer on the brane sees this state break up into a set of scalars $\psi^{\mu=p+1,\ldots,9}\,|ii;k\rangle$ describing the embedding of the brane in spacetime, plus a $U(1)$ gauge boson $\psi^{\mu=0,\ldots,p}\,|ii;k\rangle$ confined to the brane. If we consider N D-branes stacked on top of each other, then there are N^2 states $\psi^\mu_{-\frac{1}{2}}\,|ij;k\rangle\,\lambda_{ij}$ corresponding to the N^2 ways in which strings may attach themselves between the branes. These states form a massless vector in the adjoint of $U(N)$: a gauge boson.

2.4.1 The one-loop partition function

A primary element in the computation of one-loop amplitudes between branes is the *partition function*, which is the one-loop amplitude with no vertex operator insertions. In this case, the prescription described in sec. 2.3 appears problematic, since we cannot fix the position of the required $\kappa = 1$ operators. Fortunately, the group of CKVs on the annulus is of finite volume and so we may divide out by it, fixing the b and c ghosts at the same time, with the result:

$$\mathcal{Z} = \sum_{\alpha\beta} \int \frac{\mathrm{d}t}{2t} \left\langle b^1(0) c^1(0) \right\rangle_{\mathrm{C}_2} . \tag{2.101}$$

The factor of $\frac{1}{2}$ is to correct for a discrete $\mathbb{Z}_2$ symmetry from interchanging the boundaries of the annulus, and t is the modular parameter of the annulus.

Although evaluation of $\mathcal{Z}$ is possible in a path-integral formalism [14], the calculation is most straightforward when performed with operator algebra. The idea is to consider the annulus in the open string channel, and sum over all possible string states running in the loop. For the X fields and a single dimension,

$$Z \equiv \left\langle b^1(0) c^1(0) \right\rangle_{\mathrm{C}_2} = \sum_n \langle n | \, q^H \, | n \rangle = \mathrm{tr} \, q^H , \tag{2.102}$$

where $|n\rangle$ is intended to represent a state of given occupation number, and $q \equiv \mathrm{e}^{-2\pi t H}$ takes strings once around the worldsheet. Setting $l_s = \sqrt{2\alpha'} = 1$, the open-string Hamiltonian is

$$H = L_0 = \frac{1}{2} p^2 + N + a \tag{2.103}$$

with the number operator N defined by eq. 2.47. The trace breaks up into a (Gaussian) integral over the momenta, plus a $\mathrm{tr} q^N$ part. Associating the momentum integral with the X fields, one finds for a Neumann dimension that

$$Z_{X,N} = (2\pi t)^{-\frac{1}{2}} \eta \left(\mathrm{i}t\right)^{-1} . \tag{2.104}$$

The Dedekind function η is defined in appendix A. In a Dirichlet dimension, the momentum is zero, but H acquires an extra factor $(Y/2\pi)^2$ from the (classical) tension of the stretched string, so that

$$Z_{X,D} = \mathrm{e}^{-tY^2/\pi} \eta \left(\mathrm{i}t\right)^{-1} . \tag{2.105}$$

For the ψ fields, there are four possible spin structures upon the annulus to

consider. In the spatial direction, the two possibilities are just the R and NS sectors of the open string; in the time direction, inserting the operator $(-1)^F$ from the GSO projection flips the boundary condition, so that the relevant traces are

$$\begin{aligned} Z_{00} &= \mathrm{tr}_{\mathrm{NS}}\, q^H & Z_{10} &= \mathrm{tr}_{\mathrm{R}}\, q^H \\ Z_{01} &= \mathrm{tr}_{\mathrm{NS}}\, (-1)^F q^H & Z_{11} &= \mathrm{tr}_{\mathrm{R}}\, (-1)^F q^H . \end{aligned} \tag{2.106}$$

These may be explicitly evaluated as

$$Z_{\alpha\beta} = \eta\,(\mathrm{i}t)^{-1}\,\vartheta_{\alpha\beta}\,(0|\mathrm{i}t) \tag{2.107}$$

where the Jacobi theta-functions $\vartheta_{\alpha\beta}(0|\mathrm{i}t)$ are also defined in appendix A. The full partition function is then

$$\mathcal{Z} = \frac{\mathrm{i}V_{10}}{(2\pi)^{10}} \int_0^\infty \frac{\mathrm{d}t}{4t} t^{-\frac{1}{2}(p+1)} \mathrm{e}^{-tY^2/\pi} \eta\,(\mathrm{i}t)^{-12} \sum_{\alpha\beta} \delta_{\alpha\beta} \vartheta_{\alpha\beta}^4\,(0|\mathrm{i}t)\ , \tag{2.108}$$

where an (infinite) volume factor $\mathrm{i}V_{10}$ has been inserted along with an extra factor of $\frac{1}{2}$ coming from the GSO projection. A factor of $\left[\eta\,(\mathrm{i}t)^{-2}\,\vartheta_{\alpha\beta}\,(0|\mathrm{i}t)\right]^2$ has been dropped as only transverse dimensions contribute to the trace; this can be seen formally by computing the ghost contributions to $\mathcal{Z}$. Y should now be taken as a $(9-p)$-vector describing the brane separation.

The phases $\delta_{\alpha\beta}$ are

$$\delta_{00} = \delta_{11} = +1, \quad \delta_{01} = \delta_{10} = -1\,. \tag{2.109}$$

This choice may be determined by computing the closed-string partition function (from which the open string function may be obtained), and noting that only (2.109) is consistent with a property of the torus known as *modular invariance*. Furthermore, it is exactly the choice for which $\mathcal{Z}$ vanishes by the identity (A.11), reflecting that there is no net force between parallel Dp-branes.

2.4.2 Branes at a relative angle

So far, we have assumed that all branes in spacetime are parallel. It is interesting to also consider the case where they lie at a relative angle $\pi\theta$ [15]. Begin by considering branes in a single pair of dimensions (figure 2.4). First group the X into complex dimensions, as

$$X = X^8 + \mathrm{i}X^9 \tag{2.110}$$

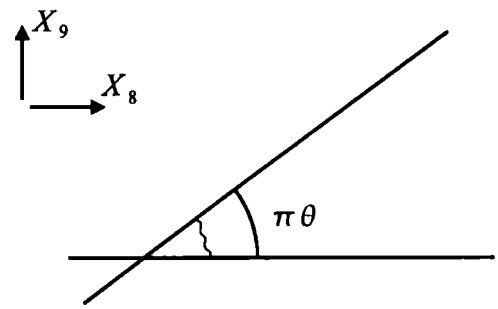

Figure 2.4: Two branes at a relative angle $\pi\theta$.

and so on. In one complex dimension, the boundary conditions on X are then

$$\begin{aligned} \sigma = 0: &\quad \partial_\sigma \mathrm{Re}\, X = \mathrm{Im}\, X = 0 \\ \sigma = \pi: &\quad \partial_\sigma \mathrm{Re}\, \mathrm{e}^{\mathrm{i}\pi\theta} X = \mathrm{Im}\, \mathrm{e}^{\mathrm{i}\pi\theta} X = 0\,, \end{aligned} \tag{2.111}$$

which are satisfied by the mode expansion

$$X(z,\bar{z}) = \mathrm{i}\sqrt{\frac{\alpha'}{2}} \sum_{n\in\mathbb{Z}} \left(\frac{\alpha_{n-\theta}}{n-\theta} \mathrm{e}^{\mathrm{i}(n-\theta)z} + \frac{\alpha^\dagger_{n+\theta}}{n+\theta} \mathrm{e}^{-\mathrm{i}(n+\theta)\bar{z}} \right) \tag{2.112}$$

where α, $\alpha^\dagger$ are now suitable independent combinations of α^8 and α^9. The string has now become localized at the intersection point, with zero momentum, and the oscillator coefficients have been shifted by θ relative to the usual result. This is exactly what happens to twisted closed strings in orbifold compactifications, suggesting an equivalence between the two approaches. A similar result is found for the ψ fields, where the n are shifted by a further factor of $\frac{1}{2}$ in the R sector.

Vertex operators for strings at the intersection of branes may be computed by making use of the bosonized spin fields $\mathrm{e}^{\mathrm{i}s\cdot H}$ discussed in section 2.3.2, with the coefficients s appropriately modified by θ. However, as the conformal weight of the spin field is $\frac{1}{2}s^2$, the total conformal weight of the vertex operators will no longer be correct in general, and we must introduce a field which returns the conformal weight to unity. Such a field is the bosonic *twist field* σ_θ, originally introduced in the context of closed strings on orbifolds [16,17], which has conformal weight $\frac{1}{2}\theta(1-\theta)$. It is then possible to construct a combination of $\mathrm{e}^{\mathrm{i}s\cdot H}$, σ_θ, $\mathrm{e}^{\mathrm{i}k\cdot X}$ and $\mathrm{e}^{\alpha\phi}$ which has weight 1. Physically, one should interpret the twist fields as worldsheet operators which shift us from one brane to another in spacetime. We discuss vertex operators

for intersecting branes further in chapter 4.

As a final comment, we point out that it is possible to construct a partition function of the form (2.108) between a pair of branes at relative angles [11], which is extremely similar in form to the partition function for branes at orbifold singularities [18]. However, we will not need it in this work.

Chapter 3

Kinetic Mixing in Brane Models

3.1 Introduction

Kinetic Mixing occurs in theories that have, in addition to some visible $U(1)_a$, an additional $U(1)_b$ factor in the hidden sector. The effect occurs when the hidden $U(1)_b$ couples to the visible $U(1)_a$ through the diagram in figure 3.1. This diagram, proportional to $\mathrm{Tr}(Q_a Q_b)$, results in a Lagrangian of the form

$$\mathcal{L}_{\text{gauge}} = -\frac{1}{4g_a^2}F_a^{\mu\nu}F_{a\mu\nu} - \frac{1}{4g_b^2}F_b^{\mu\nu}F_{b\mu\nu} - \frac{\chi}{2g_a g_b}F_a^{\mu\nu}F_{b\mu\nu}\,. \tag{3.1}$$

The consequences of this type of mixing were first studied by Holdom in the context of millicharged particles [19]. Later, Dienes *et al* pointed out that Kinetic Mixing can contribute significantly and even dominantly to supersymmetry-breaking mediation [20] resulting in additional contributions to the scalar mass-squared terms proportional to their hypercharge. In this chapter we will be considering both the generation of millicharged particles (that is, particles carrying fractionally shifted

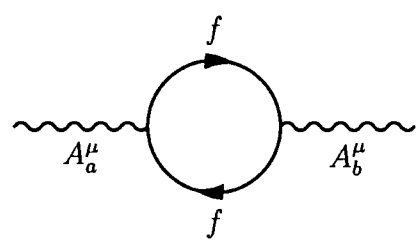

Figure 3.1: Kinetic Mixing in field theory. f is a fermion carrying charge under both $U(1)$'s.

units of electric charge) and the mediation of supersymmetry breaking, in models involving stacks of D-branes and (anti) $\overline{\text{D}}$-branes. This is a particularly interesting context in which to consider Kinetic Mixing because the stacks of branes and anti-branes carry $U(N)$ gauge factors, so that Kinetic Mixing naturally occurs between these groups.

The string equivalent of the Kinetic Mixing diagram is shown in figure 3.2. This is a non-planar annulus diagram, with the states in the loop corresponding to open strings stretched between the 'MSSM branes' and anti-branes across the bulk. However, going to the closed string channel, it can also be seen as a closed string tree-level diagram with closed string dilaton, graviton and RR fields propagating in the bulk. This is simply gravitational mediation, and as such one expects the Kinetic Mixing parameter χ to receive a suppression from the bulk space. Therefore, before evaluating the diagram in detail (which we do in the following section), let us first use dimensional arguments to estimate the expected relative strengths of various effects.

Effects that are propagated through closed string modes in the bulk suffer a suppression of order Y^{p-7} where Y is the interbrane separation in units of the fundamental scale. Thus we expect

$$\frac{\chi}{g_a g_b} \sim \text{Tr}(\lambda_a)\text{Tr}(\lambda_b) V_{\text{NN}} Y^{p-7}\,, \tag{3.2}$$

where V_{NN} is the ($p-3$ dimensional) world-volume of the p branes in the compactified space. The prefactors are the traces of the Chan-Paton matrices, and the Kinetic Mixing is therefore between the central $U(1)$'s of the $U(N)$ gauge groups. These vanish only if the gauge group on either the branes or anti-branes is orthogonal. Now consider a set-up where the interbrane separation and compactification scales are all of the same order, R, in fundamental units. The compactification scale and string scale are related by the Planck mass which can be obtained by dimensional reduction of the 10D theory; specifically [21],

$$\frac{M_s}{M_P} \sim \alpha_p R^{(p-6)}\,, \tag{3.3}$$

where α_p is the fine-structure constant on the brane. The latter can be set to be of order one (it is supposed to correspond to some Standard Model value) by adjusting the string coupling to compensate for the potentially large V_{NN} factor. We then have

$$\frac{\chi}{g_a g_b} \sim \left(\frac{M_s}{M_P}\right)^{\frac{2(5-p)}{6-p}}\,. \tag{3.4}$$

Experimental upper bounds on χ are presented in [22]. Assuming that the hidden sector contains some massless fields, the relevant bound is $\chi \lesssim 2 \times 10^{-14}$. Inserting into the above we find that we require $M_s \lesssim 10^8$ GeV for $p = 3, 4$, while for $p \geq 5$ it is impossible to avoid the millicharged particle bounds.

The above limit holds if the hidden $U(1)$ symmetry remains unbroken. If the hidden $U(1)$ is broken with $\langle D_b \rangle \neq 0$ then one expects a different kind of effect to be important, namely that the supersymmetry breaking D-term VEV of order M_s^2 be communicated to the visible sector via the Kinetic Mixing terms. It is easy to see that such terms would generally dominate in communicating supersymmetry breaking, as they do in the heterotic case [20]. The potential due to the brane-antibrane attraction goes as Y^{p-7} and so the corresponding effective supersymmetry breaking mass-squareds go as $\partial^2 V/\partial Y^2 \sim Y^{p-9}$. By contrast the SUSY breaking mass-squareds communicated by Kinetic Mixing go simply as Y^{p-7}, and so are dominant. The expected SUSY breaking terms in the visible sector are then of order

$$m_{\rm KM}^2 \sim M_s^2 \frac{\chi}{g_a g_b} \sim M_s^2 \left(\frac{M_s}{M_P}\right)^{\frac{2(5-p)}{6-p}} . \tag{3.5}$$

Requiring that $m_{\rm KM}^2 \lesssim M_W^2$ gives a similar bound on the string scale, $M_s \lesssim 10^8$ GeV for $p = 3, 4$. When the bound is saturated, SUSY breaking terms of order M_W are induced by $\overline{D3}$-branes or $\overline{D4}$-branes in the bulk.

One class of models to which our analysis is particularly relevant are the so-called intermediate scale models [2, 4, 23–38]. In these models the string scale M_s is assumed to be of order $M_s \sim \sqrt{M_W M_P} \sim 10^{11}$ GeV. One adopts a brane configuration that *locally* reproduces the spectrum of the MSSM but which breaks supersymmetry globally by for example the inclusion of $\overline{\rm D}$-branes somewhere in the bulk of the compactified space. (Such supersymmetry breaking configurations may still be consistent with the constraints of RR tadpole cancellation.) In this set-up, the large Planck mass is a result of the dilution of gravity by a large bulk volume as usual. As above, supersymmetry breaking communication is realized as interactions between $\overline{\rm D}$-branes in the bulk and visible sector MSSM branes. This communication gets the same volume suppression that gives the four-dimensional M_P, and so purely dimensional arguments have led to the conclusion that supersymmetry breaking terms of order $M_{\not{\rm SUSY}} \sim M_s(M_s/M_P) \sim M_W$ are induced in the visible sector. Indeed, this effect corresponds precisely to the Y^{p-9} suppression above. However Kinetic Mixing terms can drastically modify this picture. If they are present a more natural fundamental scale would be $M_s \sim 10^8$ GeV.

It may seem odd that in the end an *upper* bound on the string scale is ob-

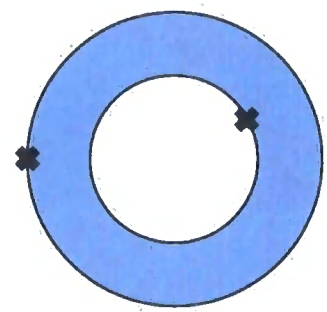

Figure 3.2: Kinetic Mixing in string theory: Annulus diagram with two open-string vertex operator insertions.

tained. To see why, note that there are two competing effects. The first obvious effect is that high string scales generate larger supersymmetry breaking. However, the overwhelming effect for the bounds is that low string scales require larger compactification volumes to generate the correct effective Planck mass. Consequently low string scales allow a greater brane-antibrane separation and a reduced Kinetic Mixing.

In the following sections we give a more detailed exposition of these bounds, beginning with a study of Kinetic Mixing between Dp-branes and $\overline{\text{D}p}$-branes in a simplified type II set-up. One particular aspect that needs some attention is the question of NS-NS tadpoles which are generally present in nonsupersymmetric set-ups. We will also discuss what happens in configurations that have asymmetric compactification radii. This is important for two reasons. Firstly, because making some directions transverse to the brane much smaller than the overall brane separation modifies the rate of fall-off. However, we find that when we recalculate the above constraints the degenerate case we have outlined above is the optimum one, in the sense that the bounds obtained are the least restrictive. Secondly, one would like to avoid having a too large string coupling since then the perturbative calculation (*i.e.* based on strings propagating in a D-brane background) breaks down. Because of this the compact world-volumes of the branes (V_{NN}) typically need to be much smaller than the large transverse volumes required to dilute gravity, since the former also dilute the gauge couplings. For D3-branes our conclusions are the same as above (since $V_{\text{NN}} = 1$) and the degenerate case is optimal. If $p > 3$, the conclusions can be somewhat different: a large string scale may be recovered for extremely asymmetric dimensions ($R/r \gtrsim 10^9$ and larger). However, this loophole is not particularly helpful since most models constructed to date contain $\overline{\text{D3}}$-branes,

where the more restrictive bounds apply. Hence our main conclusions will indeed be as presented above.

3.2 String calculation of Kinetic Mixing

In this section we will carry out a calculation of Kinetic Mixing in a simplified type II set-up. Many features of the end result have to do with volume dilution and are common to all brane/antibrane exchanges taking place in a compact space. Much of the important behaviour can therefore already be seen in the partition function, a factor in our final answer. In particular by looking at the partition function we can see how Kaluza-Klein modes and winding modes reproduce the volume dilution one intuitively expects in both degenerate and asymmetric compactifications. We also discuss the NS-NS tadpole which is uncancelled and which in a perfect world would be treated by modifying the background. Lastly we include the vertex factors, discuss correlation functions on the annulus, and evaluate the final result.

Consider a setup consisting of parallel Dp and $\overline{\text{D}p}$ branes a distance Y apart. Let each of these branes have an open string stuck to it, representing a $U(1)$ gauge boson. The two open strings interact by exchanging a closed string cylinder, which we map to an annulus with two vertex operators inserted on the boundary (fig. 3.2). Let coordinates on the worldsheet be defined by $z = x+\mathrm{i}y$, with $x \in [0, \pi]$ worldsheet space and $y \in [0, 2\pi t]$ Euclideanized worldsheet time. From the spacetime point of view, $t \to 0$ corresponds to a long cylinder, and $t \to \infty$ a long strip. A formal expression for the amplitude is

$$\Pi^{\mu\nu}(k_1, k_2) = \sum_{\alpha\beta} \int_0^\infty \frac{\mathrm{d}t}{2t} \left\langle b^1(0)c^1(0) \int \mathrm{d}z_1\, \mathrm{d}z_2\, \mathcal{V}^\mu(k_1, z_1)\mathcal{V}^\nu(k_2, z_2) \right\rangle_{C_2} \tag{3.6}$$

with $b^1(0)$ and $c^1(0)$ the spatial components of ghost fields, $\alpha\beta$ spin structures on the worldsheet and $\mathcal{V}^\mu(k, z)$ vertex operators. The factor of $2t$ corrects for the discrete symmetry coming from interchanging the ends of the cylinder plus the continuous translational symmetry around the annulus.

The most straightforward way to evaluate (3.6) is to take the partition function $\mathcal{Z}_{p\bar{p}}$, and insert appropriate contributions from the vertex operators. In a non-compact spacetime, $\mathcal{Z}_{p\bar{p}}$ can be obtained by taking the result (2.108) for two p-branes separated by a distance Y in their co-volume, and accounting for the relative flip of RR charge between a brane and antibrane by flipping the sign of the term coming from RR closed strings. Measuring distances in terms of the string length

(*i.e.* setting $l_s = \sqrt{2\alpha'} = 1$),

$$\mathcal{Z}_{p\bar{p}} = \frac{iV_4}{(2\pi)^4}\int_0^\infty \frac{dt}{4t} t^{-\frac{1}{2}(p+1)} e^{-tY^2/\pi}\eta(it)^{-12}\left[\underbrace{\vartheta_{00}(0|it)^4 - \vartheta_{10}(0|it)^4}_{\text{NS-NS strings}} + \underbrace{\vartheta_{01}(0|it)^4}_{\text{RR strings}}\right]. \tag{3.7}$$

where the Dedekind function η and the Jacobi functions ϑ_{ab} are defined in appendix A. Unlike the result for parallel p-branes this does not vanish, reflecting the fact that the brane-antibrane configuration breaks all spacetime supersymmetries. Using the expansions given in appendix A, it can be shown that the small-t limit of this result gives an attractive potential between the branes that goes as $1/Y^{7-p}$ [39]. On the other hand, the large-t limit gives a divergence from the tachyon at $Y < \pi$ which is associated with annihilation of the brane-antibrane system at small Y [40].

3.2.1 The partition function in compact spacetimes

We introduce the Kinetic Mixing calculation with a prototypical set-up in which spacetime has the topology $\mathcal{M}_4 \times (T^2)^3$. We require the branes to fill $\mathcal{M}_4$ and allow them separations Y_i in the six compact dimensions. Modifications must be made to (3.7) to account for the compact nature of some of the dimensions. In particular, for a noncompact dimension, integration over the string zero modes contributes a factor $V/2\pi t^{1/2}$ (where V is formally infinite). For a compact dimension of size $2\pi R$, we have a sum over Kaluza-Klein modes,

$$\sum_{n=-\infty}^{\infty} e^{-\pi t n^2/R^2} = \begin{cases} 1 & : \quad t/R^2 \to \infty \\ R/t^{1/2} & : \quad t/R^2 \to 0 \end{cases}. \tag{3.8}$$

The second limit is obtained from the Poisson resummation formula,

$$\sum_{n=-\infty}^{\infty} e^{-\pi a n^2 + 2\pi i b n} = a^{-1/2}\sum_{m=-\infty}^{\infty} e^{-\pi(m-b)^2/a}. \tag{3.9}$$

Strings occupying dimensions where the boundary conditions on the brane are Dirichlet can also wind around that dimension, if it is compact. This stretching is just an extension of the brane separation term in (3.7):

$$e^{-tY^2/\pi} \to \sum_{w=-\infty}^{\infty} e^{-t(Y+2\pi R w)^2/\pi}. \tag{3.10}$$

In each dimension, the winding modes can also be Poisson resummed,

$$\sum_{w=-\infty}^{\infty} \mathrm{e}^{-t(Y+2\pi Rw)^2/\pi} = \frac{1}{Rt^{1/2}}\left[1+\sum_{m>0} 2\cos\left(m\frac{Y}{R}\right)\mathrm{e}^{-\pi m^2/4R^2 t}\right]. \tag{3.11}$$

In the limit $R^2 t \to 0$, we should take only the leading term.

As in the noncompact case, we can examine the amplitude in the large and small-t limits. First, let us examine the large-t limit (which we denote as $t > t_c \simeq \pi$, since $\mathrm{e}^{-t/\pi}$ is our expansion parameter). Kaluza-Klein modes do not contribute at large t, so after expanding the ϑ and η functions, we have

$$\mathcal{Z}_{p\bar{p}} \simeq \frac{\mathrm{i}V_4}{(2\pi)^4}\int_{t_c}^{\infty} \mathrm{d}t\, t^{-3} \sum_{w\in\Gamma_{9-p}} \mathrm{e}^{-t\left((Y+2\pi Rw)^2-\pi^2\right)/\pi} \tag{3.12}$$

where w is a $9-p$ vector of integers that sums over the integer lattice Γ_{9-p}, and we are also treating Y and R as vectors. Since we are here interested in $Y \gg \pi$ we can neglect the $w \in \Gamma_{9-p} - \{0\}$ contribution and retain only the zeroth mode, giving

$$\mathcal{Z}_{p\bar{p}} \simeq \frac{\mathrm{i}V_4}{(2\pi)^4} t_c^{-2} E_3\left(t_c(Y^2-\pi^2)/\pi\right) \tag{3.13}$$

where $E_n(z) = \int_1^\infty \mathrm{d}t\; t^{-n}\mathrm{e}^{-zt}$ is the standard exponential integral function. Note that this function diverges when its argument is negative, so we still get the usual appearance of a tachyon when $Y < \pi$.

The remainder of the partition function is evaluated in the small t limit $t < t_c$, and this is where we will find interesting results. The Kaluza-Klein modes do now contribute, and so after expanding (3.7) we have

$$\mathcal{Z}_{p\bar{p}} = \frac{\mathrm{i}V_4 V_{\mathrm{NN}}}{(2\pi)^4}\int_0^{t_c} \mathrm{d}t\, t^{-\frac{1}{2}(p-5)} \sum_{w\in\Gamma_{9-p}} \mathrm{e}^{-t(Y+2\pi Rw)^2/\pi}. \tag{3.14}$$

We have written $V_{\mathrm{NN}} = (\prod_{i=4}^{p} R_i)$ for the volume of the compact space occupied by the branes. There is a tadpole term coming from a closed string infrared divergence (*i.e.* the limit $t \to 0$). In this limit, we can deal with the sum over windings by Poisson resumming all dimensions, giving

$$\mathcal{Z}_{p\bar{p}} = \frac{\mathrm{i}V_4}{(2\pi)^4}\frac{V_{\mathrm{NN}}}{V_{\mathrm{DD}}}\int_0^{t_c} \mathrm{d}t\, t^{-2} \prod_{i=p+1}^{9}\frac{1}{2}\left[1+\sum_{m_i>0} 2\cos\left(m_i\frac{Y_i}{R_i}\right)\mathrm{e}^{-\pi m_i^2/4R_i^2 t}\right] \tag{3.15}$$

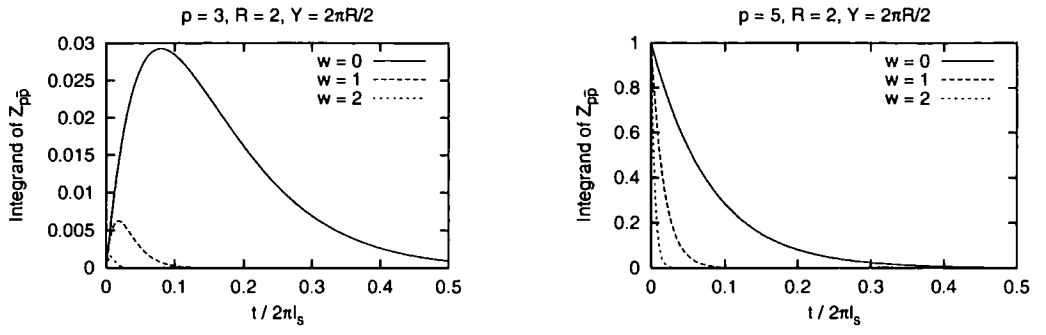

Figure 3.3: Relative contribution of different winding modes to $Z_{p\bar{p}}$, for $p = 3$ and $p = 5$. Even if $Y = 2\pi R/2$, we see that the zero-winding contribution is strongly dominant.

where $V_{\rm DD} = \left(\prod_{i=p+1}^{9} R_i\right)$ is the volume of the compact space transverse to the branes. Cutting off $t > 1/\mu^2$ and taking $t_c \to \infty$ gives a tadpole divergence of order μ^2 from the leading term:

$$\mathcal{Z}_{\rm tadpole} = \frac{{\rm i}V_4}{(2\pi)^4}\frac{V_{\rm NN}}{2^{9-p}V_{\rm DD}}\mu^2 . \tag{3.16}$$

This expression corresponds to the propagation of a massless closed string state, and we will discuss it shortly. Before we do so, let us deal with the remaining, 'threshold', contribution where we are on a surer footing. To address these we need to be more discerning when deciding to Poisson resum a particular dimension in eq.(3.14). First, note that for $p < 5$ the integrand is dominated by peaks at

$$t_s = \frac{(5-p)\pi}{2(Y+2\pi Rw)^2} . \tag{3.17}$$

Figure 3.3 illustrates this. The magnitude of the peaks is exponentially suppressed as the winding number increases, and so the threshold contribution is dominated by the first peak, corresponding to strings stretched a distance Y with no winding. The tadpole divergence we saw earlier comes from an infinite number of these peaks piling up on the origin.

Next we note that, from (3.11), resummation in a given dimension i is only valid when $R_i^2 t \ll 1$. Since we know that the dominant value of t will be the t_s given

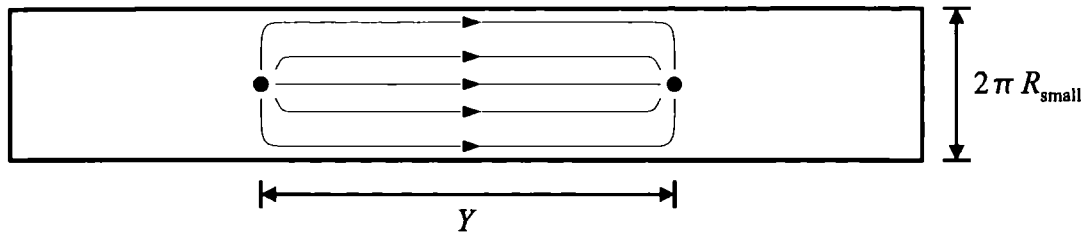

Figure 3.4: When to resum winding modes; a dimension that has $R_i \ll |Y|$ ceases to contribute to the exchange of closed string modes between the branes as lines of flux are confined. Winding modes in that dimension are then resummed.

above, we should resum the windings in a given dimension only if

$$R_i \ll |Y| \,. \tag{3.18}$$

The familiar physical situation corresponding to resumming or not is shown in figure 3.4.

Degenerate radii

If we take all radii to be degenerate, $R_i \equiv R$, we see that successful resummation requires $R < Y$, which cannot be. Hence, we choose instead to impose a small cut-off w_0 on the winding lattice, indicating that we take just the leading terms.

Also, note that the larger Y the further t_s is below t_c and the better the approximation of small t asymptotics. We can therefore neglect the large-t contribution (3.12) (which is an exponentially small correction) in the $Y \gg \pi$ limit, and take $t_c \to \infty$ in (3.14). The threshold corrections then look like

$$\mathcal{Z}_{\text{threshold}} \approx \frac{iV_4V_{\text{NN}}}{(2\pi)^4} \int_0^\infty \mathrm{d}t\, t^{-\frac{1}{2}(p-5)} \sum_{|w|<|w_0|} \mathrm{e}^{-t(Y+2\pi Rw)^2/\pi} \tag{3.19}$$

$$= \frac{iV_4V_{\text{NN}}}{(2\pi)^4} \Gamma\left(\frac{1}{2}(7-p)\right) \sum_{|w|<|w_0|} \left(\frac{\pi}{(Y+2\pi Rw)^2}\right)^{\frac{1}{2}(7-p)} . \tag{3.20}$$

For $p \geq 5$ both the divergence and the threshold terms are maximal at $t = 0$ so it is less obvious that this prescription is correct for them also. To see that it is correct, it is useful to consider the tadpole contribution in the un-resummed "many winding" picture. Consider the $|w| \gg 1$ contribution to $\mathcal{Z}_{\text{threshold}}$ that we have removed, with

$Y = 0$ for convenience:

$$\mathcal{Z}_\infty = \frac{iV_4 V_{NN}}{(2\pi)^4}\Gamma\left(\frac{1}{2}(7-p)\right)\sum_{|w|>|w_0|}\left(\frac{\pi}{(2\pi Rw)^2}\right)^{\frac{1}{2}(7-p)}. \tag{3.21}$$

We may approximate the divergent sum involved by an integral, imposing a large cutoff w_μ on the winding,

$$\sum_{|w_0|<|w|<|w_\mu|}\frac{1}{|2\pi Rw|^{(7-p)}} \approx \int_{w_0}^{w_\mu}\frac{\Omega_{8-p}w^{8-p}\mathrm{d}w}{(2\pi Rw)^{(7-p)}} \tag{3.22}$$

$$= \frac{\Omega_{8-p}}{(2\pi R)^{9-p}}\frac{1}{2}\left[(2\pi Rw_\mu)^2 - (2\pi Rw_0)^2\right] \tag{3.23}$$

where Ω_{8-p} is the area of a unit $(8-p)$-sphere. Then,

$$\mathcal{Z}_\infty = \frac{iV_4}{(2\pi)^4}\frac{V_{NN}}{2^{9-p}V_{DD}}\Gamma\left(\frac{1}{2}(7-p)\right)\pi^{-\frac{1}{2}(7-p)}\Omega_{8-p}\frac{1}{2}\left[(2Rw_\mu)^2 - (2Rw_0)^2\right]. \tag{3.24}$$

Clearly this is the μ^2 divergence of the massless closed string with

$$\mu^2 = \frac{1}{2}\Gamma\left(\frac{1}{2}(7-p)\right)\pi^{-\frac{1}{2}(7-p)}\Omega_{8-p}(2Rw_\mu)^2. \tag{3.25}$$

The tadpole contribution may be excised by removing the contributions with many windings, leaving the threshold contribution which corresponds to just the leading term. This picture does not rely on the presence of the saddle.

Asymmetric radii

Suppose now that the R_i are not all equal, and that we have d dimensions which meet the criterion (3.18) for resummation, leaving $9-p-d$ dimensions which require a cutoff on w. By (3.11), the resummed dimensions contribute a factor $1/R_i t^{1/2}$ to $\mathcal{Z}_{p\bar{p}}$, so that

$$\mathcal{Z}_{\text{threshold}} = \frac{iV_4}{(2\pi)^4}\frac{V_{NN}}{2^d V_{DD,\text{small}}}\Gamma\left(\frac{1}{2}(7-p-d)\right)\sum_{|w|<|w_0|}\left(\frac{\pi}{(Y+2\pi Rw)^2}\right)^{\frac{1}{2}(7-p-d)}, \tag{3.26}$$

where $V_{DD,\text{small}}$ is the volume of the small Dirichlet-Dirichlet dimensions that have been resummed. Physically, the reduction in the power to which Y is raised comes from the volume restriction on closed string modes exchanged between the branes (figure 3.4). Note that we need $p + d < 7$ to avoid a divergence in $\mathcal{Z}_{p\bar{p}}$. Hence,

scenarios with $d = 4$ appear untenable.

We now return to the tadpole contribution. As we have seen this piece corresponds to the propagation of a massless closed string mode. In principle the contribution would be one particle reducible, corresponding to the exchange of an on-shell massless closed string state between the two gauge fields. Thus at this stage it is not appropriate to include the tadpole contribution to χ. The correct way to deal with it would be a generalization of the Fischler-Susskind mechanism [41, 42], in which the background is modified to take account of the extra tadpole term in the effective potential, upon which as shown in ref. [43] 'spontaneous compactification' can occur. Intuitively one expects the propagation of the massless modes to be screened by the Fischler-Susskind mechanism, so that the cut-off we have imposed by hand on the effective potential, $\mu \sim Rw_\mu$, may take on a physical meaning as some kind of screening length. Since we do not wish to address the Fischler-Susskind mechanism in any detail, we will simply work in the toroidal background and use the 1PI argument to excise the tadpole from χ. One should bear in mind however that volume factors involving the radius along the Y direction should possibly be understood as the size of some spontaneously compactified dimension.

3.2.2 Inclusion of vertex operators

Let us now proceed to evaluate the Kinetic Mixing amplitude (3.6) by including vertex operators in $\mathcal{Z}_{p\bar{p}}$. For the annulus, it is necessary that the vertex operators' superghost charges sum to zero. Hence, we work with vertex operators in the 0-picture, in which a $U(1)$ gauge boson corresponds to

$$\mathcal{V}_0^\mu(k,z) = \mathrm{i}g_O\lambda\left(\dot{X}^\mu + \mathrm{i}\,(k\cdot\psi)\,\psi^\mu\right)\mathrm{e}^{\mathrm{i}k\cdot X}\,(z)\ . \tag{3.27}$$

Here, g_O is the open string coupling and λ the Chan-Paton matrix for the brane or stack of branes associated with the vertex operator. The index μ runs over the noncompact dimensions. We have again set $l_s = \sqrt{2\alpha'} = 1$.

The correlation between two such vertex operators can be calculated either by summing over all contractions or via a path integral approach; a path-integral approach for the X fields is described in Appendix B. By (B.6), an expression for the

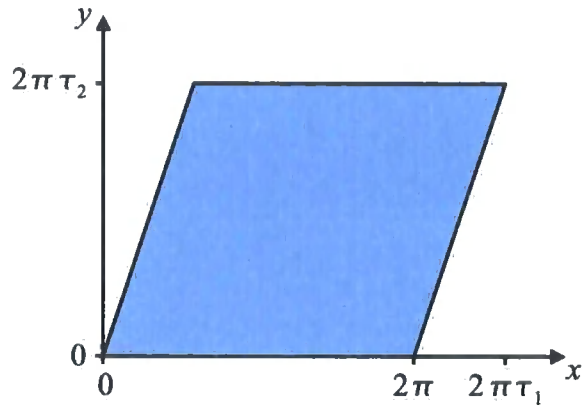

Figure 3.5: The torus with modulus τ in the complex plane. The upper and lower, and left and right, edges are identified.

amplitude is

$$\Pi^{\mu\nu} = -g_O^2 \mathrm{Tr}\left(\lambda_a\right) \mathrm{Tr}\left(\lambda_b\right) \left[k^\mu k^\nu - \eta^{\mu\nu} k^2\right] \sum_{\alpha\beta} \mathcal{Z}_{\alpha\beta} \int_0^{2\pi t} \mathrm{d}y_1 \int_0^{2\pi t} \mathrm{d}y_2 \, \mathrm{e}^{k^2 G(y_{12})} \left[(2\pi)^2 G'(y_{12})^2 - S\left(y_{12}\right)^2\right] . \quad (3.28)$$

Here, $\mathcal{Z}_{\alpha\beta}$ is the $(\alpha\beta)$ spin structure term in $\mathcal{Z}_{p\bar{p}}$, and it is to be understood that the integration over t contained in $\mathcal{Z}_{p\bar{p}}$ is applied to the entire expression. $G\left(z\right)$ and $S\left(z\right)$ are the respective correlators for bosons and fermions on opposite side of the annulus, which we now discuss.

Correlation functions on the annulus

A torus may be defined as a region of the complex plane with periodic boundary conditions

$$z = z + 2\pi\left(m + n\tau\right) \qquad m, n \in \mathbb{Z} \quad (3.29)$$

where $\tau = \tau_1 + \mathrm{i}\tau_2$. This describes a parallelogram in the complex plane (figure 3.5). If we set $\tau_1 = 1$ so that the parallelogram becomes a square, then we have only one modulus $t \equiv \tau_2$. Then, identifying $z = -\bar{z}$ gives us the annulus (figure 3.6).

Using this identification, we can obtain the correlator on an annulus from that

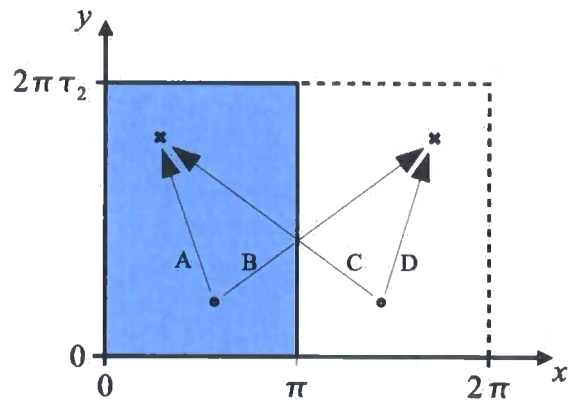

Figure 3.6: The annulus as obtained from the torus by setting $\tau_1 = 1$ and identifying under $x = -x$ ($z = -\bar{z}$). A fundamental region is shown shaded. The propagator is obtained by supplementing each transition (marked A,D) by an image charge piece (marked B,C).

on a torus. On a torus parameterized as described, the correlator is [44]

$$G_{T^2}(z) = -\frac{1}{4}\log\left|\frac{\vartheta_1\left(\frac{z}{2\pi}\middle|\,\tau\right)}{\eta(\tau)^3}\right|^2 + \frac{[\mathrm{Im}z]^2}{8\pi\tau_2}\,. \tag{3.30}$$

Here, $\vartheta_1(\nu|\tau)$ and $\eta(\tau)$ are the Jacobi theta- and Dedekind eta-functions, as defined in [10]. Now, by including image charges as shown in figure 3.6, we can find the correlator on an annulus.

In general, we have a choice of Neumann or Dirichlet conditions on the world-sheet boundaries. About a Neumann boundary, the open string mode expansion is symmetric, whilst about a Dirichlet boundary it is antisymmetric. We can impose N or D boundary conditions on our correlator by requiring it to have similar characteristics. In our situation, open string vertex operators are confined to the two branes and their have momenta parallel to both. Hence, NN boundary conditions are appropriate; we require our correlator be symmetric under both $z_1 \to -\bar{z}_1$ and $z_2 \to -\bar{z}_2$:

$$G(z_2 - z_1) = \left[G_{T^2}(z_2 - z_1|it) + G_{T^2}(z_2 + \bar{z}_1|it)\right]\,. \tag{3.31}$$

For vertex operators on opposite sides of the annulus, take $z_1 = 0 + iy_1$, $z_2 = \pi + iy_2$. Defining $y_{12} = y_2 - y_1$ and using $\vartheta_1\left(\nu \pm \frac{1}{2}\middle|\,\tau\right) = \vartheta_2(\nu|\tau)$, plus the fact that the

appropriate theta-functions are always real for purely imaginary ν, τ, we find

$$G\left(y_{12}\right) = -\log\left[\frac{\vartheta_2\left(\frac{iy_{12}}{2\pi}\middle|\, it\right)}{\eta(it)^3}\right] + \frac{y_{12}^2}{4\pi t}\,. \tag{3.32}$$

The fermion correlator on a torus with periodic boundary conditions can be obtained by noting that the derivative of a solution to the bosonic action solves the Dirac action. For the three 'even' spin structures where the boundary conditions are not periodic (*i.e.* $(\alpha\beta) \neq (11)$), the torus is artificially extended by a factor of two in both directions and the method of images is used [45]. The result is [46]

$$S_{T^2}(z) = 2\pi\frac{\vartheta_{\alpha\beta}\left(\frac{z}{2\pi},\tau\right)\vartheta_1'\left(0|\tau\right)}{\vartheta_1\left(\frac{z}{2\pi}\middle|\,\tau\right)\vartheta_{\alpha\beta}(0,\tau)}\,. \tag{3.33}$$

Note that this correlator is spin-structure dependent.

We can convert these to the annulus by the method of images as before. There is an extra complication due to the way in which the involutions applied to the torus exchange left- and right-moving fermions, which requires us to insert gamma-matrices appropriately [45]. For Neumann-Neumann boundary conditions on the annulus,

$$\begin{aligned}\mathbf{S}\left(z_2 - z_1\right) &= \frac{1}{2}\left[S_{T^2}\left(z_2 - z_1\right) + \gamma_1 S_{T^2}\left(-\bar{z}_2 - z_1\right)\right. \\ &\qquad \left. + S_{T^2}\left(z_2 + \bar{z}_1\right)\gamma_1^T + \gamma_1 S_{T^2}\left(-\bar{z}_2 + \bar{z}_1\right)\gamma_1^T\right] \\ &= \begin{pmatrix} S^{T^2}\left(z_2 - z_1\right) & S^{T^2}(z_2 + \bar{z}_1) \\ S^{T^2}(z_2 + \bar{z}_1) & S^{T^2}(z_2 - z_1)\end{pmatrix}\,.\end{aligned} \tag{3.34}$$

In the last line we have used the result that $S_{T^2}(z) = S_{T^2}\left(-\bar{z}\right)$, which comes directly from the theta-function identity $\vartheta_{\alpha\beta}\left(\nu,\tau\right) = \vartheta_{\alpha\beta}\left(-\bar{\nu},\tau\right)$. Attempts to construct a correlator with either Dirichlet-Dirichlet or Neumann-Dirichlet boundary conditions fail, as all terms then cancel.

The off-diagonal terms represent correlators between fermions moving in opposite directions, and are not of interest to us. Thus, we have found that on the annulus with Neumann conditions on the boundaries, the correlator is the same as that for a torus:

$$S\left(z_2 - z_1\right) = S_{T^2}\left(z_2 - z_1\right)\,. \tag{3.35}$$

Now, using the identity [47]

$$\left[\frac{\vartheta_{\alpha\beta}(z,\tau)\,\vartheta_1'(0|\tau)}{\vartheta_1(z|\tau)\,\vartheta_{\alpha\beta}(0,\tau)}\right]^2 = \frac{\partial_z^2\vartheta_{\alpha\beta}\left(\frac{z}{2\pi}\middle|\,it\right)\Big|_{z=0}}{\vartheta_{\alpha\beta}\left(\frac{z}{2\pi}\middle|\,it\right)\Big|_{z=0}} - \frac{\partial^2}{\partial z^2}\log\vartheta_1(z,\tau)\ , \tag{3.36}$$

we can write for the even spin structures, with vertex operators on opposite boundaries of the annulus as before,

$$S(y_{12})^2 = (2\pi)^2\left[\frac{\partial_x^2\vartheta_{\alpha\beta}\left(\frac{iy_{12}}{2\pi}\middle|\,it\right)\Big|_{y_{12}=0}}{\vartheta_{\alpha\beta}\left(\frac{iy_{12}}{2\pi}\middle|\,it\right)\Big|_{y_{12}=0}} - \frac{\partial^2}{\partial y_{12}^2}\log\vartheta_2\left(\frac{iy_{12}}{2\pi}\middle|\,it\right)\right]. \tag{3.37}$$

Calculation of $\Pi^{\mu\nu}$

We now return to the evaluation of equation 3.28. Since the only physical degree of freedom in the problem is y_{12}, a change of variables $\{y_1, y_2\} \to \{y_1, y_{12}\}$ is appropriate:

$$\int_0^{2\pi t} dy_1 \int_0^{2\pi t} dy_2 = 2\pi t \int_0^{2\pi t} dy_{12}\,.$$

Furthermore, it is not necessary to integrate y_{12} over the entire annulus; by symmetry, we can just integrate halfway round and multiply by two. The second line of $\Pi^{\mu\nu}$ is then

$$-4\pi t\int_0^{\pi t} dy_{12}\, e^{k^2G(y_{12})}\left[(2\pi)^2 G'(y_{12})^2 + S(y_{12})^2\right]. \tag{3.38}$$

From experience with the partition function, we expect the interesting physics to come from small values of t. Hence, we modular-transform the correlators so that their expansions will be in $1/t$, finding

$$(2\pi)^2 G'(y_{12})^2 + S(y_{12})^2 = (2\pi)^2\left[\frac{\partial_{y_{12}}^2\vartheta_4\left(\frac{iy_{12}}{2\pi t}\middle|\,\frac{i}{t}\right)}{\vartheta_4\left(\frac{iy_{12}}{2\pi t}\middle|\,\frac{i}{t}\right)} - \frac{\partial_{y_{12}}^2\vartheta_{\beta\alpha}\left(\frac{iy_{12}}{2\pi t}\middle|\,\frac{i}{t}\right)\Big|_{y_{12}=0}}{\vartheta_{\beta\alpha}\left(\frac{iy_{12}}{2\pi t}\middle|\,\frac{i}{t}\right)\Big|_{y_{12}=0}}\right]. \tag{3.39}$$

Terms involving first derivatives of the theta functions have cancelled between the bosonic and fermionic correlators in $\Pi^{\mu\nu}$. For the analogous calculation on the torus, the spin-structure independent terms cancel entirely [46, 48, 49], but this does not occur on the annulus. Using the theta-function expansions in appendix A, we have

$$e^{k^2G(y_{12})} = \left[t^{-1}\frac{\eta\left(\frac{i}{t}\right)^3}{\vartheta_4\left(\frac{iy_{12}}{2\pi t}\middle|\,\frac{i}{t}\right)}\right]^{k^2} \simeq t^{-k^2}e^{-\pi k^2/4t} \tag{3.40}$$

and

$$\frac{\partial_{y_{12}}^2 \vartheta_4\left(\frac{iy_{12}}{2\pi t}\middle|\frac{i}{t}\right)}{\vartheta_4\left(\frac{iy_{12}}{2\pi t}\middle|\frac{i}{t}\right)} = 2e^{-\pi/t}t^{-2}\cos\left(y_{12}/t\right) + 2e^{-4\pi/t}(2t)^{-2}\cos\left(2y_{12}/t\right) + \cdots \tag{3.41}$$

Since $\int_0^{\pi t} dx\ \cos(nx/2t) = 0$, the first term in (3.38) will disappear when we integrate over the vertex operator positions. Effectively, then, we care only about the second term, which is

$$-(2\pi)^2 \frac{\partial_{y_{12}}^2 \vartheta_{\beta\alpha}\left(\frac{iy_{12}}{2\pi t}\middle|\frac{i}{t}\right)\Big|_{y_{12}=0}}{\vartheta_{\beta\alpha}\left(\frac{iy_{12}}{2\pi t}\middle|\frac{i}{t}\right)\Big|_{y_{12}=0}} = (2\pi)^2 \begin{cases} 2e^{-\pi/t}t^{-2} & : (\alpha\beta) = (00) \\ -2e^{-\pi/t}t^{-2} & : (\alpha\beta) = (10) \\ \frac{1}{4}t^{-2} & : (\alpha\beta) = (01) \end{cases}. \tag{3.42}$$

Using these expansions, we may write the spin-structure-dependent portion of $\Pi^{\mu\nu}$ as

$$\begin{aligned} &\sum_{\alpha\beta} \bar{\delta}_{\alpha\beta}\vartheta_{\alpha\beta}\left(0|it\right)^4 \left(-4\pi t\right) \int_0^{2\pi t} dy_{12} e^{k^2 G(y_{12})} \left[(2\pi)^2 G'(y_{12})^2 + S\left(y_{12}\right)^2\right] \\ &= -t^{-2}\, 4\pi t\, \pi t\, t^{-k^2} e^{-\pi k^2/4t} (2\pi)^2 \left[2e^{-\pi/t}t^{-2} - \left(-2e^{-\pi/t}t^{-2}\right) + \left(16e^{-\pi/t}\right)\left(\frac{1}{4}t^{-2}\right)\right] \\ &= 8\left(2\pi\right)^4 t^{-k^2-2} e^{-\pi/t} e^{-\pi k^2/4t}. \end{aligned} \tag{3.43}$$

where the signs $\bar{\delta}_{\alpha\beta}$ are defined by (3.7).

We are now in a position to write down the final amplitude. As discussed in section 3.2.1, this will contain both a 'tadpole' contribution and a 'threshold' contribution. Taking the tadpole contribution first, we have

$$\Pi^{\mu\nu}_{\text{tadpole}} = 2iV_4 \frac{V_{\text{NN}}}{2^{9-p}V_{\text{DD}}} g_O^2 \text{Tr}(\lambda_a)\text{Tr}(\lambda_b) \left[k^\mu k^\nu - \eta^{\mu\nu}k^2\right] \int_{1/\mu^2}^{\infty} dt\ t^{-k^2-2} e^{-\pi k^2/4t}. \tag{3.44}$$

The t integral diverges on-shell; however, as we have argued, the interesting physics ought to come from the threshold contribution, which we now examine. For notational simplicity, we take the degenerate radii result for $\mathcal{Z}_{p\bar{p}}$, leading to

$$\Pi^{\mu\nu}_{\text{threshold}} = 2iV_4 V_{\text{NN}} g_O^2 \text{Tr}(\lambda_a)\text{Tr}(\lambda_b) \left[k^\mu k^\nu - \eta^{\mu\nu}k^2\right] \tag{3.45}$$

$$\int_0^{\infty} dt\ t^{-k^2-\frac{1}{2}(p-5)} e^{-\pi k^2/4t} \sum_{|w|<|w_0|} e^{-t(Y+2\pi Rw)^2/\pi}. \tag{3.46}$$

As in section 3.2.1, we have imposed a small cut-off $|w_0|$ on the winding lattice to

avoid the tadpole, so that the integral is

$$\int_0^\infty \mathrm{d}t\, t^{-k^2-\frac{1}{2}(p-5)} \mathrm{e}^{-\pi k^2/4t} \mathrm{e}^{-tY^2/\pi} = 2\left(\frac{k\pi}{2Y}\right)^{\frac{1}{2}(7-p)-k^2} K_{\frac{1}{2}(p-7)+k^2}(kY)\,.$$

For non-integral $\nu < 0$, the Bessel K function expands as

$$K_\nu(z) = \frac{1}{2}\left(\frac{z}{2}\right)^{-\nu}\left[\Gamma(\nu) - \left(\frac{z}{2}\right)^2 \Gamma(\nu-1)\right] + \mathcal{O}\left(z^{4-\nu}\right)\,, \tag{3.47}$$

hence

$$\int_0^\infty \mathrm{d}t\, t^{-k^2-\frac{1}{2}(p-5)} \mathrm{e}^{-\pi k^2/4t} \mathrm{e}^{-tY^2/\pi} = \left(\frac{\pi}{Y^2}\right)^{\frac{1}{2}(7-p)} \Gamma\left(\frac{1}{2}(7-p)\right) + \mathcal{O}(k^2) \qquad (p<7)\,. \tag{3.48}$$

Taking $k^2 \to 0$ and ignoring all winding modes except the zeroth, we have

$$\Pi^{\mu\nu}_{\text{threshold}} = 2\mathrm{i}V_4 V_{\text{NN}} g_O^2 \mathrm{Tr}(\lambda_a)\mathrm{Tr}(\lambda_b)\left[k^\mu k^\nu - \eta^{\mu\nu}k^2\right]\left(\frac{\pi}{Y^2}\right)^{\frac{1}{2}(7-p)} \Gamma\left(\frac{1}{2}(7-p)\right)\,. \tag{3.49}$$

As for the partition function, the necessary modifications for asymmetric radii are to introduce a factor $2^d V_{\text{DD,small}}$ on the bottom and to replace $p \to p+d$. Rewriting the k^μ in terms of $F^{\mu\nu}$ (with an appropriate normalization to remove factors of the string coupling g_O), the relevant parameter measuring the mixing is

$$\frac{\chi}{g_a g_b} = \frac{2}{N}\mathrm{Tr}\left(\lambda_a\right)\mathrm{Tr}\left(\lambda_b\right)\frac{V_{\text{NN}}}{2^d V_{\text{DD,small}}}\left(\frac{\pi l_s^2}{Y^2}\right)^{\frac{1}{2}(7-p-d)} \Gamma\left(\frac{1}{2}\left(7-p-d\right)\right)\,. \tag{3.50}$$

We have explicitly restored l_s in this expression, except for the volume factors which are expressed in units of string lengths.

There are two further subtleties we should mention: orbifolds, and branes of differing dimensionality. Firstly, suppose we make our internal space $(T^2)^3/\mathbb{Z}_N$, and fix the branes at two different orbifold singularities. The resulting theory contains an untwisted sector, in which the states are just those in the non-orbifolded theory, plus $N-1$ twisted sectors consisting of states that survive the orbifold projection. The boundary conditions on twisted states prevent them from having momentum [17], which keeps them stuck at fixed points. Hence, figure 4.1 cannot occur for twisted states in the theory. We therefore neglect twisted-sector contributions to the amplitude, and simply divide $\Pi^{\mu\nu}$ by a factor N to get the result for Kinetic Mixing with a $\mathbb{Z}_N$ orbifold.

Secondly, suppose that instead of a Dp-$\overline{\text{D}p}$ combination, we have a setup consisting of Dp and $\overline{\text{D}q}$ branes (or equivalently, Dq and $\overline{\text{D}p}$ branes), where $q > p$. Let dimensions $i = 4, \ldots, p$ be shared Neumann-Neumann, $i = p+1, \ldots, q$ be Neumann-Dirichlet and $i = q+1, \ldots, 9$ be Dirichlet-Dirichlet. The nonzero number of ND dimensions will not affect our results since there correlation functions between vertex operators in ND dimensions vanish. The only changes to the amplitudes calculated is that V_{NN} should be taken as the volume of compact Neumann-Neumann dimensions *shared* by the branes, and V_{DD} should be appropriately reduced.

3.3 Millicharged particles from Kinetic Mixing

We first assume that $U(1)_b$ is unbroken, so that millicharged particles are generated by Kinetic Mixing. As we argued in section 3.2, only the amplitude contribution (3.49) is relevant here. One can now look at the consequences of this mixing in different scenarios, using experimental data on the maximum size of millicharged particles. To do this, we will need the following relation, obtained from dimensional reduction of the type I string action [21],

$$\left(\frac{M_s}{M_P}\right)^2 = 2\alpha_p^2 \frac{V_{\text{NN}}}{2^{9-p} V_{\text{DD}}}. \tag{3.51}$$

$M_s = 1/l_s$ is the string scale, and α_p is the coupling on the brane. Since the type I theory can be considered as an orientifold of type IIB, and type IIA is related to type IIB by a symmetry known as T-duality [11, 12], this result is valid in all brane-based models.

3.3.1 Degenerate radii

Let us first consider the case of degenerate extra dimensions, $R_i \equiv R$ with $d = 0$. Take the brane separation to be $Y = \pi R$ and write $g_a g_b = 4\pi\alpha_p$, so

$$\chi_{\text{degen}} = \frac{2}{N}\text{Tr}\,(\lambda_a)\,\text{Tr}\,(\lambda_b)\left(\frac{2^{\frac{1}{2}(8-p)}}{\alpha_p}\frac{M_s}{M_P}\right)^{\frac{2(5-p)}{(6-p)}} 4\pi\alpha_p \pi^{\frac{1}{2}(p-7)}\Gamma\left(\frac{1}{2}(7-p)\right). \tag{3.52}$$

The mixing parameter χ is related to the observable charge shift ϵ simply by $\chi = -\frac{e_a}{e_b}\epsilon$ [19]. Experimental upper bounds on ϵ are examined in [22], where it is found that for particles of mass $m_\epsilon \lesssim m_e$, $|\epsilon| \gtrsim 2 \times 10^{-14}$ is excluded.

We can use this information to put an upper bound on the string scale. For

$p = 3$, suppose we assume $e_a/e_b \sim 1$, $\mathrm{Tr}(\lambda_a)\mathrm{Tr}(\lambda_b) \sim 1$, and take $N = 3$, $\alpha_p \approx 1/24$ (the MSSM unification value). The requirement $|\epsilon| \lesssim 2 \times 10^{-14}$ then gives

$$M_s \lesssim 5 \times 10^7 \,\mathrm{GeV}. \tag{3.53}$$

By the argument at the end of section 3.2.2, the same result holds between for D3-$\overline{\mathrm{D}q}$ system, where $q > 3$; the only difference is that we ought to take $g_a g_b = 4\pi\sqrt{\alpha_p \alpha_q}$.

Note that the existence of millicharged particles at some level is necessary to avoid a nonzero M_s. If millicharged particles do not exist at all in nature, then the only resolution is to insist either that no unbroken $U(1)$'s exist on the antibrane, or that $\mathrm{Tr}(\lambda_a)\mathrm{Tr}(\lambda_b)$ is fortuitously zero. This could be the case if all antibranes present have orthogonal gauge groups on their world volumes (*e.g.* if they are located at orientifold planes).

Setting $p > 3$ leads to similar conclusions; when $p = 4$ we find $M_s \lesssim 4 \times 10^4$ GeV, $p = 5$ is clearly ruled out as χ has no dependence on any mass scale, $p = 6$ implies $M_P > M_s$, whilst χ becomes singular for $p \geq 7$.

3.3.2 Asymmetric radii

Suppose we set the number of small Dirichlet-Dirichlet dimensions to be $d > 0$, with the small dimensions having radius r whilst the others have radius R. Again set the brane separation to $Y = \pi R$. We cannot now eliminate both radii from (3.50) using (3.51), and choose to leave the free parameter as the ratio R/r.

There are two cases to consider. First, we suppose that the dimensions wrapped by the brane are of size R, *i.e.* $V_{\mathrm{NN}} = R^{p-3}$. The result is that χ is enhanced by a power of R/r relative to the degenerate case:

$$\chi_{\mathrm{asymm}} = \chi_{\mathrm{degen}} \left(\frac{R}{r}\right)^{\frac{d}{6-p}} \left(\frac{\sqrt{\pi}}{2}\right)^d \frac{\Gamma\left(\frac{1}{2}(7-p-d)\right)}{\Gamma\left(\frac{1}{2}(7-p)\right)}. \tag{3.54}$$

Since $R > r$, this enhancement factor is always greater than one for $p < 6$. Hence, we see that the degenerate case is optimal; the bound on M_s becomes more restrictive as R/r increases. The conclusion that unbroken $U(1)$'s cannot exist on the antibrane then appears unavoidable.

Alternatively, we may take $V_{\mathrm{NN}} = r^{p-3}$, so that the extra dimensions wrapped by the brane are small. This assumption is perhaps more natural given that we want to end up with gauge couplings ~ 1 without having an overly large string coupling.

In this case, we find

$$\chi_{\text{asymm}} = \chi_{\text{degen}} \left(\frac{R}{r}\right)^{\frac{d-(p-3)}{6-p}} \left(\frac{\sqrt{\pi}}{2}\right)^{d} \frac{\Gamma\left(\frac{1}{2}(7-p-d)\right)}{\Gamma\left(\frac{1}{2}(7-p)\right)} . \tag{3.55}$$

The difference with the first case is that we have $d \to d-(p-3)$ in the exponent of R/r. This shows that the small NN directions are working against the small DD directions, which is what one would expect by T-duality. For $p = 3$, things are of course the same as before since $V_{\text{NN}} = 1$. For $p > 3$, it appears possible to suppress the Kinetic Mixing effect by having $d < p-3$. However, R/r must be very large to recover a large string scale. For $p = 4$ and $d = 0$, we need $R/r \sim 10^7$ to give $M_s \lesssim 10^{11}$, for example. For $p = 5$ with $d = 0$ or $d = 1$, χ contains no dependence on M_P or M_s and so experimental data serves only to constrain $R/r \gtrsim 10^6$ or $R/r \gtrsim 10^{12}$ respectively. Even if one accepts these large values of R/r, millicharged particles must be predicted at some level.

3.4 SUSY breaking communication

It is known that, if supersymmetry is a feature of nature, then its breaking is highly restricted if experimental constraints are to be satisfied. The most frequently cited explanation for this that is that supersymmetry breaking occurs at some high scale in a hidden sector and is communicated to the visible sector by some process which both weakens it and gives it the desired form. Intermediate-scale brane models contain hidden antibranes which are present to ensure cancellation of Ramond-Ramond tadpoles. These provide natural candidates for the hidden sector.

Reference [20] showed, in the context the heterotic string, that if we suppose some physics causes a hidden $U(1)_b$ to break with a non-zero D-term VEV, then Kinetic Mixing is a candidate for the mediation process. The result is an additional contribution to supersymmetry breaking mass-squareds in the visible sector of the form

$$m^2_{\text{KM}} = g_a Q_a \chi \langle D_b \rangle . \tag{3.56}$$

Identifying $U(1)_a = U(1)_Y$, this results in extra supersymmetry breaking terms proportional to hypercharge. The authors of [20] also pointed out that it cannot be the only source of mediation, as some of the mass-squareds would have to be negative, and these authors therefore focused on placing an upper limit on χ in order to avoid destabilising the gauge hierarchy (*i.e.* to avoid supersymmetry breaking in the visible sector much larger than 1 TeV). The appropriate limit on χ then depends

on the scale of supersymmetry breaking in the hidden sector which in turn depends on the other sources of mediation (*e.g.* gravity or gauge). The conclusion was that generic models with gravity mediation would have disastrously large Kinetic Mixing if the hidden sector contained additional $U(1)$'s. The relevant bound to avoid destabilising the hierarchy is $\chi \lesssim 10^{-16}$. Such a small coupling constitutes a fine tuning according to the criterion of t'Hooft. In heterotic strings the situation can be ameliorated somewhat because the gauge groups are usually unified into some non-abelian GUT groups. The Kinetic Mixing only arises due to mass splittings once the GUT groups are broken, and one finds typical values of $\chi \sim 10^{-9}$; much less than 1 but still large enough to destabilize the hierarchy.

Let us apply the same considerations to non-supersymmetric D-brane configurations. In intermediate scale models, supersymmetry is usually assumed to be broken by annulus diagrams with no vertex operators: this is supersymmetry breaking in the bulk. In this case, $\mathcal{Z}_{p\bar{p}}$ should be treated as a potential felt by observers on the visible brane due to the presence of the antibrane. The term in an effective Lagrangian with dimensions of mass squared is then $M_s^2(\partial^2 \mathcal{Z}_{p\bar{p}}/\partial Y^2)$, and so supersymmetry breaking terms are of the order

$$m^2_{\not{\text{SUSY}}} \sim M_s^2 \frac{\partial^2 \mathcal{Z}_{p\bar{p}}}{\partial Y^2} \sim M_s^2 \frac{V_{\text{NN}}}{Y^{9-p}} \sim M_s^2 \frac{V_{\text{NN}}}{V_{\text{DD}}} \sim \frac{M_s^4}{M_P^2}\,. \tag{3.57}$$

We have used (3.51) in the last step, and ignored extraneous factors.

However if supersymmetry is broken on the antibrane it will be communicated across to the visible sector by Kinetic Mixing. Let us now suppose that there is a $U(1)_b$ present on the antibrane, and that some physics causes the D-term of this $U(1)$ to acquire a VEV. The scale of supersymmetry breaking is then

$$m^2_{\text{KM}} \sim M_s^2 \chi \tag{3.58}$$

where χ includes just the threshold contributions. For asymmetric dimensions with $V_{\text{NN}} = R^{p-3}$, we find

$$m^2_{\text{KM}} \sim M_s^2 \left(\frac{M_s}{M_P}\right)^{\frac{2(5-p)}{(6-p)}} \left(\frac{R}{r}\right)^{\frac{d}{6-p}}\,. \tag{3.59}$$

The key point is that the usual bulk breaking contribution goes as $1/M_P$, whereas the Kinetic Mixing contribution receives less suppression. Of the two effects then, Kinetic Mixing will always be dominant if it is present (*i.e.* if $\text{Tr}(\lambda_a)\text{Tr}(\lambda_b) \neq 0$).

In that case, requiring $m_{\rm KM} \sim M_W$ gives us

$$M_s \sim M_P \left(\frac{M_W}{M_P}\right)^{\frac{6-p}{11-2p}} \left(\frac{r}{R}\right)^{\frac{d}{2(11-2p)}} . \tag{3.60}$$

We are led to the conclusion that the string scale must be much lower than the usual $M_s \sim 10^{11}\,\text{GeV}$ in order to generate the right sort of visible supersymmetry breaking in the visible sector. For instance, with degenerate extra dimensions and $p = 3$, we find $M_s \sim 10^8\,\text{GeV}$. Including all numerical factors from (3.50, 3.56) raises this by perhaps an order of magnitude, but the general conclusion is the same. In most cases, asymmetric extra dimensions only serve to lower the string scale further. The exception is if the visible sector is a $p > 3$-brane when one might try to circumvent this restriction by identifying $V_{\rm NN} = r^{p-3}$ and demanding a large value of R/r, as discussed above in the context of millicharged particles. In this case, one obtains (3.60), but with $d \to d - (p-3)$. However, R/r must be extremely large to recover $M_s \sim 10^{11}\,\text{GeV}$: for $p = 4$ we need $R/r \gtrsim 10^{20}$, and for $p = 5$, $R/r \gtrsim 10^9$.

One might alternatively assume that some unrelated effect such as gaugino condensation is responsible for supersymmetry breaking, and that Kinetic Mixing must be a sub-dominant contribution in order to avoid destabilising the hierarchy. In that case $M_{\rm KM} < M_W$ is required, and the $\sim$ in equation (3.60) becomes a $\lesssim$, giving an upper bound on the string scale.

3.5 Summary and conclusions

Kinetic Mixing provides an opportunity to constrain non-supersymmetric D-brane configurations (*e.g.* intermediate scale models) using current phenomenological data. We have shown that the effect will occur between the visible branes and hidden antibranes present in the majority of these models, and that it will have observable consequences for low-energy physics. It can be avoided only if the hidden $U(1)$ becomes heavy *without* acquiring a D-term VEV, or if all antibranes present have orthogonal gauge groups on their world volumes (*e.g.* if they are located at orientifold planes). This is a stringent demand on the global configuration.

From experimental limits on millicharged particles, we have shown that in intermediate-scale brane models, one must generally either accept a string scale which is $M_s \lesssim 10^8\,\text{GeV}$, or require that there be no unbroken $U(1)$'s on the antibrane. If we accept a lower string scale or take advantage of the discussion at the end of section 3.3, we then predict millicharged particles at some level. The

consequences are similar with hidden $U(1)$'s which have acquired a D-term VEV. If we are to avoid destabilising the hierarchy, we must either accept $M_s \lesssim 10^8\,\mathrm{GeV}$, or again ensure $\mathrm{Tr}\,(\lambda_a)\,\mathrm{Tr}\,(\lambda_b)$ always vanishes.

The overall conclusion must be that intermediate-scale models – and indeed, any model containing branes and antibranes – are more strongly constrained than was previously thought. It is interesting that a strong upper bound on the string scale is obtained, as this pushes the models in a direction where they are likely to conflict with other constraints due to excessively large instanton or Kaluza-Klein couplings (*e.g.* refs. [50–54]). This upper bound is a result of the large volumes required to dilute the effect of Kinetic Mixing.

Construction of phenomenologically realistic models consistent with the demands of Kinetic Mixing remain an interesting avenue for investigation. Apart from configurations that have antibranes with only orthogonal groups, one possibility which is quite attractive is to set the string scale at $\sim 10^8\,\mathrm{GeV}$ and to use the Kinetic Mixing mediation to generate mass-squared terms in the visible sector that are proportional to hypercharge. This results in a significant amelioration of the so-called flavour problem of supersymmetry in the effective $\mathcal{N} = 1$ model. The problem to be addressed here however would be how to prevent negative mass-squareds. One alternative, to have a second non-anomalous visible sector $U(1)$, does not seem to arise very naturally in the models that have been constructed to date, but may be worth investigating.

Chapter 4

One-loop Yukawas on Intersecting Branes

4.1 Introduction

Open string models based on intersecting D-branes have stimulated new approaches in a number of areas of unification physics. They have also proven to be a useful laboratory for testing ideas initially presented in extra-dimensional field theories, without any of the concomitant renormalizability or finiteness problems.

Chief amongst these, for the purposes of this chapter, are ideas concerning Yukawa couplings and their possible hierarchies. One striking feature of intersecting branes is their natural replication of families at different intersections, which naturally leads to the idea that Yukawa hierarchies have a geometrical origin [55, 56]: small Yukawa couplings can arise if different families are located at different intersections, and the couplings can be exponentially suppressed by world-sheet instantons whose actions are the areas of the 'Yukawa triangles'. This type of picture has its equivalent in closed string orbifold models where the couplings between twisted states at different fixed points are similarly suppressed [57–60]. There has been significant interest in the phenomenological implications of such a set-up and many extra-dimensional ideas (for example, the contribution of Kaluza-Klein states to flavour changing [52]) found their natural realization here. On a more formal level, Yukawa couplings have important applications in understanding brane recombination processes [61].

Going beyond tree-level, there are ideas about Yukawa couplings that have not yet been addressed in a string theory context. One that will concern us here is power law running. Any model with extra dimensions enjoys the possibility of

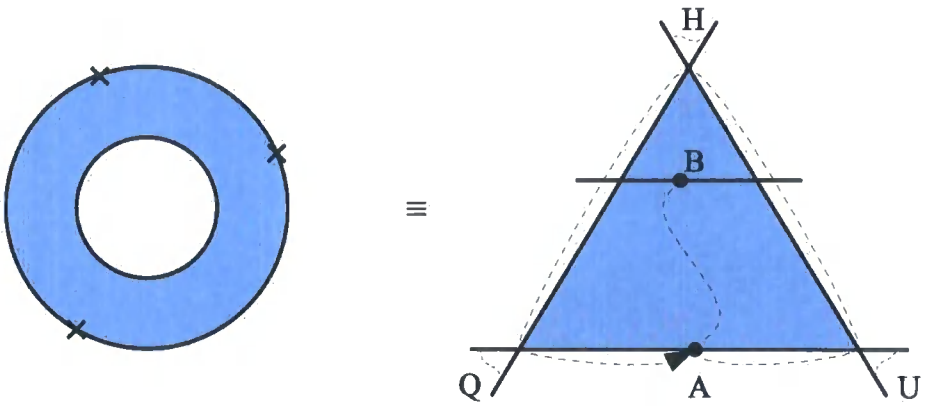

Figure 4.1: The annulus diagram corresponds to taking an open string stretched between two branes as shown, and moving one end around the Yukawa triangle.

greatly accelerated renormalization group running of gauge and Yukawa couplings due to the contribution of Kaluza-Klein states. This effect was originally suggested in the context of large extra dimensions [62–64], based on the ultra-violet cut-off dependence of couplings at one loop in field theory with extra dimensions. It has since been explored for gauge couplings in extra-dimensional field theory (despite its non-renormalizability) by calculating one-loop vacuum polarization diagrams off-shell and computing their energy-scale dependence in various regularization schemes [65, 66]. A genuine energy-scale dependence has been established and agrees (up to subdominant scheme dependent pieces) with the IR-cut-off dependence in various string compactifications [67, 68].

There are a number of reasons why a similarly direct comparison of power law running has not yet been done for the Yukawa couplings, most notably the fact that the tree-level Yukawa couplings are set (at least in the intersecting brane picture) by non-perturbative classical world sheet instantons. There is no easy prescription for inserting these non-perturbative tree-level couplings into one-loop diagrams other than simply truncating to the extra dimensional field theory, which would be begging the question. If we want to derive power law running of Yukawas from intersecting brane configurations, we have to make sure that the *one-loop* classical instantons give the expected factors of *tree-level* Yukawa couplings in the field theory limits of the string diagram. An additional complicating factor is the technical difficulty of calculating the one-loop correlation functions that are required to describe interactions between fields living at intersections.

So, with this aim in mind, we present the calculation of Yukawa couplings at one-

loop on intersecting branes. (A more general motivation for our study is simply that we would like to know how to do perturbation theory at one-loop on intersecting branes, anyway.) Our main focus will be the annulus diagram with no orbifold twists, shown in figures 4.1 and 4.2.

We will for concreteness consider D6 branes (although the techniques can easily be extended to other configurations) intersecting at angles in a factorizable torus $T_2 \times T_2 \times T_2$ whose sub-tori may be tilted and may contain orientifold planes. A general $\mathcal{N} = 1$ set-up will usually involve orbifolds and orientifolds so that there will also be twisted diagrams if the D-branes go through orbifold fixed points, and there will be Möbius strip diagrams as well. All of the techniques we are going to describe can be used for those diagrams as well as the untwisted annulus. However, one can get all the extra information required about these additional diagrams by factorizing on the one-loop partition function, and so it is possible to present results quite generally in terms of the latter. The net effect of the other diagrams is, as one would expect, simply to add new twisted sectors or to project out states in the spectrum. Consequently, we will focus on the untwisted diagram, but our results are easily converted to the twisted case.

The first figure spells out the physical principle of the calculation, discussed in ref. [69]. This is to take a string stretched between two branes as shown and keep one end (B) fixed on a particular brane, whilst the opposing end (A) sweeps out a Yukawa triangle. Quark and Higgs states are deposited at each vertex of the triangle as the endpoint A switches from one brane to the next. The corresponding world-sheet diagram is then the annulus with two fermion and two boson vertex operator insertions on the boundary. There is no constraint on the relative positioning of the B brane (although the usual rule that the action goes as the square of the brane separation will continue to be obeyed), and it may be one of the other three branes (in fact, all renormalization diagrams in the effective field theory will be of this type, and diagrams involving four branes generically separated correspond to string scale masses circulating in the loop).

In the second figure we have mapped the annulus world-sheet to the rectangular domain shown, which has width $\frac{1}{2}$ and height it. The 'branch-cuts' are there to indicate that many correlation functions (for example those involving ∂X) will get a phase as they go round the vertex. This takes account of the change in angle of the allowed motion of the string end-point A as it switches from one brane to another at the intersection. The regions between vertices then correspond to separate branes (with corresponding phases of ∂X), so the region with no branch cut on the left is the *same brane as* (or at least parallel to) the brane on the right. The technology of

mapping a triangle with a hole in it to a fundamental domain such as this is known as Schwarz-Christoffel mapping. It was discussed in ref. [53] for the tree level case, so we will not dwell on it here except to say that we expect the correlation functions to involve products of elliptic functions in the one loop case. Note that it is possible to have branes on the right that are not parallel to any on the left in which case one has branch-cuts up the entire height of the fundamental domain. We will not consider this possibility for reasons that will become clear shortly.

The overriding goal of this calculation will be to show how to recover beta functions for the Yukawa couplings in the field theory limit. We will therefore mainly be interested in the limit of large t (where t is the ratio of the annulus length to its width, and plays the role of the Schwinger time) and in particular the dependence of the results on the IR (large-t) cut-off. In this limit the beta functions are dominated by the various field theory limits in which one or more of the vertices are pinched together. The relevant diagrams for discussing beta functions will be those that factor on a Yukawa coupling times field renormalization diagram. There are four different limiting cases shown in figure 4.2, which we will refer to as limits 0 to 4. Limit 0 is the partition function factorization limit where all the vertices come together, and the string diagram factorizes into the product of a one-loop annulus diagram and the tree-level Yukawa coupling.

Adjacent to the other diagrams are their nearest field theory equivalents. Concentrating on the quantum part of the amplitude for a moment, limit 1 (non-degenerate vertices) is a coupling renormalization diagram and so in supersymmetric theories this 'limit' should give zero. In $\mathcal{N} = 0$ models such diagrams will be non-zero and will represent an actual coupling renormalization. (However, the $t \to 0$ limit would yield UV divergences in these cases due to non-vanishing tadpoles in the closed string channel, indicating a non-trivial background.) One of our tasks therefore will be to show the vanishing of this contribution in supersymmetric configurations due to a ϑ-function identity. This is the stringy version of the non-renormalization theorem. The only opportunity to obtain non-zero contributions is therefore when there is a pole, corresponding to limits 2 and 3.

One diagram that we will not consider is the the one which would be a Yukawa renormalization with three intersection (twisted) fields in the loop. It is this case which corresponds to the diagram with a non-parallel fourth brane and branch-cut all the way up. Calculating them would involve a significant complication, but since they can only be relevant for non-supersymmetric theories anyway, we feel justified in neglecting them.

Our expectations for the classical worldsheet-instanton contributions to the am-

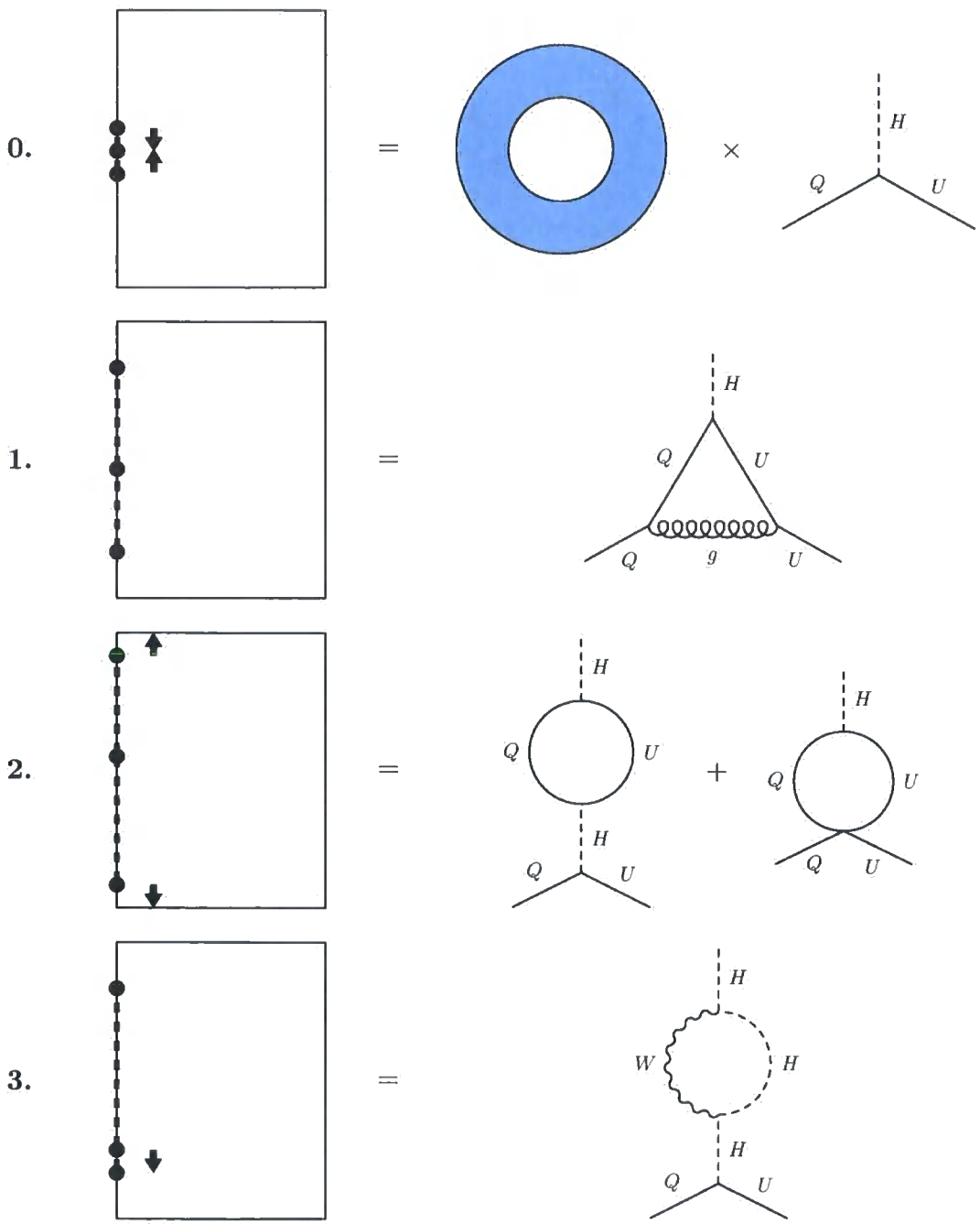

Figure 4.2: Field-theory diagrams from various limits on the worldsheet.

plitudes are based on the quantum part. Field theoretically the closest diagram to limit 1 would be proportional to $\mathcal{Y}g^2$ where $\mathcal{Y}$ is the Yukawa coupling and g the relevant gauge coupling of the gauge field in the loop. The Yukawa coupling at tree level is determined by the worldsheet instanton whose action is simply the sum of the projected triangle areas swept out by the worldsheet in the three sub-tori, $S_{\text{tree}} = \sum_{i=1}^{3} (\text{Area})_i$ (the tree-level Yukawa is proportional to $e^{-S_{\text{tree}}}$). The same sum of triangle areas should appear in the one-loop action in this limit.

Limit 2 gives the field theory diagram corresponding to a Yukawa contribution with a bubble on one of the legs, which has two twisted states running in the loop. We can see this heuristically by noting that the imaginary direction on the annulus represents the loop, and that the branch-cut free part of the annulus is pinched in this limit. These contributions should be proportional to $\mathcal{Y}\mathcal{Y}^\dagger\mathcal{Y}$. This means that the one-loop classical action should yield $S_{\text{one-loop}} = \sum S_{\text{tree}}$ in this limit, where the sum is over Yukawas appearing in the field theory diagram. The diagram should also have a $1/k^2$ pole that requires the k^2 term in the quantum prefactor; this is simply the contribution to the Yukawa beta function coming from field renormalization. As all states are twisted, there should be no Kaluza-Klein (KK) modes in this limit.

Limit 3 gives the field theory diagram with one twisted state and one untwisted (gauge) state in the loop. These contributions should still be proportional to $\mathcal{Y}g^2$. Note that we should get contributions from all the KK modes of the gauge field, generating power-law running of the Yukawa coupling in this limit. This sum over KK contributions comes from a Poisson resummation of the classical action contribution to the amplitude.

The chapter is organized as follows. In the next section we set up the string theory calculation, discussing vertex operators and charge conservation, and extract the general form of the amplitudes in terms of correlators. We then evaluate all necessary correlators, including the spin and twist fields, on the annulus. In section 4.3, we collect the necessary correlators together and discuss the quantum part of the amplitude, elucidating the emergence of the non-renormalization theorem. Section 4.4 is devoted to deriving the classical instanton action via monodromy conditions. Section 4.5 discusses the factorization of the classical part onto the various limits discussed above, while section 4.6 discusses the extraction of the beta functions and power law running.

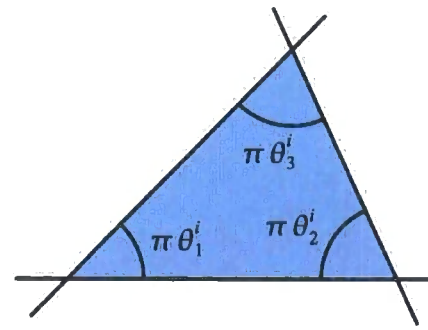

Figure 4.3: We work with internal angles, and always stick to the notation where subscripts on angles label intersections, and superscripts label tori.

4.2 Elements of the calculation

Before we begin, it is perhaps worthwhile to give a brief review of background literature. The supersymmetric non-renormalization theorem has been demonstrated explicitly for a $\mathbb{Z}_3$ orbifold using only untwisted states [70], and more general rules have also been derived for other $D = 4$ models [71]. Also, an extraction of the β-function for gauge fields was performed for supersymmetric orbifolds [72].

Key elements in our calculation will be the conservation of the H-charge of bosonized states, correlation functions of spin operators and correlation functions of twist operators. H-charge conservation and consequent selection rules are discussed for orbifold models in [73–79]. Spin field operators for closed strings at one loop have been given explicitly for flat backgrounds [80–82], and implicitly for orbifold backgrounds [83]; we give an explicit result and generalize to open strings in section 4.2.4. Similarly, twist field correlators are known at one loop for closed strings [84], which we generalize to open strings in section 4.2.6. We also examine correlation functions of excited twist operators at one loop, which have been discussed for the orbifold case in [16, 85, 86].

We will work with type IIA theory compactified on a factorizable T^6, with D6-branes at angles wrapping in the compact space. In each sub-torus, the intersection of the branes makes a triangle. The rotations which take us from one brane to another are taken as shown: hence, $\theta_1^i + \theta_2^i + \theta_3^i = 1$ in each sub-torus. Unless displayed explicitly, we set $\alpha' = \frac{1}{2}$.

4.2.1 Vertex operators and H-charge

At any given intersection, an analysis of the mode expansions of strings stretched between the branes [87] tells us that we obtain from the R sector a massless fermion. Introducing a set H_i of bosonic fields on the worldsheet, where i labels pairs of complex dimensions, the most canonical vertex operator for this state is [15, 50, 88]

$$\mathcal{V}_{-\frac{1}{2}}(u,k,z) = \mathrm{e}^{-\frac{1}{2}\phi} u S^{\pm} \mathrm{e}^{\mathrm{i}k\cdot X} \mathrm{e}^{\mathrm{i}q\cdot H} \Sigma(z) \quad \text{with} \quad q = \left(\tfrac{1}{2}-\theta^1, \tfrac{1}{2}-\theta^2, \tfrac{1}{2}-\theta^3\right), \tag{4.1}$$

where u is the four-dimensional polarization, $S^{\pm} = \mathrm{e}^{\pm\frac{1}{2}\mathrm{i}(H_1+H_2)}$ is a four-dimensional spin field, $\mathrm{e}^{\mathrm{i}q\cdot H}$ is the spin field for the internal co-ordinates, and $\Sigma = \sigma^1\sigma^2\sigma^3$ are bosonic twist fields [16, 17]. Our convention for angles means that the operators σ correspond to 'anti-twist' fields, sometimes denoted σ_- or $\sigma_{1-\theta}$ in the literature. The plane wave portion of the vertex operators, $\mathrm{e}^{\mathrm{i}k\cdot X}$, is present only in the non-compact space – k^μ is a four-vector. We have suppressed factors of the string coupling g_O and Chan-Paton factors in this expression, and will do so throughout the rest of this work.

A vertex operator of the opposite chirality may also be created, representing strings stretched with the opposite orientation, but as our final result ought to be comparable to a quark Yukawa term, in which both fermions have the same chirality, we will not need it.

In the NS sector, the scalars surviving the GSO projection are generally massive [87]: see table 4.1. With a suitable choice of angles, we may make any one (but only one) of these states massless, in which case it becomes the $\mathcal{N}=1$ superpartner of the massless fermion in the R sector. The other three states are then massive, and so must be superpartners of other heavy fermions. It may appear strange that we have a choice of four NS-sector vertex operators but only one R-sector vertex operator. In fact, up to chirality, there are *four* choices which could have been made for (4.1), the other three being obtained by flipping the sign of the $\frac{1}{2}$ in any pair of sub-tori.

For the choice shown in 4.1, we may identify the Higgs from factorization of the tree level four-point function [53] as the state $\psi_{\frac{1}{2}-\theta^1}\psi_{\frac{1}{2}-\theta^2}\psi_{\frac{1}{2}-\theta^3}|0\rangle$. The $\mathcal{N}=1$ supersymmetry condition on our set-up is then

$$\theta^1 + \theta^2 + \theta^3 = 1\,, \tag{4.2}$$

State	q	m^2
$\psi_{\frac{1}{2}-\theta^1}\|0\rangle$	$(-\theta^1, 1-\theta^2, 1-\theta^3)$	$\theta^1-\theta^2-\theta^3+1$
$\psi_{\frac{1}{2}-\theta^2}\|0\rangle$	$(1-\theta^1, -\theta^2, 1-\theta^3)$	$-\theta^1+\theta^2-\theta^3+1$
$\psi_{\frac{1}{2}-\theta^3}\|0\rangle$	$(1-\theta^1, 1-\theta^2, -\theta^3)$	$-\theta^1-\theta^2+\theta^3+1$
$\psi_{\frac{1}{2}-\theta^1}\psi_{\frac{1}{2}-\theta^2}\psi_{\frac{1}{2}-\theta^3}\|0\rangle$	$(-\theta^1, -\theta^2, -\theta^3)$	$\theta^1+\theta^2+\theta^3-1$

Table 4.1: NS-sector states for strings localized at the intersection of two D6-branes.

and the most canonical vertex operator for the Higgs is

$$\mathcal{V}_{-1}(k,z) = \mathrm{e}^{-\phi}\mathrm{e}^{\mathrm{i}k\cdot X}\mathrm{e}^{\mathrm{i}q\cdot H}\Sigma(z) \quad \text{with} \quad q = \left(-\theta^1, -\theta^2, -\theta^3\right) . \tag{4.3}$$

One may verify that (4.3) correctly has unit conformal weight, provided that $k^2 = -m^2$.

Another way to see that that we have identified the correct state as the Higgs is to note that since the H are a set of free bosonic fields, non-vanishing terms in $\mathcal{A}$ must obey H-charge (momentum) conservation:

$$\sum_{i=1}^{3} q_i^j = 0 \tag{4.4}$$

in each complex dimension j. If we were interested in calculating the *tree-level* Yukawa coupling,

$$\mathcal{Y} = \left\langle \mathcal{V}_{-\frac{1}{2}}\mathcal{V}_{-\frac{1}{2}}\mathcal{V}_{-1} \right\rangle , \tag{4.5}$$

we would see that H-charge conservation is correctly obeyed by the vertex operators given: in an external dimension, $\pm\frac{1}{2} \mp \frac{1}{2} = 0$, and in an internal dimension $\frac{1}{2} - \theta_1 + \frac{1}{2} - \theta_2 - \theta_3 = 0$.

Using the simple tool of H-charge conservation, the reader may verify that choices for the quantum numbers of the fermion vertex operator other than those displayed in (4.1) will lead to the Higgs being identifed as one of the other three NS-sector states in the table; the $\mathcal{N} = 1$ supersymmetry condition on the angles will then be that which makes the appropriate state massless. For concreteness, we will stick to the choices (4.1) and (4.3).

4.2.2 One-loop amplitudes and picture-changing

On the annulus, the appropriate string scattering amplitude is given by finding the correlation function of two fermions plus one boson, then integrating over all possible configurations of vertex operators plus the modular parameter t of the annulus:

$$\mathcal{A} = \int_0^\infty \frac{\mathrm{d}t}{t} f(t) \int \mathrm{d}z_1 \mathrm{d}z_2 \mathrm{d}z_3 \; A(z_1, z_2, z_3) \; . \tag{4.6}$$

$f(t)$ is an overall normalization which will be determined later by coalescing the three vertex operators (limit 0 of figure 4.2). For now, we focus on the computation of A.

At tree-level, the amplitude (4.5) has an overall ϕ-charge of $-\frac{1}{2}-\frac{1}{2}-1=-2$. On the annulus, $\mathcal{A}$ must have an overall ϕ-charge of zero if it is to be non-anomalous, and we have to perform 'picture-changing' operations [89] on our vertex operators:

$$\mathcal{V}_{i+1}(z) = \lim_{w \to z} \mathrm{e}^{\phi} T_F(w) \, \mathcal{V}_i(z) \; . \tag{4.7}$$

Here, T_F is the generator of worldsheet supersymmetry,

$$T_F = \frac{1}{2}(\partial \overline{X}^i \psi_i + \partial X^i \overline{\psi}_i) \, , \tag{4.8}$$

with $\psi \sim \mathrm{e}^{\mathrm{i}H}$ and $\overline{\psi} \sim \mathrm{e}^{-\mathrm{i}H}$ bosonized fermions in each complex pair of dimensions,

$$X^i = X^{\mu=2i} + \mathrm{i}X^{\mu=2i+1} \qquad \overline{X}^i = X^{\mu=2i} - \mathrm{i}X^{\mu=2i+1} \, . \tag{4.9}$$

To obtain the correct ϕ-charge, we need to insert two picture-changing operators somewhere in our amplitude. It will be convenient to apply one operator to one of the fermions, and one to the boson, so that the relevant correlation function is

$$\mathcal{A} = \left\langle \mathcal{V}_{-\frac{1}{2}}(\overline{u}_1, k_1, z_1) \lim_{w_2 \to z_2} \mathrm{e}^{\phi} T_F(w_2) \, \mathcal{V}_{-\frac{1}{2}}(u_2, k_2, z_2) \lim_{w_3 \to z_3} \mathrm{e}^{\phi} T_F(w_3) \, \mathcal{V}_{-1}(u_3, k_3, z_3) \right\rangle \, . \tag{4.10}$$

Our picture-changing operators must be inserted in such a way as not to affect the overall H-charge, meaning that for each complex dimension, we should make one $\partial \overline{X} \psi$ and one $\partial X \overline{\psi}$ insertion. In other words, only terms of the form

$$\mathcal{V}_{-\frac{1}{2}}(z_1) \, \partial \overline{X}^i \psi^i(w_2) \, \mathcal{V}_{-\frac{1}{2}}(z_2) \, \partial X^i \overline{\psi}^i(w_3) \, \mathcal{V}_{-1}(z_3) \tag{4.11}$$

and

$$\mathcal{V}_{-\frac{1}{2}}(z_1)\,\partial X^i\overline{\psi}^i(w_2)\,\mathcal{V}_{-\frac{1}{2}}(z_2)\,\partial\overline{X}^i\psi^i(w_3)\,\mathcal{V}_{-1}(z_3) \tag{4.12}$$

may contribute to A (no summation over i is implied).

We may see explicitly the effect of the picture-changing operators on the vertex operators (4.1) and (4.3) by using the OPEs

$$\begin{aligned}
e^{iaH}(w)\,e^{ibH}(z) &\sim (w-z)^{ab}\,e^{i(a+b)H}(z)\\
\partial X(w)\,e^{ik\cdot X}(z) &\sim \frac{ik}{w-z}e^{ik\cdot X}(z)\\
\partial\overline{X}(w)\,e^{ik\cdot X}(z) &\sim \frac{i\overline{k}}{w-z}e^{ik\cdot X}(z)\,,
\end{aligned} \tag{4.13}$$

where k^i is defined in exactly the same way as X^i, so that $k\cdot X=\frac{1}{2}\left(k^i\overline{X}^i+\overline{k}^iX^i\right)$, and

$$\begin{aligned}
\partial X(w)\,\sigma(z) &\sim (w-z)^{-\theta}\,\tau(z)\\
\partial\overline{X}(w)\,\sigma(z) &\sim (w-z)^{-(1-\theta)}\,\tau'(z)\,,
\end{aligned} \tag{4.14}$$

with τ and τ' excited twist fields[1].

Since the vertex operators are segregated into operators which act only in the internal dimensions ($S^{\pm}$, $e^{ik\cdot X}$) and operators which act only in the external dimensions ($e^{iq\cdot H}$, Σ), we need to treat internal and external indices differently. Beginning with the case where i is an internal index, we have for the fermion,

$$\begin{aligned}
\frac{1}{2}\lim_{w\to z}e^{\phi}\partial\overline{X}^i\psi^i(w)\,\mathcal{V}_{-\frac{1}{2}}(z) &= \frac{1}{2}e^{\frac{1}{2}\phi}uS^{\pm}e^{ik\cdot X}e^{i\tilde{q}\cdot H}\tau'^i\sigma^j\sigma^k(z) \quad \text{with} \quad \tilde{q}^i=\tfrac{3}{2}-\theta^i\\
\frac{1}{2}\lim_{w\to z}e^{\phi}\partial X^i\overline{\psi}^i(w)\,\mathcal{V}_{-\frac{1}{2}}(z) &= \frac{1}{2}e^{\frac{1}{2}\phi}uS^{\pm}e^{ik\cdot X}e^{i\tilde{q}\cdot H}\tau^i\sigma^j\sigma^k(z) \quad \text{with} \quad \tilde{q}^i=-\tfrac{1}{2}-\theta^i\,,
\end{aligned} \tag{4.15}$$

again with no summation implied over i.

For the boson,

$$\begin{aligned}
\frac{1}{2}\lim_{w\to z}e^{\phi}\partial\overline{X}^i\psi^i(w)\,\mathcal{V}_{-1}(z) &= \frac{1}{2}e^{ik\cdot X}e^{i\tilde{q}\cdot H}\tau'^i\sigma^j\sigma^k(z) \quad \text{with} \quad \tilde{q}^i=1-\theta^i\\
\frac{1}{2}\lim_{w\to z}e^{\phi}\partial X^i\overline{\psi}^i(w)\,\mathcal{V}_{-1}(z) &= 0\,.
\end{aligned} \tag{4.16}$$

Therefore, the internal dimensions contribute only to $\mathcal{A}$ via terms of the form (4.12).

[1] We have made the replacement $\theta\to 1-\theta$ with respect to the usual definition of these OPEs, reflecting the fact that we work with internal angles as shown in figure 4.3.

Sub-torus / H-charge	i	j	k
q_1	$\frac{1}{2}-\theta_1^i$	$\frac{1}{2}-\theta_1^j$	$\frac{1}{2}-\theta_1^k$
$\tilde{q}_2$	$-\frac{1}{2}-\theta_2^i$	$\frac{1}{2}-\theta_2^j$	$\frac{1}{2}-\theta_2^k$
$\tilde{q}_3$	$1-\theta_3^i$	$-\theta_3^j$	$-\theta_3^k$

Table 4.2: H-charge assignments in the contribution $\mathcal{A}_1$. The sum in each column is zero, preserving charge conservation in each sub-torus.

We label these contributions as A_1:

$$A_1 = \frac{1}{4}\overline{u}_1 u_2 \left\langle \mathrm{e}^{-\frac{1}{2}\phi}(z_1)\,\mathrm{e}^{\frac{1}{2}\phi}(z_2)\right\rangle \left\langle S^{\mp}(z_1)\,S^{\pm}(z_2)\right\rangle \left\langle \mathrm{e}^{\mathrm{i}k_1\cdot X}(z_1)\,\mathrm{e}^{\mathrm{i}k_2\cdot X}(z_2)\,\mathrm{e}^{\mathrm{i}k_3\cdot X}(z_3)\right\rangle$$
$$\sum_{i\neq j\neq k} \left\langle \mathrm{e}^{\mathrm{i}q_1\cdot H(z_1)}\mathrm{e}^{\mathrm{i}\tilde{q}_2\cdot H(z_2)}\mathrm{e}^{\mathrm{i}\tilde{q}_3\cdot H(z_3)}\right\rangle \left\langle \sigma^i(z_1)\tau^i(z_2)\tau'^i(z_3)\right\rangle \left\langle \sigma^j(z_1)\sigma^j(z_2)\sigma^j(z_3)\right\rangle$$
$$\left\langle \sigma^k(z_1)\sigma^k(z_2)\sigma^k(z_3)\right\rangle . \quad (4.17)$$

The arrangement of picture-changed H-charge in the spin operators here is displayed explicitly in table 4.2.

Now consider the case when i is an external index. There are two different possibilities for the result of the picture-changing operation on the fermion operator $\mathcal{V}_{-\frac{1}{2}}$, depending upon whether it contains an $S^+ = \mathrm{e}^{+\frac{1}{2}\mathrm{i}(H_1+H_2)}$ or an $S^- = \mathrm{e}^{-\frac{1}{2}\mathrm{i}(H_1+H_2)}$ operator. If $\mathcal{V}_{-\frac{1}{2}}$ contains an S^+, then we have

$$\frac{1}{2}\lim_{w\to z}\mathrm{e}^{\phi}\partial\overline{X}^i\psi^i(w)\,\mathcal{V}_{-\frac{1}{2}}(z) = \frac{1}{2}\mathrm{i}k^i\mathrm{e}^{\frac{1}{2}\phi}\mathrm{e}^{\mathrm{i}k\cdot X}S_{\uparrow}^{+}\mathrm{e}^{\mathrm{i}q\cdot H}\Sigma(z)$$
$$\frac{1}{2}\lim_{w\to z}\mathrm{e}^{\phi}\partial X^i\overline{\psi}^i(w)\,\mathcal{V}_{-\frac{1}{2}}(z) = \frac{1}{2}\partial X^i\mathrm{e}^{\frac{1}{2}\phi}\mathrm{e}^{\mathrm{i}k\cdot X}S_{\downarrow}^{+}\mathrm{e}^{\mathrm{i}q\cdot H}\Sigma(z) + \text{singular term} \quad (4.18)$$

where

$$S_{\uparrow}^{+} = \mathrm{e}^{\mathrm{i}\left(\frac{3}{2}H_i+\frac{1}{2}H_j\right)} \qquad \text{and} \qquad S_{\downarrow}^{+} = \mathrm{e}^{\mathrm{i}\left(-\frac{1}{2}H_i+\frac{1}{2}H_j\right)}. \quad (4.19)$$

The singular term will vanish via the Dirac equation, just as it does in the picture-changing of $\mathcal{V}_{-\frac{1}{2}}$ when no branes are present [89,90]; this vanishing has been obscured by the 'helicity basis' used to represent the spin operators.

If $\mathcal{V}_{-\frac{1}{2}}$ contains an S^- operator,

$$\begin{aligned}\frac{1}{2}\lim_{w\to z} e^{\phi}\partial\overline{X}^i\psi^i(w)\,\mathcal{V}_{-\frac{1}{2}}(z) &= \frac{1}{2}\partial\overline{X}^i e^{\frac{1}{2}\phi}e^{ik\cdot X}S_{\uparrow}^- e^{iq\cdot H}\Sigma(z) + \text{singular term}\\ \frac{1}{2}\lim_{w\to z} e^{\phi}\partial X^i\overline{\psi}^i(w)\,\mathcal{V}_{-\frac{1}{2}}(z) &= \frac{1}{2}ik^i e^{\frac{1}{2}\phi}e^{ik\cdot X}S_{\downarrow}^- e^{iq\cdot H}\Sigma(z)\end{aligned} \tag{4.20}$$

where

$$S_{\uparrow}^- = e^{i\left(\frac{1}{2}H_i-\frac{1}{2}H_j\right)} \qquad \text{and} \qquad S_{\downarrow}^- = e^{i\left(-\frac{3}{2}H_i-\frac{1}{2}H_j\right)}. \tag{4.21}$$

For the boson,

$$\begin{aligned}\lim_{w\to z} e^{\phi}\partial\overline{X}^i\psi^i(w)\,\mathcal{V}_{-1}(z) &= \frac{1}{2}i\overline{k}^i\psi^i e^{ik\cdot X}e^{iq\cdot H}\Sigma(z)\\ \lim_{w\to z} e^{\phi}\partial X^i\overline{\psi}^i(w)\,\mathcal{V}_{-1}(z) &= \frac{1}{2}ik^i\overline{\psi}^i e^{ik\cdot X}e^{iq\cdot H}\Sigma(z)\,.\end{aligned} \tag{4.22}$$

Since we should consider both possibilities for the boson, there are four possible terms from picture-changing the external dimensions: two from the H-charge conserving combinations of (4.18) and (4.22), and two from the H-charge conserving combinations of (4.20) and (4.22). The terms naturally group into two pairs:

$$\begin{aligned}A_2^+ = \frac{1}{4}\overline{u}_1 u_2\mathcal{I}\left\langle e^{-\frac{1}{2}\phi}(z_1)\,e^{\frac{1}{2}\phi}(z_2)\right\rangle \sum_{i\neq j}^{2} i\overline{k}_3^i\left\langle e^{ik_1\cdot X}(z_1)\,\partial X^i e^{ik_2\cdot X}(z_2)\,e^{ik_3\cdot X}(z_3)\right\rangle\\ \left\langle e^{-\frac{1}{2}iH_i}(z_1)\,e^{-\frac{1}{2}iH_i}(z_2)\,e^{iH_i}(z_3)\right\rangle\left\langle e^{-\frac{1}{2}iH_j}(z_1)\,e^{\frac{1}{2}iH_j}(z_2)\right\rangle\end{aligned} \tag{4.23}$$

$$\begin{aligned}A_2^- = \frac{1}{4}\overline{u}_1 u_2\mathcal{I}\left\langle e^{-\frac{1}{2}\phi}(z_1)\,e^{\frac{1}{2}\phi}(z_2)\right\rangle \sum_{i\neq j}^{2} ik_3^i\left\langle e^{ik_1\cdot X}(z_1)\,\partial X^i e^{ik_2\cdot X}(z_2)\,e^{ik_3\cdot X}(z_3)\right\rangle\\ \left\langle e^{\frac{1}{2}iH_i}(z_1)\,e^{\frac{1}{2}iH_i}(z_2)\,e^{-iH_i}(z_3)\right\rangle\left\langle e^{\frac{1}{2}iH_j}(z_1)\,e^{-\frac{1}{2}iH_j}(z_2)\right\rangle,\end{aligned} \tag{4.24}$$

and

$$\begin{aligned}A_3^+ = -\frac{1}{4}\overline{u}_1 u_2\mathcal{I}\left\langle e^{-\frac{1}{2}\phi}(z_1)\,e^{\frac{1}{2}\phi}(z_2)\right\rangle\left\langle e^{ik_1\cdot X}(z_1)\,e^{ik_2\cdot X}(z_2)\,e^{ik_3\cdot X}(z_3)\right\rangle\\ \sum_{i\neq j}^{2} k_2^i\overline{k}_3^i\left\langle e^{-\frac{1}{2}iH_i}(z_1)\,e^{\frac{3}{2}iH_i}(z_2)\,e^{-iH_i}(z_3)\right\rangle\left\langle e^{-\frac{1}{2}iH_j}(z_1)\,e^{\frac{1}{2}iH_j}(z_2)\right\rangle\end{aligned} \tag{4.25}$$

$$A_3^- = -\frac{1}{4}\bar{u}_1 u_2 \mathcal{I} \left\langle e^{-\frac{1}{2}\phi}(z_1)\, e^{\frac{1}{2}\phi}(z_2)\right\rangle \left\langle e^{ik_1\cdot X}(z_1)\, e^{ik_2\cdot X}(z_2)\, e^{ik_3\cdot X}(z_3)\right\rangle$$
$$\sum_{i\neq j}^{2} \bar{k}_2^i k_3^i \left\langle e^{\frac{1}{2}iH_i}(z_1)\, e^{-\frac{3}{2}iH_i}(z_2)\, e^{iH_i}(z_3)\right\rangle \left\langle e^{\frac{1}{2}iH_j}(z_1)\, e^{-\frac{1}{2}iH_j}(z_2)\right\rangle , \quad (4.26)$$

where the contribution from the internal dimensions is

$$\mathcal{I} = \left\langle e^{iq_1\cdot H}(z_1)\, e^{iq_2\cdot H}(z_2)\, e^{iq_3\cdot H}(z_3)\right\rangle \left\langle \Sigma_1(z_1)\, \Sigma_2(z_2)\, \Sigma_3(z_3)\right\rangle . \quad (4.27)$$

So, overall, we have five different terms contributing to A. Heuristically, the difference between them is that A_1 contains excited twist operators but contains no kinematic factors, whereas the $A_2^\pm$ and $A_3^\pm$ terms contain only ordinary twist operators but have kinematic factors in front of them. These kinematic factors will generally cause the $A_2^\pm$ and $A_3^\pm$ terms to be suppressed relative to the A_1 contribution, unless we bring two of the vertex operators close together. Therefore, it seems appropriate to identify the term A_1 with limit 1 in figure 4.2, and $A_2^\pm$, $A_3^\pm$ with the other cases [70]. When we compute these terms explicitly, we will see that this identification is indeed correct; first, however, we must find explicit expressions for the correlation functions in A_1, A_2 and A_3. The discussion is somewhat technical, so for reference we have collected the results at the beginning of the section 4.3, where we start to build the amplitudes.

4.2.3 Bosonic fields

Just as in chapter 3, the correlators involving the fields X^μ may be found from those on the torus via the method of images. This time, we avoid spurious factors of 2π by defining the annulus as the rectangular region of the complex plane $x \in \left[0, \frac{1}{2}\right]$, $y \in [0, t]$, and write (3.31) as

$$\langle X(z_1)\, X(z_2)\rangle = -\frac{1}{2}\left|\log \vartheta_1(z_2 - z_1|it)\right| + \frac{\pi\left[\mathrm{Im}(z_2 - z_1)\right]^2}{2t}$$
$$-\frac{1}{2}\left|\log \vartheta_1(z_2 + \bar{z}_1|it)\right| + \frac{\pi\left[\mathrm{Im}(z_2 + \bar{z}_1)\right]^2}{2t} + r(t) , \quad (4.28)$$

absorbing the various factors which regulate the propagator as $z_1 \to z_2$ into the function $r(t)$. All of our fields are on the same end of the annulus, so we can set $z_1 = iy_1$, $z_2 = iy_2$ with $y_1, y_2 \in [0, t]$. Then, since the theta functions are real for

purely imaginary arguments,

$$\langle X(y_1)\, X(y_2)\rangle = -\log\vartheta_1(\mathrm{i}y_{12}) + \frac{\pi y_{ij}^2}{t}\,, \tag{4.29}$$

with the notation $y_{ij} = |y_j - y_i|$. For brevity, we have suppressed the explicit t-dependence in ϑ_1. We have also left out the function $r(t)$; it will not become important until we begin to care about the t-dependence of A in section 4.6, and we will deal with it then.

With this simplification, the $\mathrm{e}^{\mathrm{i}k\cdot X}$ correlations in A are

$$\left\langle \prod_i \mathrm{e}^{\mathrm{i}k_i\cdot X}(y_i)\right\rangle = \prod_{i<j}\left[\vartheta_1(\mathrm{i}y_{ij})\,\mathrm{e}^{-\pi y_{ij}^2/t}\right]^{k_i\cdot k_j}\,, \tag{4.30}$$

while including one factor of ∂X^μ pulls down kinematic factors (c.f. eq. B.7):

$$\left\langle \partial X^\mu(y_k)\prod_i \mathrm{e}^{\mathrm{i}k_i\cdot X}(y_i)\right\rangle = \prod_{\substack{i<j\\ i\neq k}} \mathrm{i}k_j^\mu\left[\frac{\theta_1'(\mathrm{i}y_{jk})}{\theta_1(\mathrm{i}y_{jk})} - \frac{2\pi y_{jk}}{t}\right]\left[\vartheta_1(\mathrm{i}y_{ij})\,\mathrm{e}^{-\pi y_{ij}^2/t}\right]^{k_i\cdot k_j}\,. \tag{4.31}$$

4.2.4 Spin fields

The correlators between the the fermion spin fields $\mathrm{e}^{\mathrm{i}q\cdot H}$ are more difficult to compute. The problem is that we must respect spin structures on the underlying torus, which prevents us from dealing with the H fields in the same way as the X fields. We may resolve the issue by using the stress-tensor method [16], generalising the results of ref. [82].

As above, we first perform the calculation on a torus, and then specialize the result to the annulus. Begin by bosonizing the holomorphic fermions,

$$\psi(z) = \mathrm{e}^{\mathrm{i}H(z)} \qquad \overline{\psi}(z) = \mathrm{e}^{-\mathrm{i}H(z)}\,, \tag{4.32}$$

and defining holomorphic spin operators,

$$\mathcal{S}_a(z) = \mathrm{e}^{\mathrm{i}aH(z)}\,. \tag{4.33}$$

From (4.13), we see the the OPEs between fermions and spin fields take the form

$$\begin{aligned}
\psi(z)\,\overline{\psi}(w) &\sim (z-w)^{-1} \\
\psi(z)\,\mathcal{S}_a(w) &\sim (z-w)^{a}\,\mathcal{S}_{a+1}(w) \\
\overline{\psi}(z)\,\mathcal{S}_a(w) &\sim (z-w)^{-a}\,\mathcal{S}_{a-1}(w) \\
\mathcal{S}_a(z)\,\mathcal{S}_b(w) &\sim (z-w)^{ab}\,\mathcal{S}_{a+b}(w)\ .
\end{aligned} \tag{4.34}$$

We will work out the correlation between an arbitrary number of spin fields, since it is no more complicated than that between three such fields. Define an auxiliary Green's function as

$$g(z,w;z_i) = \frac{\left\langle \overline{\psi}(z)\,\psi(w)\prod_i S_{a_i}(z_i)\right\rangle}{\left\langle \prod_i S_{a_i}(z_i)\right\rangle}\ . \tag{4.35}$$

The OPEs (4.34) show that this function must satisfy

$$\begin{aligned}
g(z,w;z_i) &= (z-w)^{-1} + \text{finite as } z \to w \\
g(z,w;z_i) &\propto (z-w)^{-a_i} + \text{finite as } z \to z_i \\
g(z,w;z_i) &\propto (z-w)^{a_i} + \text{finite as } w \to z_i.
\end{aligned} \tag{4.36}$$

Furthermore, it must be periodic on the torus as a function of z and w. A suitable function satisfying these conditions is

$$g(z,w;z_i) = \frac{\vartheta_1'(0)}{\vartheta_1(z-w)}\frac{\vartheta_{\alpha\beta}(z-w+\sum a_i z_i)}{\vartheta_{\alpha\beta}(\sum a_i z_i)}\prod_i\left(\frac{\vartheta_1(w-z_i)}{\vartheta_1(z-z_i)}\right)^{a_i}\ , \tag{4.37}$$

where $(\alpha\beta) = (00)\ldots(11)$ label the four possible spin structures on the torus. The reason for the specific form of the term $\sum_{i=1}^{n} a_i z_i$ in the argument of $\vartheta_{\alpha\beta}$ will become clear shortly; for the moment we press on.

The stress-energy tensor for the ψ, $\overline{\psi}$ CFT may be written as

$$T(z) = \lim_{z\to w}\left[\frac{1}{2}\partial_z\overline{\psi}(z)\,\psi(w) - \frac{1}{2}\overline{\psi}(z)\,\partial_w\psi(w) + \frac{1}{(z-w)^2}\right]\ , \tag{4.38}$$

and so using the definition (4.35), we may form the function

$$\frac{\left\langle T(z)\prod_i S_{a_i}(z_i)\right\rangle}{\left\langle \prod_i S_{a_i}(z_i)\right\rangle} = \lim_{z\to w}\left[\frac{1}{2}\partial_z g(z,w;z_i) - \frac{1}{2}\partial_w g(z,w;z_i) + \frac{1}{(z-w)^2}\right]\ . \tag{4.39}$$

Using $\lim_{z\to 0}\vartheta_1(z) = \vartheta_1'(0)\,z$, and derivatives thereof, one finds

$$\frac{\langle T(z)\prod_i S_{a_i}(z_i)\rangle}{\langle\prod_i S_{a_i}(z_i)\rangle} = \frac{1}{2}\left[\sum_{i=1}^{n} a_i \frac{\vartheta_1'(z-z_i)}{\vartheta_1(z-z_i)}\right]^2 - \left[\sum_{i=1}^{n} a_i \frac{\vartheta_1'(z-z_i)}{\vartheta_1(z-z_i)}\right] \frac{\vartheta'_{\alpha\beta}(\sum_i a_i z_i)}{\vartheta_{\alpha\beta}(\sum_i a_i z_i)}\,.$$

The next step is to take the limit $z \to z_j$ on both sides. In this limit, the right-hand side may be evaluated directly, whilst the left-hand side is simplified by the fact that the OPE of any tensor operator with the stress-energy tensor takes the prescribed form

$$T(z)\,\mathcal{S}_{a_j}(z_j) \sim \frac{h}{(z-z_j)^2}\mathcal{S}_{a_j}(z_j) + \frac{1}{z-z_j}\partial_{z_j}\mathcal{S}_{a_j}(z_j)\,, \tag{4.40}$$

with h the conformal weight of the field $\mathcal{S}_{a_j}(z)$. The result is

$$\begin{aligned}\lim_{z\to z_j}&\left\{\frac{h}{(z-z_j)^2} + \frac{1}{z-z_j}\partial_{z_j}\log\left\langle\prod_i \mathcal{S}_{a_i}(z_i)\right\rangle\right\} \\ &= \lim_{z\to z_j}\left\{\frac{\frac{1}{2}a_j^2}{(z-z_j)^2} + \frac{a_j}{z-z_j}\left[\left(\sum_{i\neq j} a_i\frac{\vartheta_1'(z-z_i)}{\vartheta_1(z-z_i)}\right) - \frac{\vartheta'_{\alpha\beta}(\sum_i a_i z_i)}{\vartheta_{\alpha\beta}(\sum_i a_i z_i)}\right]\right\}\,. \end{aligned}\tag{4.41}$$

Comparing coefficients in $(z-z_j)$ shows that $\mathcal{S}_{a_j}(z)$ correctly has conformal weight $\frac{1}{2}a_j^2$, and that

$$\partial_{z_j}\log\left\langle\prod_i \mathcal{S}_{a_i}(z_i)\right\rangle = a_j\left[\left(\sum_{i\neq j} a_i\frac{\vartheta_1'(z-z_i)}{\vartheta_1(z-z_i)}\right) - \frac{\vartheta'_{\alpha\beta}(\sum_i a_i z_i)}{\vartheta_{\alpha\beta}(\sum_i a_i z_i)}\right]\,, \tag{4.42}$$

with solution

$$\left\langle\prod_i \mathcal{S}_{a_i}(z_i)\right\rangle = K_{\alpha\beta}\left[\prod_{i<j}\vartheta_1(z_i-z_j)^{a_i a_j}\right]\vartheta_{\alpha\beta}\left(\sum_i a_i z_i\right) \tag{4.43}$$

where $K_{\alpha\beta}$ is an overall normalization.

The reason for the argument of $\vartheta_{\alpha\beta}$ in (4.37) to take the form it does is now revealed: when $a_i = \pm\frac{1}{2}$, the three translations $z_i \to z_i+1$, $z_i \to z_i+\tau$ and $z_i \to z_i+1+\tau$ transform a given theta function $\vartheta_{\alpha\beta}$ into the other three theta functions. Under the same translations, the correlator (4.43) for a given spin structure transforms into the correlator for one of the other spin structures (up to a phase), just as it should. For the internal spin fields, on the other hand, translational invariance implies $\sum_i a_i = 0$, which is just the H-charge conservation condition that we used

in section 4.2.1.

We can convert our result for general spin operators on the torus to that for the annulus quite easily, by defining an open-string auxiliary Green's function through the method of images,

$$g_{\text{open}}(z, w; z_i) = g(z, w; z_i) + g(z, \bar{w}; z_i) , \tag{4.44}$$

and proceeding through with the calculation as before. The outcome is that we end up with two identical copies of equation 4.42; we see, then, that the correlator for spin fields on the annulus is just the same as that on the torus.

4.2.5 Ghost spin fields

Also required are correlators for the ghost spin fields, $e^{a\phi}$. These may be calculated by an analogous method, but with the OPEs and stress tensor appropriately modified to account for the fact that the ghost fields ϕ inhabit the (β, γ) rather than the $(\overline{\psi}, \psi)$ CFT [81]. The result turns out to be the reciprocal of (4.43):

$$\left\langle e^{a_i\phi}(z_i)\right\rangle = K^g_{\alpha\beta}\left[\prod_{i<j}\vartheta_1(z_i - z_j)^{-a_i a_j}\right]\vartheta^{-1}_{\alpha\beta}\left(\sum_i a_i z_i\right) . \tag{4.45}$$

4.2.6 Twist fields

Twist fields correlators are also tricky, this time because they do not possess a natural interpretation as local operators on the worldsheet. Again, the resolution is to use the stress-tensor method, and again we begin on a torus before converting our result to the annulus.

On a torus, the twist fields have the OPEs (4.14), given by the local monodromy conditions for the twist fields. Things are complicated somewhat by the *global* monodromy conditions – that is, the behaviour of the X fields as they are transported around collections of twist fields. If we define a closed loop γ as a loop on the worldsheet as a loop enclosing twist operators whose twists sum to zero, then around such a loop,

$$\Delta_\gamma X = \oint_\gamma dz\, \partial X + \oint_\gamma d\bar{z}\, \overline{\partial} X = v_\gamma . \tag{4.46}$$

Here v_γ represents a consistent displacement on the network of branes. If the branes are on a compact space then the contours may generate a displacement that wraps a number of times around the compactified brane before returning to the same place.

We may choose to split X into a 'classical' part and a 'quantum fluctuation' part,

$$X = X_{\rm cl} + X_{\rm qu}\,, \tag{4.47}$$

with the requirement that the quantum part be unchanged by transportation around a closed loop while the classical part takes care of the displacement,

$$\Delta_\gamma X_{\rm qu} = \oint_\gamma \mathrm{d}z\,\partial X_{\rm qu} + \oint_\gamma \mathrm{d}\bar{z}\,\bar{\partial} X_{\rm qu} = 0\,. \tag{4.48}$$

$$\Delta_\gamma X_{\rm cl} = \oint_\gamma \mathrm{d}z\,\partial X_{\rm cl} + \oint_\gamma \mathrm{d}\bar{z}\,\bar{\partial} X_{\rm cl} = v_\gamma\,. \tag{4.49}$$

Then, the correlator for L twist operators also splits into a quantum and a classical part,

$$\left\langle \prod_{i=1}^{L} \sigma_i\left(z_i\right) \right\rangle = Z_\sigma \mathrm{e}^{-S_{\rm cl}}\,. \tag{4.50}$$

The classical portion of the twist correlators will play a key role in our calculation, and as such we defer discussion of it until section 4.4, considering first just the quantum part Z_σ.

Using the stress-tensor method to compute this correlator in a manner consistent with both the local and global monodromy conditions, plus the periodicity of the torus, is not a trivial task. Fortunately such a calculation has been performed on the torus by Atick *et al.* [84], with the result[2]

$$Z_\sigma = \left|\det W\right|^{-1} \overline{\vartheta_1\left(Y\right)}^{(L-M-1)} \vartheta_1\left(Y'\right)^{(M-1)} \prod_{i<j}^{L-M} \frac{}{\vartheta_1\left(z_{\alpha_i} - z_{\alpha_j}\right)} \prod_{i<j}^{M} \vartheta_1\left(z_{\beta_i} - z_{\beta_j}\right) \prod_{i<j}^{L} \overline{\vartheta_1\left(z_i - z_j\right)}^{-(1-\theta_i)(1-\theta_j)} \vartheta_1\left(z_i - z_j\right)^{-\theta_i\theta_j}\,, \tag{4.51}$$

where $M = \sum_{i=1}^{L} \theta_i$ is an integer, z_{α_i} are a set of $L - M$ twist insertion points chosen from z_i and z_{β_j} are a set of M twist insertion points chosen from z_i (not necessarily

[2]The OPEs in [84] have $\theta \to 1-\theta$ with respect to our OPEs (4.14); in the conventional orbifold language, we are interested in the correlator of anti-twist operators, rather than twist operators. We deal with the disparity by reversing the notions of holomorphic and anti-holomorphic with respect to the work of Atick *et al.*, leading to the result shown in eq. 4.51. Formally, we should also replace $W \to \overline{W}$ everywhere; however, this does not affect our results, so we stick with the simpler notation.

related to z_{α_i}). The elements of the elements of the $L \times L$ matrix W are given by

$$\begin{aligned} W_a^i &= \oint_{\gamma_a} \mathrm{d}z\, \omega_i(z) \qquad i = 1, \ldots, L-M \\ W_a^i &= \oint_{\gamma_a} \mathrm{d}\bar{z}\, \overline{\omega_i'(\bar{z})}, \qquad i = L-M+1, \ldots, L, \end{aligned} \tag{4.52}$$

with γ_a a basis for L closed loops on the worldsheet. ω and ω' are so-called 'cut differentials',

$$\begin{aligned} \omega_i(z) &= \gamma(z)\,\vartheta_1(z - z_{\alpha_i} - Y) \prod_{i \neq j}^{L-M} \vartheta_1(z - z_{\alpha_j}) \\ \omega_i'(z) &= \gamma'(z)\,\vartheta_1(z - z_{\beta_i} - Y') \prod_{i \neq j}^{M} \vartheta_1(z - z_{\beta_j}) \end{aligned} \tag{4.53}$$

with the contributions

$$\begin{aligned} \gamma(z) &= \prod_{j=1}^{L} \vartheta_1(z - z_j)^{-(1-\theta_j)} \\ \gamma'(z) &= \prod_{j=1}^{L} \vartheta_1(z - z_j)^{-\theta_j} \end{aligned} \tag{4.54}$$

chosen to obey the local monodromy. These cut differentials form a basis for ∂X_{cl};

$$\begin{aligned} \partial \overline{X}_{\mathrm{cl}} &= \sum_{i=1}^{L-M} c_i \omega_i \\ \partial X_{\mathrm{cl}} &= \sum_{i=L-M+1}^{L} c_i \omega_i'. \end{aligned} \tag{4.55}$$

The terms Y and Y' in (4.53) are

$$\begin{aligned} Y &= \sum_{i=1}^{L} (1 - \theta_i) z_i - \sum_{j=1}^{L-M} z_{\alpha_j} \\ Y' &= \sum_{i=1}^{L} \theta_i z_i - \sum_{j=1}^{M} z_{\beta_j}, \end{aligned} \tag{4.56}$$

and have the function of keeping ω and ω' periodic on the torus.

This result may be converted to the annulus by applying the method of images,

just as for the spin fields. This time, the two terms in the open-string Green's function lead to *different* differential equations; this is a reflection of the fact that the twist operators respond differently to holomorphic and anti-holomorphic fields on the torus, as we see from the OPEs above. Taking the vertex operators to lie along the annulus boundary, $z_i = \mathrm{i}y_i$, we find that both differential equations are in the same variable and so we may add them before solving. The result turns out to be the square root of (4.51), which is exactly what similar calculations at tree level [50, 51, 53] lead us to expect.

We are interested in the case where we have three twist operators, and the angles at the intersections add up to π; hence, $L = 3$ and $M = 1$. We choose the $3 - 1 = 2$ points z_{α_i} as $\{z_{\alpha_1}, z_{\alpha_2}\} = \{\mathrm{i}y_1, \mathrm{i}y_2\}$, and the one point $z_{\beta_1} = \mathrm{i}y_3$. Then, for a single complex dimension and up to an overall normalization,

$$Z_\sigma = |\det W|^{-\frac{1}{2}} \vartheta_1\left(\mathrm{i}\left(\theta_1 y_1 + \theta_2 y_2 - (1-\theta_3) y_3\right)\right)^{\frac{1}{2}} \vartheta_1\left(\mathrm{i}y_{12}\right)^{\frac{1}{2}} \prod_{i<j}^{3} \vartheta_1\left(\mathrm{i}y_{ij}\right)^{-\frac{1}{2}(1-\theta_i)(1-\theta_j)-\frac{1}{2}\theta_i\theta_j} \tag{4.57}$$

(an overall phase having been taken out of the first ϑ_1), with

$$\begin{aligned} W_\alpha^1 &= \oint_{\gamma_\alpha} \mathrm{d}z\, \gamma(z)\, \vartheta_1\left(z - (1-\theta_1)\,\mathrm{i}y_1 + \theta_2 \mathrm{i}y_2 - (1-\theta_3)\, y_3\right) \vartheta_1\left(z - \mathrm{i}y_2\right) \\ W_\alpha^2 &= \oint_{\gamma_\alpha} \mathrm{d}z\, \gamma(z)\, \vartheta_1\left(z + \theta_1 \mathrm{i}y_1 - (1-\theta_2)\, y_2 - (1-\theta_3)\, y_3\right) \vartheta_1\left(z - \mathrm{i}y_1\right) \\ W_\alpha^3 &= \oint_{\gamma_\alpha} \mathrm{d}\bar{z}\, \overline{\gamma'(\bar{z}) \vartheta_1\left(\bar{z} - \mathrm{i}\left(\theta_1 y_1 + \theta_2 y_2 + \theta_3 y_3\right)\right)}\,. \end{aligned} \tag{4.58}$$

Three suitable independent contours γ_a are shown in figure 4.4. They consist of a cycle γ_1 running around the annulus, a cycle γ_2 around the covering torus and a Pochhammer contour γ_3. This latter contour encircles each of the twist operators once in each direction, so that the net twist enclosed by γ_3 is correctly zero. We choose γ_3 to encircle the branch cut $\mathrm{i}y_1 < z < \mathrm{i}y_2$, but we could just have easily have chosen it to encircle the other cut; indeed, one may deform between the two by taking linear combinations of γ_3 together with the two cycles.

Note that the cycle γ_2, which generates a displacement between the branes, is always chosen such that it does not pass through a branch cut. This corresponds to taking the displacement to be between two parallel pairs of branes.

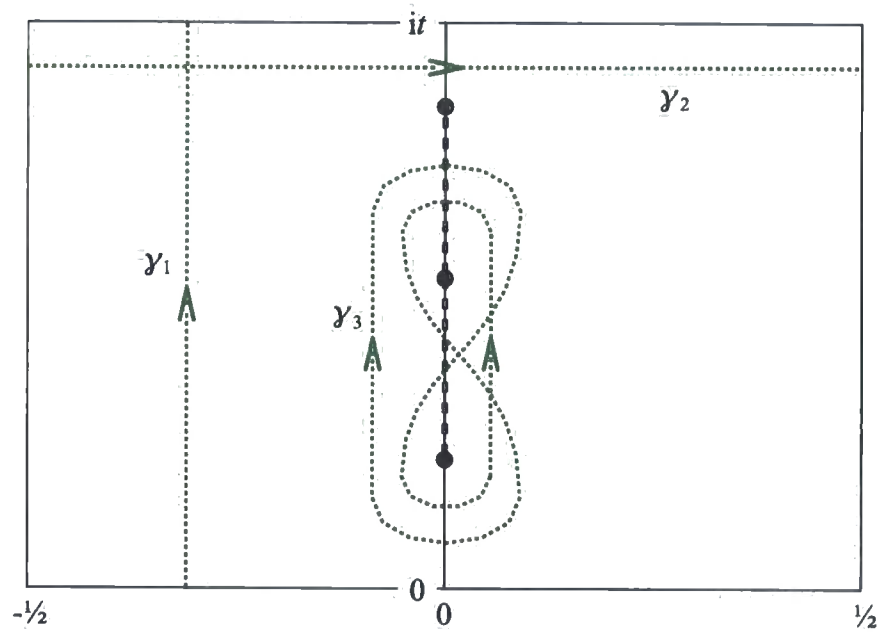

Figure 4.4: Independent contours on the worldsheet: two cycles and a Pochhammer loop. The annulus corresponds to the region $z > 0$.

4.2.7 Excited twist fields

Finally, we must deal with the excited twist correlator $\langle \sigma(z_1)\tau(z_2)\tau'(z_3)\rangle$ which is present in A_1 (eq. 4.17). This correlator may be obtained from the basic twist correlator as follows: using the OPEs (4.14), write

$$\langle \sigma(z_1)\tau(z_2)\tau'(z_3)\rangle = \lim_{\substack{z\to z_2\\ w\to z_3}} (z-z_2)^{\theta_2}(w-z_3)^{1-\theta_3} \langle \sigma(z_1)\partial X(z)\sigma(z_2)\partial\overline{X}(w)\sigma(z_3)\rangle \ . \quad (4.59)$$

Writing $X = X_{\rm qu} + X_{\rm cl}$, this second correlator splits into a quantum and a classical piece,

$$\langle \sigma(z_1)\partial X(z)\sigma(z_2)\partial\overline{X}(w)\sigma(z_3)\rangle = \langle \sigma(z_1)\partial X_{\rm qu}(z)\sigma(z_2)\partial\overline{X}_{\rm qu}(w)\sigma(z_3)\rangle + \partial X_{\rm cl}(z)\partial\overline{X}_{\rm cl}(w)\langle \sigma(z_1)\sigma(z_2)\sigma(z_3)\rangle \ , \quad (4.60)$$

and we deal with each portion separately.

Taking the quantum part first, define a function $g(z,w;z_i)$ as

$$g(z,w;z_i) = \frac{\langle \partial X_{\rm qu}(z)\,\partial\overline{X}_{\rm qu}(w)\prod_{i=1}^{3}\sigma(z_i)\rangle}{\langle\prod_{i=1}^{3}\sigma(z_i)\rangle}\,. \tag{4.61}$$

so that

$$\langle\sigma_1(z_1)\,\tau_2(z_2)\,\tau_3'(z_3)\rangle_{\rm qu} = \left\langle\prod_i \sigma(z_i)\right\rangle \lim_{\substack{z\to z_2\\ w\to z_3}} (z-z_2)^{\theta_2}(w-z_3)^{1-\theta_3}\,g(z,w;z_i)\,. \tag{4.62}$$

Since g is a function only of holomorphic variables, this result will be equally true on the torus or annulus; there is no need to take square roots anywhere except in the base twist correlator $\langle\prod_i \sigma_i(z_i)\rangle$.

An explicit expression for $g(z,w;z_i)$ is[3] [84]

$$g(z,w;z_i) = g_s(z,w) + \omega_1(w)\sum_{i=1}^{2} B_i\omega_i'(z)\,. \tag{4.63}$$

Using the result $\lim_{z\to 0}\vartheta_1(z) = \vartheta_1'(0)\,z$, we see

$$\begin{aligned}\lim_{w\to z_3}(w-z_3)^{1-\theta_3}\,\omega_i(w) &\propto \lim_{w\to z_3}(w-z_3)^{1-\theta_3}\,\vartheta_1(w-z_3)^{-(1-\theta_3)}\,\vartheta_1(w-z_3) \\ &= 0\,,\end{aligned} \tag{4.64}$$

and so the second term in $g(z,w;z_i)$ disappears when we take the limit in equation 4.62. Therefore, the term of interest to us is $g_s(z,w)$, which is given by

$$g_s(z,w) = \gamma(w)\,\gamma'(z)\left[\frac{\vartheta_1'(0)}{\vartheta_1(w-z)}\right]^2 \sum_{i=1}^{3}\theta_i F_i(w,z)\,\vartheta_1(z-z_i)\prod_{j\neq i}\vartheta_1(w-z_j)\,, \tag{4.65}$$

with

$$F_i(w,z) = \frac{\vartheta_1(w-z+U_i^0)}{\vartheta_1(U_i^0)}\,\frac{\vartheta_1(w-z+Y_i-U_i^0)}{\vartheta_1(Y_i-U_i^0)} \tag{4.66}$$

$$Y_i = \left(\sum_{j=1}^{3}\theta_j z_j\right) - z_i\,, \tag{4.67}$$

and U_i^0 chosen so as to satisfy the equation $\partial_w F_i(w,z) = 0$. Taking the limit (4.62),

[3] As in the previous section, we deal with the $\theta \to 1-\theta$ issue by exchanging $X \leftrightarrow \overline{X}$, which corresponds simply to swapping $z \leftrightarrow w$ relative to the work of Atick *et al.*

one finds

$$\langle \sigma_1(z_1)\,\tau_2(z_2)\,\tau_3'(z_3)\rangle_{\rm qu} = \left\langle \prod_i \sigma_i(z_i) \right\rangle \theta_3 F_3(z_3,z_2) \\ \vartheta_1(z_{12})^{-\theta_1}\,\vartheta_1(z_{13})^{\theta_1}\,\vartheta_1(z_{23})^{\theta_2-\theta_3-1}\,. \quad (4.68)$$

To evaluate the classical part of (4.60) we insert (4.55) for the case of three twist operators,

$$\begin{aligned} \partial\overline{X}_{\rm cl} &= \sum_{i=1}^{2} c_i\omega_i \\ \partial X_{\rm cl} &= c_3\omega_3'\,, \end{aligned} \quad (4.69)$$

and take the limit (4.62) to find

$$\langle \sigma_1(z_1)\,\tau_2(z_2)\,\tau_3'(z_3)\rangle_{\rm cl} = \left\langle \prod_i \sigma_i(z_i) \right\rangle \vartheta_1(z_{12})^{-\theta_1}\,\vartheta_1(z_{13})^{\theta_1-1}\,\vartheta_1(z_{23})^{\theta_2-\theta_3-1} \\ [c_1\vartheta_1(z_{23})\,\vartheta_1(-z_1(1-\theta_1)+z_2\theta_2+z_3\theta_3)+c_2\vartheta_1(z_{13})\,\vartheta_1(z_1\theta_1+z_2\theta_2-z_3(1-\theta_3))] \\ c_3\vartheta_1(z_1\theta_1-z_2(1-\theta_2)+z_3\theta_3)\,. \quad (4.70)$$

The factors of $\vartheta_1(z_{ij})^{\pm\theta}$ in both the quantum and classical parts of this excited twist correlator compensate exactly for the changes in the spin correlator introduced by picture-changing.

4.3 The quantum part

We are now in a position to construct the quantum part of A explicitly. In everything that follows it should be understood that the vertex operators z_i are positioned along the imaginary axis as shown, so that $z_i = \mathrm{i}y_i$. For ease of reference, we collect together the relevant correlators (4.30), (4.31), (4.43), (4.45), (4.57), (4.68) and (4.70) in figure 4.5.

Recall that in section 4.2, we found three contributions to A, which we denoted A_1, A_2 and A_3. We begin here with the term A_1, which we previously argued ought to correspond to a vertex renormalization, limit 1 of figure 4.2. Using the correlators

$$\left\langle \prod_i \mathrm{e}^{\mathrm{i}k_i\cdot X}(z_i) \right\rangle = \prod_{i<j} \left[\vartheta_1(z_{ij})\,\mathrm{e}^{\pi z_{ij}^2/t}\right]^{k_i\cdot k_j}$$

$$\left\langle \partial X^\mu(w) \prod_i \mathrm{e}^{\mathrm{i}k_i\cdot X}(z_i) \right\rangle = \prod_{i<j} \mathrm{i}k_j^\mu \left[\frac{\theta_1'(w-z_j)}{\theta_1(w-z_j)} - \frac{2\pi}{t}\,|w-z_j|\right] \left[\vartheta_1(z_{ij})\,\mathrm{e}^{\pi z_{ij}^2/t}\right]^{k_i\cdot k_j}$$

$$\left\langle \prod_i \mathrm{e}^{\mathrm{i}a_i H}(z_i) \right\rangle = K_{\alpha\beta} \left[\prod_{i<j} \vartheta_1(z_i-z_j)^{a_i a_j}\right] \vartheta_{\alpha\beta}\left(\sum_i a_i z_i\right)$$

$$\left\langle \prod_i \mathrm{e}^{a_i\phi}(z_i) \right\rangle = K^g_{\alpha\beta} \left[\prod_{i<j} \vartheta_1(z_i-z_j)^{-a_i a_j}\right] \vartheta^{-1}_{\alpha\beta}\left(\sum_i a_i z_i\right)$$

$$\left\langle \prod_i \sigma_i(z_i) \right\rangle = \mathrm{e}^{-S_{\mathrm{cl}}} \left|\det W\right|^{-\frac{1}{2}} \vartheta_1(\theta_1 z_1 + \theta_2 z_2 - (1-\theta_3) z_3)^{\frac{1}{2}}$$
$$\vartheta_1(z_{12})^{\frac{1}{2}} \prod_{i<j}^{3} \vartheta_1(z_{ij})^{-\frac{1}{2}(1-\theta_i)(1-\theta_j)-\frac{1}{2}\theta_i\theta_j}$$

$$\langle \sigma(z_1)\,\tau(z_2)\,\tau'(z_3)\rangle = \left\langle \prod_i \sigma_i(z_i) \right\rangle \vartheta_1(z_{12})^{-\theta_1}\,\vartheta_1(z_{13})^{\theta_1}\,\vartheta_1(z_{23})^{\theta_2-\theta_3-1}$$
$$\Phi(z_1,z_2,z_3)$$

with

$$\Phi(z_1,z_2,z_3) \equiv \Big\{ \theta_3 F_3(z_3,z_2) + \Big[c_1 \frac{\vartheta_1(z_{23})}{\vartheta_1(z_{13})} \vartheta_1(-z_1(1-\theta_1) + z_2\theta_2 + z_3\theta_3)$$
$$+ c_2 \vartheta_1(z_1\theta_1 + z_2\theta_2 - z_3(1-\theta_3)) \Big] c_3 \vartheta_1(z_1\theta_1 - z_2(1-\theta_2) + z_3\theta_3) \Big\}$$

Figure 4.5: Correlators required for the calculation of $\mathcal{A}$, up to overall normalization factors. The term $F_3(w,z)$ is given by (4.66).

given, we find the rather involved expression

$$A_1 = \frac{1}{4}\overline{u}_1 u_2 \mathrm{e}^{-S_{\mathrm{cl}}} \left(\sum_{i=1}^{3} \Phi^i\left(z_1, z_2, z_3\right) \right) \mathrm{e}^{\pi\left(k_1\cdot k_2 z_{12}^2 + k_1\cdot k_3 z_{13}^2 + k_2\cdot k_3 z_{23}^2\right)/t}$$
$$\vartheta_1\left(z_{12}\right)^{k_1\cdot k_2 - \frac{3}{2}} \vartheta_1\left(z_{13}\right)^{k_1\cdot k_3 + \frac{1}{2}\left(\theta_1^1+\theta_1^2+\theta_1^3\right)-1} \vartheta_1\left(z_{23}\right)^{k_2\cdot k_3 + \frac{1}{2}\left(\theta_2^1+\theta_2^2+\theta_2^3\right)-3}$$
$$\left(\prod_{i=1}^{3} \left|\det W^i\right|^{-\frac{1}{2}} \vartheta_1\left(\theta_1^i z_1 + \theta_2^i z_2 + (\theta_3^i - 1) z_3\right)^{\frac{1}{2}} \vartheta_1\left(z_{12}\right)^{\frac{1}{2}} \right)$$
$$\sum_{\alpha\beta} \delta_{\alpha\beta} \vartheta_{\alpha\beta}\left(\tfrac{1}{2}\left(z_2 - z_1\right)\right) \prod_{i=1}^{3} \vartheta_{\alpha\beta}\left(z_1 q_1^i + z_2 \tilde{q}_2^i + z_3 \tilde{q}_3^i\right) . \quad (4.71)$$

The function $\Phi^i\left(z_1, z_2, z_3\right)$ in the first line comes from the excited twist correlators, and is displayed explicitly in figure 4.5. Factors in the second line come from the combination of all correlators, the third from the ordinary twist correlation and the fourth from the spin and ghost spin field correlators. The values of q_1^i, $\tilde{q}_2^i$, $\tilde{q}_3^i$ are given in table 4.2.

The phases $\delta_{\alpha\beta}$ may be determined by the requirement that as $z_1 \longrightarrow z_2 \longrightarrow z_3$, the amplitude ought to factor onto the partition function $\mathcal{Z}$ for two D6-branes, which contains the term

$$\mathcal{Z} \propto \sum_{\alpha\beta} \delta_{\alpha\beta} \vartheta_{\alpha\beta}\left(0\right)^4 \qquad \left(\delta_{00} = \delta_{11} = +1,\ \delta_{01} = \delta_{10} = -1\right) . \quad (4.72)$$

The H-charge conservation rule $q_1^i + \tilde{q}_2^i + \tilde{q}_2^i = 0$ guarantees that (4.71) does indeed have this property, and so the relative phases in A_1 must be the same as those in $\mathcal{Z}$. Therefore, we may apply the Riemann identity (A.11), with the result

$$A_1 \propto \vartheta_1\left(\tfrac{1}{2}\sum_i z_i \left(1 - \sum_j \theta_i^j\right)\right) . \quad (4.73)$$

Using the $\mathcal{N} = 1$ supersymmetry condition $\sum_j \theta_i^j = 1$ and the result $\vartheta_1\left(0\right) = 0$, we see that A_1 always vanishes in supersymmetric models. This appears to support our identification of A_1 as a vertex renormalization, since those diagrams vanish in $\mathcal{N} = 1$ theories by the non-renormalization theorem.

We now turn to the terms $A_2^{\pm}$. Note first that after correlators have been inserted explicitly, the main difference between (4.23) and (4.24) comes from the spin-

dependent parts coming from the external space: A_2^+ contains a factor of

$$\vartheta_{\alpha\beta}^{-1}\left(\tfrac{1}{2}\left(z_2-z_1\right)\right)\vartheta_{\alpha\beta}\left(\tfrac{1}{2}\left(z_2-z_1\right)\right)\vartheta_{\alpha\beta}\left(z_3-\tfrac{1}{2}\left(z_2+z_1\right)\right)\,,$$

whilst A_2^- contains a factor of

$$\vartheta_{\alpha\beta}^{-1}\left(\tfrac{1}{2}\left(z_2-z_1\right)\right)\vartheta_{\alpha\beta}\left(-\tfrac{1}{2}\left(z_2-z_1\right)\right)\vartheta_{\alpha\beta}\left(-z_3+\tfrac{1}{2}\left(z_2+z_1\right)\right)\,.$$

Since the ϑ-functions are odd or even, the difference is superficial and the terms $A_2^{\pm}$ may be joined together to give one single term:

$$\begin{aligned}A_2 = \frac{1}{2}\overline{u}_1 u_2 \mathrm{e}^{-S_{\mathrm{cl}}}\mathrm{e}^{\pi\left(k_1\cdot k_2 z_{12}^2+k_1\cdot k_3 z_{13}^2+k_2\cdot k_3 z_{23}^2\right)/t}\\ \left[k_1\cdot k_3\left(\frac{\theta_1'\left(z_{12}\right)}{\theta_1\left(z_{12}\right)}+\frac{2\pi\mathrm{i}}{t}z_{12}\right)+k_3\cdot k_3\left(\frac{\theta_1'\left(z_{23}\right)}{\theta_1\left(z_{23}\right)}+\frac{2\pi\mathrm{i}}{t}z_{23}\right)\right]\\ \vartheta_1\left(z_{12}\right)^{k_1\cdot k_2-\frac{1}{2}}\vartheta_1\left(z_{13}\right)^{k_1\cdot k_3+\frac{1}{2}\left(\theta_1^1+\theta_1^2+\theta_1^3\right)-2}\vartheta_1\left(z_{23}\right)^{k_2\cdot k_3+\frac{1}{2}\left(\theta_2^1+\theta_2^2+\theta_2^3\right)-2}\\ \left(\prod_{i=1}^{3}\left|\det W^i\right|^{-\frac{1}{2}}\vartheta_1\left(\theta_1^i z_1+\theta_2^i z_2+\left(\theta_3^i-1\right)z_3\right)^{\frac{1}{2}}\vartheta_1\left(z_{12}\right)^{\frac{1}{2}}\right)\\ \sum_{\alpha\beta}\delta_{\alpha\beta}\vartheta_{\alpha\beta}\left(-\tfrac{1}{2}z_1-\tfrac{1}{2}z_2+z_3\right)\prod_{i=1}^{3}\vartheta_{\alpha\beta}\left(\left(\tfrac{1}{2}-\theta_1^i\right)z_1+\left(\tfrac{1}{2}-\theta_2^i\right)z_2-\theta_3 z_3\right)\,.\end{aligned}\tag{4.74}$$

In a supersymmetric set-up, A_2 may be seen to vanish in exactly the same way as A_1. However, as it has kinematic factors in front, it does not contribute significantly when the vertex operators are far apart and so we do not associate it with a vertex renormalization.

More interesting are the terms $A_3^{\pm}$, which also join together to give

$$\begin{aligned}A_3 = -\frac{1}{2}\overline{u}_1 u_2 \mathrm{e}^{-S_{\mathrm{cl}}}k_2\cdot k_3\mathrm{e}^{\pi\left(k_1\cdot k_2 z_{12}^2+k_1\cdot k_3 z_{13}^2+k_2\cdot k_3 z_{23}^2\right)/t}\\ \vartheta_1\left(z_{12}\right)^{k_1\cdot k_2-\frac{3}{2}}\vartheta_1\left(z_{13}\right)^{k_1\cdot k_3+\frac{1}{2}\left(\theta_1^1+\theta_1^2+\theta_1^3\right)-1}\vartheta_1\left(z_{23}\right)^{k_2\cdot k_3+\frac{1}{2}\left(\theta_2^1+\theta_2^2+\theta_2^3\right)-3}\\ \left(\prod_{i=1}^{3}\left|\det W^i\right|^{-\frac{1}{2}}\vartheta_1\left(\theta_1^i z_1+\theta_2^i z_2+\left(\theta_3^i-1\right)z_3\right)^{\frac{1}{2}}\vartheta_1\left(z_{12}\right)^{\frac{1}{2}}\right)\\ \sum_{\alpha\beta}\delta_{\alpha\beta}\vartheta_{\alpha\beta}\left(-\tfrac{1}{2}z_1+\tfrac{3}{2}z_2-z_3\right)\prod_{i=1}^{3}\vartheta_{\alpha\beta}\left(\left(\tfrac{1}{2}-\theta_1^i\right)z_1+\left(\tfrac{1}{2}-\theta_2^i\right)z_2-\theta_3 z_3\right)\,.\end{aligned}\tag{4.75}$$

Again the phases may be determined from factorization on the partition function

Term	Vanishes by Riemann identity?	Kinematic prefactors?
A_1	$\surd$	$\times$
A_2	$\surd$	$\surd$
A_3	$\times$	$\surd$

Table 4.3: Properties of the three terms A_i.

and so we may apply the Riemann identity, leading to

$$\begin{aligned} A_3 = &-\overline{u}_1 u_2 \mathrm{e}^{-S_{\mathrm{cl}}} k_2 \cdot k_3 \mathrm{e}^{\pi\left(k_1\cdot k_2 z_{12}^2 + k_1\cdot k_3 z_{13}^2 + k_2\cdot k_3 z_{23}^2\right)/t} \\ &\vartheta_1\left(z_{12}\right)^{k_1\cdot k_2 - \frac{3}{2}} \vartheta_1\left(z_{13}\right)^{k_1\cdot k_3 + \frac{1}{2}\left(\theta_1^1+\theta_1^2+\theta_1^3\right)-1} \vartheta_1\left(z_{23}\right)^{k_2\cdot k_3 + \frac{1}{2}\left(\theta_2^1+\theta_2^2+\theta_2^3\right)-3} \\ &\left(\prod_{i=1}^{3} \left|\det W^i\right|^{-\frac{1}{2}} \vartheta_1\left(\theta_1^i z_1 + \theta_2^i z_2 + \left(\theta_3^i - 1\right) z_3\right)^{\frac{1}{2}} \vartheta_1\left(z_{12}\right)^{\frac{1}{2}}\right) \\ &\vartheta_1\left(\tfrac{1}{2}\sum_i \left(1 - \sum_j \theta_i^j\right) z_i + z_2 - z_3\right) \prod_k \vartheta_1\left(\tfrac{1}{2}\sum_{i,j} M_{kj}\theta_i^j z_i + \tfrac{1}{2}\left(z_2 - z_1 - z_3\right)\right), \end{aligned} \tag{4.76}$$

where the matrix M is

$$M_{kj} = \begin{pmatrix} -1 & 1 & 1 \\ 1 & -1 & 1 \\ 1 & 1 & -1 \end{pmatrix}.$$

This time, the result does *not* vanish in an $\mathcal{N} = 1$ theory, which suggests that we should identify A_3 as a field renormalization. Also, since A_3 has kinematic factors in front, it will be most significant when we take two vertex operators to be close together; therefore, we confirm the intuitive results of figure 4.2.

The properties of the terms A_1–A_3 are summarized in table 4.3. It appears that we have a problem if we want an $\mathcal{N} = 1$ theory, since the only term which is not killed by a Riemann identity, A_3, appears to disappear on-shell via

$$k_2 \cdot k_3 = \frac{1}{2}m^2 = 0. \tag{4.77}$$

In fact, we shall see in section 4.6 that the integral over y_i yields poles which should be cancelled with the kinematic prefactor before going on-shell. In this manner finite answers are obtained. In non-supersymmetric theories, we will see that the

structure of A_2 and A_3 (and in particular, the relative minus sign between them) is such that the poles in the combined expression cancel.

In the case where one of the branes go through an orbifold fixed point, the correlators of spin and twist operators will be modified [84]. However, the differences must only be in the spin-dependent terms, *i.e.* the last lines of (4.71), (4.74) and (4.75). In order that the amplitude factor onto the twisted partition function, these modifications must be exactly those that are made to the spin-dependent terms in the partition function, and so it is possible to write down the above expressions in the case of orbifold fixed points without repeating the calculation explicitly. The situation is similar in the presence of O-planes, where Möbius strip diagrams may be present.

4.4 The classical action

We now return to the question of how to treat the global monodromy conditions and extract the classical contribution to the action. The classical action for each pair of complex coordinate can be written

$$S_{\rm cl} = \frac{1}{4\pi\alpha'} \int \mathrm{d}^2 z \, \left(\partial X_{\rm cl} \overline{\partial X}_{\rm cl} + \bar{\partial} X_{\rm cl} \partial \overline{X}_{\rm cl} \right) . \tag{4.78}$$

The linear decomposition of $X_{\rm cl}$ can be defined,

$$\Delta_\gamma X_{\rm cl} = v_a = W_a^i c_i \tag{4.79}$$

where the displacements v_a are determined from the global monodromy conditions (*i.e.* by comparing the displacement of X under combinations of twists that add up to zero), as discussed earlier. The coefficients c_i are to be determined from them;

$$c_i = v_a (W^{-1})_i^a . \tag{4.80}$$

From the definition of ΔX we see that we must have

$$\begin{aligned} \partial \overline{X}_{\rm cl} &= \sum_{i=1}^{2} c_i \omega_i \\ \partial X_{\rm cl} &= c_3 \omega_3' . \end{aligned} \tag{4.81}$$

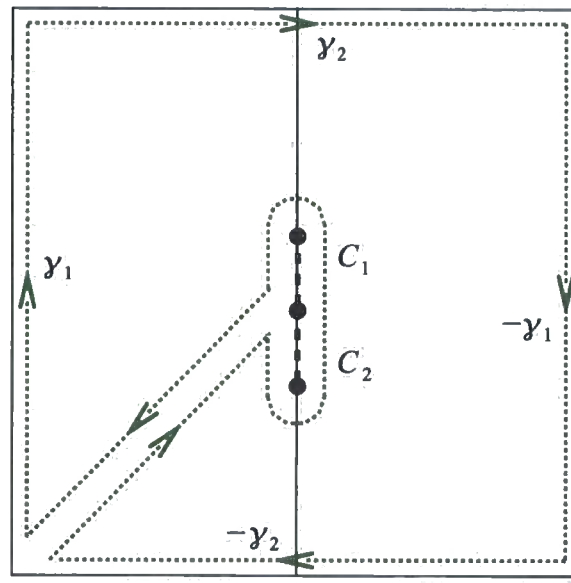

Figure 4.6: The dissection of the torus for three point diagrams.

Inserting into S_{cl} gives

$$S_{\rm cl} = \frac{1}{4\pi\alpha'}\left(\sum_{i,j}^{2} c_i c_j^* I_{ij} + |c_3|^2 I_{33}\right) \tag{4.82}$$

where

$$\begin{aligned} I_{ij} &= \int \mathrm{d}^2 z\, \omega^i \bar{\omega}^j \\ I_{33} &= \int \mathrm{d}^2 z\, |\omega^3| \end{aligned} \tag{4.83}$$

In order to determine the I_{ij} we may perform a canonical dissection of the torus [84]. In this case the dissection is as shown in figure 4.6. In terms of the cycles and two spurs shown in the figure, the I_{ij} are given by [84]

$$\begin{aligned} I_{ij} = \oint_{\gamma_1} \mathrm{d}z\, \omega^i \oint_{\gamma_2} \mathrm{d}\bar{z}\, \bar{\omega}^j - \oint_{\gamma_2} \mathrm{d}z\, \omega^i \oint_{\gamma_1} \mathrm{d}\bar{z}\, \bar{\omega}^j \\ + \int_{C_1} \omega^i \int_{C_2} \bar{\omega}^j + \sum_{l=1}^{2} \frac{1}{(1 - e^{-2\pi i \theta_l})} \int_{C_l} \omega^i \int_{C_l} \bar{\omega}^j . \end{aligned} \tag{4.84}$$

Evaluating the contour integrals explicitly we find the relations

$$\begin{aligned}
\int_{C_1} \bar{\omega}^3 &= \frac{-1}{1-\mathrm{e}^{-2\pi \mathrm{i}\theta_2}} W_3^3 \\
\int_{C_2} \bar{\omega}^3 &= \frac{1}{1-\mathrm{e}^{2\pi \mathrm{i}\theta_2}} W_3^3 \\
\int_{C_1} \omega^{i=1,2} &= \frac{-1}{1-\mathrm{e}^{-2\pi \mathrm{i}\theta_2}} W_3^i \\
\int_{C_2} \omega^{i=1,2} &= \frac{1}{1-\mathrm{e}^{2\pi \mathrm{i}\theta_2}} W_3^i
\end{aligned} \tag{4.85}$$

whence we determine

$$I_{ij} = W_a^i \bar{W}_b^j K^{ab} \tag{4.86}$$

where

$$K^{ab} = \begin{pmatrix} 0 & -\mathrm{i} & 0 \\ \mathrm{i} & 0 & 0 \\ 0 & 0 & \alpha \end{pmatrix} \tag{4.87}$$

and

$$\alpha = \frac{1}{8\,\sin(\pi\theta_1)\sin(\pi\theta_2)\sin(\pi\theta_3)} \,. \tag{4.88}$$

This gives

$$4\pi\alpha' S_{\mathrm{cl}} = \sum_{i,j}^{2} c_i c_j^* W_a^i \overline{W}_b^j \, K^{ab} + c_3 c_3^* W_a^3 \overline{W}_b^3 K^{ab*} \tag{4.89}$$

where we have multiplied by an extra factor of $\frac{1}{2}$ to factor out half the world sheet after the Z_2 involution. Using the monodromy conditions this can be reduced to

$$4\pi\alpha' S_{\mathrm{cl}} = v_a v_b^* K^{ab} - c_3 W_a^3 v_b^* K^{ab} - c_3^* \overline{W}_b^3 v_a K^{ab} + 2|c_3|^2 W_a^3 \overline{W}_b^{3*} K^{ab*} \,. \tag{4.90}$$

Inserting K^{ab} yields

$$\begin{aligned}
8\pi\alpha' S_{\mathrm{cl}} = \alpha \, &\left(|v_3 - c_3 W_3^3|^2 + |c_3 W_3^3|^2 \right) \\
&+ \left(\mathrm{i}\,|c_3|^2 \, W_1^3 \overline{W}_2^{3*} - \mathrm{i}\,(v_1 - c_3 W_1^3)(v_2^* - c_3^* \overline{W}_2^3) + \mathrm{H.C.} \right) \,.
\end{aligned} \tag{4.91}$$

This is the main expression for the classical action. Note that we need only determine the coefficient c_3 explicitly; otherwise, all that remains to do is to find the W_a^j in the various limits and insert their values.

4.5 Limiting cases of the classical action

We are now in a position to apply the results derived thus far to the four limiting cases laid out in figure 4.2. We begin by looking at the classical action in these limits, which we expect to factor onto combinations of the classical contribution to the partition function,

$$\mathcal{Z}_{\rm cl} = \mathrm{e}^{-tY^2/2\pi\alpha'}\,, \tag{4.92}$$

and the tree-level Yukawa coupling,

$$\mathcal{Y}_{\rm cl} = \mathrm{e}^{-\mathrm{Area}/2\pi\alpha'}\,. \tag{4.93}$$

4.5.1 The partition function limit: $y_1 \to y_2 \to y_3$, $t \to \infty$

Consider first the factorization of the classical part of the action, in a single T^2. In this limit, we expect to find

$$\mathrm{e}^{-S_{\rm cl}} \to \mathcal{Z}_{\rm cl}\,\mathcal{Y}_{\rm cl}\,, \tag{4.94}$$

which is indeed the case. To see this, one must approximate the W integrals as $y_1 \to y_2 \to y_3$. Such an approximation is presented in appendix C.1, with the result

$$W = \begin{pmatrix} it & it & -it \\ 1 & 1 & 1 \\ W_3^1 & W_3^2 & W_3^3 \end{pmatrix}\,. \tag{4.95}$$

Inserting the first two rows into the monodromy conditions $v_a = W_a^i c_i$ gives

$$\begin{aligned} it\,(c_1 + c_2 - c_3) &= v_1 \\ c_1 + c_2 + c_3 &= v_2 \end{aligned} \tag{4.96}$$

with solution

$$c_3 = \frac{v_2}{2} - \frac{v_1}{2it}\,. \tag{4.97}$$

Since W_3^3 is vanishingly small in the limit (c.f. eq. C.11), we may also write

$$W_3^3 c_3 = 0\,. \tag{4.98}$$

Inserting these results into (4.91) leads to the action

$$2\pi\alpha' S_{\rm cl} = \frac{\alpha}{4}|v_3|^2 + t\left|\frac{v_2}{2}\right|^2 + \frac{|v_1|^2}{4t}\,. \tag{4.99}$$

Values must be inserted into this expression for the physical displacements v_i. First, note that v_3 is given by the Pochhammer contour

$$v_3 = 4\sin(\pi\theta_1)\sin(\pi\theta_2)e^{i\pi(\theta_2-\theta_1)}f_{12}\,, \tag{4.100}$$

where f_{12} is the spacetime displacement between vertices one and two. Hence, the first term in the action is the area of a triangle

$$\frac{\alpha}{4}|v_3|^2 = \frac{\sin(\pi\theta_1)\sin(\pi\theta_2)|f_{12}|^2}{2\sin(\pi\theta_3)}\,, \tag{4.101}$$

and is the classical part of the tree level Yukawa coupling.

With our definitions, $|v_2|$ is twice the inter-brane separation in a given torus, $v_2 = 2iY_i$, since the contour integral goes across twice the fundamental domain of the annulus (c.f. figure 4.4). The second term in (4.99) is thus the partition function term $Y^2t/2\pi\alpha'$, seen in eq. 4.92.

From figure 4.1 we see that the displacement v_1 may be taken to zero. In a compact space, it should also be summed over all wrappings;

$$v_1 = 2\pi Ln\,, \tag{4.102}$$

where $2\pi L$ is the wrapping length of the v_1 brane. Depending on the range of t under consideration, it may be appropriate to apply the Poisson resummation formula,

$$\sum_{n=-\infty}^{\infty} \mathrm{e}^{-\pi an^2+2\pi ibn} = a^{-\frac{1}{2}} \sum_{m=-\infty}^{\infty} \mathrm{e}^{-\pi(m-b)^2/a}\,, \tag{4.103}$$

after which we see that for a single torus

$$e^{-S_{\rm cl}} = \frac{\sqrt{2\alpha' t}}{L}\mathrm{e}^{-\mathrm{Area}/2\pi\alpha'}\mathrm{e}^{-tY^2/2\pi\alpha'}\sum_{m=-\infty}^{\infty} e^{-2\pi\alpha' tm^2/L}\,. \tag{4.104}$$

The extra factors of $\sqrt{t}$ here are due to Kaluza-Klein modes propagating in the loop. The condition for the resummation to be valid is that $2\pi\alpha' t > L$, and so we will get a factor of $\sqrt{t}$ appearing in the amplitude for each torus where $2\pi\alpha' t > L_i$. We discuss the consequences of this in section 4.6 below.

4.5.2 The vertex correction limit: $(t - y_3) \to \infty$, generic y_i

A derivation of the W integrals in this limit is presented in Appendix C.2, where we show that up to terms which are suppressed by powers of t,

$$W = \begin{pmatrix} \mathrm{i}\Delta t + D & AC & -\mathrm{i}\Delta t + D + A \\ 1 & 1 & 1 \\ B & BC & B \end{pmatrix}, \tag{4.105}$$

with

$$\begin{aligned} A &= -\frac{\mathrm{i}}{2}\left[\cot(\pi\theta_1) + \cot(\pi\theta_3)\right] = -\frac{i}{2}\left(\frac{\sin(\pi\theta_2)}{\sin(\pi\theta_1)\sin(\pi\theta_3)}\right) \\ B &= -2\mathrm{i}e^{i\pi\theta_2}\sin(\pi\theta_2) \\ C &= -\frac{\Gamma(\theta_2)}{\Gamma(1-\theta_1)\Gamma(1-\theta_3)}e^{2\pi y_2\theta_1}, \\ D &= -\frac{\mathrm{i}}{2\pi}\left[2\gamma_E + \psi(1-\theta_1) + \psi(1-\theta_3)\right] \end{aligned} \tag{4.106}$$

and $\Delta t = t - y_3$.

As the nine elements of W are expressible in terms of five independent quantities, we can see that there will be some over-determination in the monodromy conditions. That is, the equation

$$v_a = W_a^i c_i \tag{4.107}$$

will yield relations between the v_a. But recall that the v_a are physical displacements, relating the sides of triangles to their heights, and consequently the W_a^i matrix we have determined ought to give displacements corresponding to the actual Yukawa triangles. We will see that it does presently.

Notice first that since W_1^2 and W_3^2 contain the factor $e^{2\pi y_2\theta_1}$, they are exponentially dominant in the v_1 and v_3 conditions and so we must have c_1, $c_3 \gg c_2$. The v_2 condition is therefore

$$c_1 + c_3 \simeq v_2\,. \tag{4.108}$$

Using this result together with the conditions for v_3 and v_1, we find

$$\begin{aligned} c_3 &= \frac{1}{2\mathrm{i}\Delta t - A}\left((\mathrm{i}\Delta t + D - A)\,v_2 - v_1 + \frac{A}{B}v_3\right) \\ &\simeq \frac{v_2}{2} + \frac{\mathrm{i}}{2\Delta t}\left(v_1 - \frac{A}{B}v_3\right). \end{aligned} \tag{4.109}$$

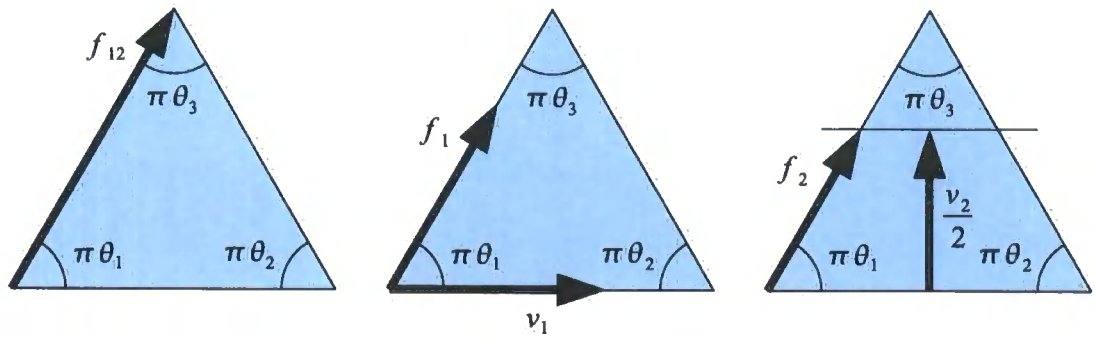

Figure 4.7: Physical vectors which appear in the global monodromy conditions $W_a^i c_i = v_a$.

To obtain the full S_{cl} via (4.78), we will need

$$c_3 W_3^3 = c_3 B = \frac{\hat{v}_2}{2} + \frac{\mathrm{i}A}{2\Delta t}\left(\hat{v}_1 - v_3\right) , \tag{4.110}$$

where

$$\begin{aligned} \hat{v}_1 &= \frac{B}{A} v_1 \\ \hat{v}_2 &= B v_2 . \end{aligned} \tag{4.111}$$

At this point it is appropriate to say something about the geometry of the situation. Notice that as A is pure imaginary, (4.110) shows that both $\hat{v}_1$ and $\hat{v}_2$ must have the same phase as v_3; arranging things so that v_1 is purely real and v_2 pure imaginary, v_3 must have an overall phase of $\mathrm{e}^{\mathrm{i}\pi\theta_2}$. However, since v_3 is also

$$v_3 = 4\sin(\pi\theta_1)\sin(\pi\theta_2) e^{i\pi(\theta_2-\theta_1)} f_{12} , \tag{4.112}$$

from the Pochhammer contour, f_{12} must have a phase of $\mathrm{e}^{\mathrm{i}\pi\theta_1}$. We may therefore define two additional vectors for $\hat{v}_1$ and $\hat{v}_2$, which we call f_1 and f_2 respectively, such that

$$\begin{aligned} \hat{v}_1 &= 4\sin\left(\pi\theta_1\right)\sin\left(\pi\theta_2\right) e^{\mathrm{i}\pi(\theta_2-\theta_1)} f_1 \\ \hat{v}_2 &= 4\sin\left(\pi\theta_1\right)\sin\left(\pi\theta_2\right) e^{\mathrm{i}\pi(\theta_2-\theta_1)} f_2 . \end{aligned} \tag{4.113}$$

With these definitions, f_1 and f_2 are projections of v_1 and $v_2/2$ along f_{12}:

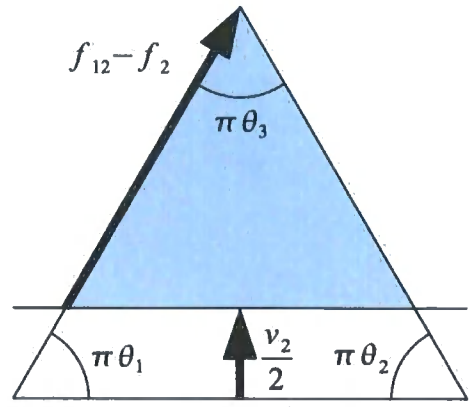

Figure 4.8: As $v_2 \to 0$, we recover the tree-level Yukawa coupling.

$$f_1 = e^{i\pi\theta_1}\frac{\sin(\pi\theta_3)\,v_1}{\sin(\pi\theta_2)}$$
$$f_2 = e^{i\pi(\theta_1-\frac{1}{2})}\frac{v_2/2}{\sin(\pi\theta_1)}\,. \tag{4.114}$$

The set-up is illustrated in figure 4.7.

Inserting (4.109, 4.110) into the result (4.78) and using $\alpha = iA/|B|^2$ gives the classical action as

$$2\pi\alpha' S_{\rm cl} = \left|\frac{v_2}{2}\right|^2(\Delta t + iD) + \frac{\alpha}{4}|v_3 - \hat{v}_2|^2 + \frac{\alpha}{8}|\hat{v}_2|^2 + \mathcal{O}\left(\frac{1}{\Delta t}\right)\,. \tag{4.115}$$

The first term in $S_{\rm cl}$ is the usual inter-brane suppression, $Y^2\Delta t/2\pi\alpha'$, showing that small $v_2 = 2iY$ is favoured. The second (and non-standard) term in $S_{\rm cl}$,

$$\frac{Y^2}{2\pi^2\alpha'}\left[2\gamma_E + \psi(1-\theta_1) + \psi(1-\theta_3)\right]\,, \tag{4.116}$$

favours small values of θ_1 and θ_3, tending to zero as $\theta_1 \to 0$, $\theta_3 \to 0$; this is just another reflection of the desire of the string not to stretch.

As $v_2 \to 0$, the third term in $S_{\rm cl}$ become the area of the large triangle (c.f. equation 4.101), and gives the tree level Yukawa coupling. The third term in the action is then the familiar effect of the propagation of a heavy (generation changing) mode of length $v_2/2$ stretched between two branes. This situation is shown in figure 4.8. The geometric interpretation of the $\frac{\alpha}{8}|\hat{v}_2|^2$ term is not obvious.

As $v_2 \to 0$, we expect to find Kaluza-Klein modes propagating in the loop. This

may be seen by retaining the $\mathcal{O}(1/\Delta t)$ terms in $S_{\rm cl}$, which when $v_2 = 0$ reads

$$2\pi\alpha' S_{cl} = \frac{\alpha}{4}|v_3|^2 + \frac{|v_1 - \tilde{v}_3|^2}{4\Delta t} + \mathcal{O}\left(\frac{1}{\Delta t^2}\right), \tag{4.117}$$

where

$$\tilde{v}_3 = \frac{A}{B}v_3 = e^{-i\pi\theta_1}\frac{\sin(\pi\theta_2)}{\sin(\pi\theta_3)}f_{12} \tag{4.118}$$

is the projection of v_3 along v_1. The displacement v_1 is allowed to wrap the brane between the 13 vertices, and we should sum over all wrappings. From figure 4.4, we see that v_1 must be at least as large as $\tilde{v}_3$ and so it is convenient to let

$$v_1 = 2\pi L n + \tilde{v}_3\,, \tag{4.119}$$

after which the resummation proceeds just as in sec. 4.5.1, with the result

$$e^{-S_{\rm cl}} = \frac{\sqrt{2\alpha'\Delta t}}{L}\mathrm{e}^{-\mathrm{Area}/2\pi\alpha'}\mathrm{e}^{-\Delta t Y^2/2\pi\alpha'}\sum_{m=-\infty}^{\infty} e^{-2\pi\alpha'\Delta t m^2/L}\,. \tag{4.120}$$

4.5.3 The purely twisted loop: $(t - y_3) \to 0$, generic y_i

As explained in Appendix C.3, we now have

$$W = \begin{pmatrix} A + i\Delta t_1' & AC & A - i\Delta t_3' \\ 1 & 1 & 1 \\ B & BC & B \end{pmatrix} \tag{4.121}$$

with A, B and C defined as per the previous section, and

$$\begin{aligned} \Delta t_1' &= \frac{\mathrm{i}}{2}\left[\frac{\pi^{\theta_1 - 1}}{\theta_1}(t - y_3)^{\theta_1} + \frac{\pi^{\theta_3 - 1}}{\theta_3}(t - y_3)^{\theta_3}\right] \\ \Delta t_3' &= \frac{\mathrm{i}}{2}\left[\frac{\pi^{-\theta_1}}{1 - \theta_1}(t - y_3)^{1-\theta_1} + \frac{\pi^{-\theta_3}}{1 - \theta_3}(t - y_3)^{1-\theta_3}\right]. \end{aligned} \tag{4.122}$$

The same argument as in section 4.5.2 then leads to

$$c_3 = \frac{v_2}{1 + \Delta t_3'/\Delta t_1'} + \frac{\mathrm{i}}{\Delta t_1' + \Delta t_3'}\left(v_1 - \frac{A}{B}v_3\right). \tag{4.123}$$

For $\theta_1 < \frac{1}{2}$ and $\theta_3 < \frac{1}{2}$, $\lim_{(t-y_3)\to 0} \Delta t_3'/\Delta t_1' = 0$, and so the first term remains finite in the limit. The second term (and therefore $S_{\rm cl}$) tends to infinity in the limit, unless

$$v_1 = \frac{A}{B} v_3 = \tilde{v}_3 \,, \tag{4.124}$$

in which case $c_3 = v_2$. Note that

$$\tilde{v}_3 = e^{-i\pi\theta_1} \frac{\sin \pi\theta_2}{\sin \pi\theta_3} f_{12} \tag{4.125}$$

is the projection of f_{12} along the v_1 direction, so this condition amounts to constraining our wrapping to triangles which are congruent to the original. As in the previous section, the origin of this constraint on v_1 lies in figure 4.4; in general, v_1 must be at least as large as $\tilde{v}_3$, but in the limit where we take vertex operators 1 and 3 to opposite sides of the worldsheet v_1 is pinched into a limit, leading to (4.124).

Substituting in to (4.91), one finds the classical action

$$2\pi\alpha' S_{\rm cl} = 2\left|\frac{v_2}{2}\right|^2 \Delta t_3' + \frac{\alpha}{4} |v_3 - \hat{v}_2|^2 + \frac{3\alpha}{4} |\hat{v}_2|^2 \,. \tag{4.126}$$

The first term, which goes to zero in the limit, is the stretching term already encountered. The second and third terms are area factors which give various combinations of Yukawa triangles. The three Yukawa couplings in the first diagram of limit 2 of figure 4.2 may be recovered by taking $v_3 = \hat{v}_2$. There are no terms suitable for Poisson resummation in this limit and so, correctly, Kaluza-Klein modes are not present.

4.5.4 The untwisted & twisted loop limit: $(t - y_3) \to \infty$, $y_2 \to y_1$

From appendix C.4, the W matrix in this limit is

$$W = \begin{pmatrix} \mathrm{i}\Delta t + E & \mathrm{i}\Delta t + E & -\mathrm{i}\Delta t - E \\ 1 & 1 & 1 \\ W_3^1 & W_3^2 & W_3^3 \end{pmatrix} \tag{4.127}$$

where

$$E = -\frac{\mathrm{i}}{2\pi} \left(2\gamma_E + \psi(\theta_3) + \psi(1-\theta_3)\right) \,. \tag{4.128}$$

The monodromy conditions $v_a = W_a^i c_i$ now lead to

$$c_3 = \frac{v_2}{2} - \frac{v_1}{2\left(\mathrm{i}\Delta t - E\right)} . \tag{4.129}$$

In this limit, $W_3^i \to 0$ (c.f. eq. C.39). Therefore, the action is

$$2\pi\alpha' S_{cl} = \left|\frac{v_2}{2}\right|^2 (\Delta t - \mathrm{i}E) + \frac{\alpha}{4}|v_3|^2 + \frac{|v_1|^2}{4\left(\Delta t - \mathrm{i}E\right)} . \tag{4.130}$$

The first specimen is the standard string stretching suppression. The term in $-\mathrm{i}E$ has a minimum around $\theta_3 = \frac{1}{2}$ - like (4.116), it is also attempting to prevent the string stretching. The third term is the tree level Yukawa coupling; as we see from figure 4.2, no other couplings are present in this diagram. The fourth term may be Poisson resummed, after which the action takes the form

$$e^{-S_{\rm cl}} = \frac{\sqrt{2\alpha'\left(\Delta t - \mathrm{i}E\right)}}{L} \mathrm{e}^{-\mathrm{Area}/2\pi\alpha'} \mathrm{e}^{-(\Delta t - \mathrm{i}E)Y^2/2\pi\alpha'} \sum_{m=-\infty}^{\infty} e^{-2\pi\alpha'(\Delta t - \mathrm{i}E)m^2/L} . \tag{4.131}$$

4.6 Extraction of β-functions

To complete our analysis, we will demonstrate how β-functions may be extracted by considering limit 3 – that is, the limit with both twisted and untwisted states in the loop. We concentrate on the field renormalization terms A_2 and A_3.

4.6.1 Factorization onto partition function

Recall that the amplitude takes the form

$$\mathcal{A} = \int_0^\infty \frac{\mathrm{d}t}{t} f(t) \int \mathrm{d}z_1 \mathrm{d}z_2 \mathrm{d}z_3 \; A(z_1, z_2, z_3) . \tag{4.132}$$

The first thing that we must do is determine the overall normalization $f(t)$ in (4.132). This may be done by the same mechanism used to determine phases previously in 4.3: factorization of the amplitude in the limit where the vertex operators come together (limit 0 of figure 4.2).

In the factorization limit one expects to find $\mathcal{A} \to \mathcal{Z}\,\mathcal{Y}$. It was shown in section 4.5.1 that the classical part of the amplitude factorizes correctly, so in what follows we concentrate on the quantum piece. For the case of D6-branes in a flat space, the

quantum part of the partition function is, in the $t \to \infty$ limit,

$$\mathcal{Z}_{\rm qu} = \int_0^\infty \frac{\mathrm{d}t}{4t} t^{-\frac{1}{2}(6+1)} \mathrm{e}^{\pi t} \sum_{\alpha\beta} \delta_{\alpha\beta} \vartheta_{\alpha\beta}(0)^4 \,, \tag{4.133}$$

where we have ignored an infinite volume factor. We will also need the quantum normalization of the tree-level Yukawa coupling, which is [50,51,91–95]

$$\mathcal{Y}_{\rm qu} = \prod_{i=1}^{3} \left[\frac{\Gamma(\theta_1^i)\,\Gamma(\theta_2^i)\,\Gamma(\theta_3^i)}{\Gamma(1-\theta_1^i)\,\Gamma(1-\theta_2^i)\,\Gamma(1-\theta_3^i)} \right]^{\frac{1}{4}} . \tag{4.134}$$

We now have nearly all the information required to write down the A_i terms in the $t \to \infty$ limit, save for one technicality: when we first began to construct correlators in terms of ϑ_1-functions in section 4.2.3, we mentioned that they ought to contain a contribution $r(t)$ which would regulate the correlators in the limit $z \to 0$. As we are now interested in the t-dependence of the correlators, we can no longer ignore this piece, which simply corresponds to making the replacement $\vartheta_1(z) \to \vartheta_1(z)/\vartheta_1'(0)$ everywhere, so that in the $t \to \infty$ limit the relevant expansion is just

$$\frac{\vartheta_1(\mathrm{i}y)}{\vartheta_1'(0)} \simeq \frac{\mathrm{i}\sinh(\pi y)}{\pi} . \tag{4.135}$$

No such replacement is made in the spin-structure dependent portion, as it does not originate from a physical propagator.

As explained in section 4.3, each of the terms A_1, A_2, A_3 factors correctly onto the partition function. We could therefore obtain $f(t)$ from any combination of these terms; we choose the field renormalization limits A_2 and A_3, as it is a field renormalization we will be ultimately interested in. To write down A_2 and A_3 in the limit, a result for $\det W$ as $y_3 \to y_2 \to 0$ is required. This is derived in appendix C.1 as

$$|\det W| = \frac{8\pi^2 t}{\Gamma(1-\theta_1)\,\Gamma(1-\theta_2)\,\Gamma(1-\theta_3)} y_{12}^{-\theta_3} y_{13}^{-\theta_2} y_{23}^{-\theta_1} y_2 \left(\theta_1 y_1 + \theta_2 y_2 - (1-\theta_3) y_3\right) . \tag{4.136}$$

Notice that the factor of $y_2\left(\theta_2^i y_2 - (1-\theta_3^i) y_3\right)$ is exactly that required to make the twist correlator (4.57) symmetric in the y_i – which of course it should be, as it it does not distinguish between fermions and bosons.

The integrals are simplified if we use translational invariance on the worldsheet

to fix $y_1 = 0$ (inserting a factor of t to compensate) and make the change of variables

$$\rho = \frac{y_2}{y_3} \qquad \lambda = \frac{t - y_3}{t}\,, \tag{4.137}$$

so that the integration over all vertex operator positions (4.6) is performed as

$$\mathcal{A}_2 + \mathcal{A}_3 = -\mathrm{i} \int_0^\infty \frac{\mathrm{d}t}{t} f(t)\, t^3 \int_0^1 \mathrm{d}\rho \int_0^1 \mathrm{d}\lambda\ (A_2 + A_3)\,. \tag{4.138}$$

Inserting (4.135) and (4.136) into (4.74) and (4.75), one finds

$$\begin{aligned}\mathcal{A}_2 = &\int_0^\infty \frac{\mathrm{d}t}{t} f(t)\, g(t) \sum_{\alpha\beta} \delta_{\alpha\beta}\vartheta_{\alpha\beta}\,(0)^4 \\ &\Big[k_1\cdot k_3 \int_0^1 \mathrm{d}\rho\ \rho^{-1+k_1\cdot k_2+\frac{1}{2}m^2}\,(1-\rho)^{-1+k_2\cdot k_3-\frac{1}{2}m^2} \int_0^1 \mathrm{d}\lambda\ (1-\lambda)^{-1+k_1\cdot k_2+k_1\cdot k_3+k_2\cdot k_3-\frac{1}{2}m^2} \\ &+k_3^2 \int_0^1 \mathrm{d}\rho\ \rho^{k_1\cdot k_2+\frac{1}{2}m^2}\,(1-\rho)^{-2+k_2\cdot k_3-\frac{1}{2}m^2} \int_0^1 \mathrm{d}\lambda\ (1-\lambda)^{-2+k_1\cdot k_2+k_1\cdot k_3+k_2\cdot k_3-\frac{1}{2}m^2}\Big]\end{aligned} \tag{4.139}$$

and

$$\begin{aligned}\mathcal{A}_3 = &-\int_0^\infty \frac{\mathrm{d}t}{t} f(t)\, g(t) \sum_{\alpha\beta} \delta_{\alpha\beta}\vartheta_{\alpha\beta}\,(0)^4 \\ &k_2\cdot k_3 \int_0^1 \mathrm{d}\rho\ \rho^{-1+k_1\cdot k_2+\frac{1}{2}m^2}\,(1-\rho)^{-2+k_2\cdot k_3-\frac{1}{2}m^2} \int_0^1 \mathrm{d}\lambda\ (1-\lambda)^{-2+k_1\cdot k_2+k_1\cdot k_3+k_2\cdot k_3-\frac{1}{2}m^2}\end{aligned} \tag{4.140}$$

where

$$g(t) = t^{-\frac{3}{2}+k_1\cdot k_2+k_1\cdot k_3+k_2\cdot k_3-\frac{1}{2}m^2} \prod_{i=1}^{3} \left[\frac{\Gamma(1-\theta_1^i)\,\Gamma(1-\theta_2^i)\,\Gamma(1-\theta_3^i)}{8\pi^2}\right]^{\frac{1}{2}}\,, \tag{4.141}$$

and an irrelevant overall phase has been dropped. All explicit angular dependence in the exponents of (4.139, 4.140) has vanished via the relation $m^2 = \sum_i \theta_3^i - 1$.

On shell, the momenta obey $k_1^2 = 0$, $k_2^2 = 0$, $k_3^2 = -m^2$, and so

$$k_1\cdot k_2 = -\frac{1}{2}m^2\,, \qquad k_1\cdot k_3 = \frac{1}{2}m^2\,, \qquad k_2\cdot k_3 = \frac{1}{2}m^2\,. \tag{4.142}$$

It is therefore clear that the integrals over ρ contain poles on-shell. We deal with

these by writing the integrals as gamma functions which may then be expanded about the poles: in A_3, for instance,

$$\int_0^1 \mathrm{d}\rho\, \rho^{-1+k_1\cdot k_2+\frac{1}{2}m^2}\,(1-\rho)^{-2+k_2\cdot k_3-\frac{1}{2}m^2} = \frac{\Gamma\left(k_1\cdot k_2+\frac{1}{2}m^2\right)\Gamma\left(k_2\cdot k_3-\frac{1}{2}m^2-1\right)}{\Gamma\left(k_1\cdot k_2+k_2\cdot k_3-1\right)} \simeq \frac{\left(k_1\cdot k_2+k_2\cdot k_3\right)}{\left(k_1\cdot k_2+\frac{1}{2}m^2\right)\left(k_2\cdot k_3-\frac{1}{2}m^2\right)}\,. \tag{4.143}$$

Performing a similar expansion in A_2 and taking everything on-shell that does not lead to a pole, we end up with

$$\mathcal{A}_2+\mathcal{A}_3 = \int_0^\infty \frac{\mathrm{d}t}{t} f(t)\, g(t) \sum_{\alpha\beta} \delta_{\alpha\beta}\vartheta_{\alpha\beta}(0)^4\, \frac{k_1\cdot k_2+k_2\cdot k_3}{k_1\cdot k_2+\frac{1}{2}m^2}\left[\frac{k_2\cdot k_3-k_1\cdot k_3}{k_2\cdot k_3-\frac{1}{2}m^2}-m^2\right]. \tag{4.144}$$

The $k_2\cdot k_3-k_1\cdot k_3$ pole occurs because of the relative minus sign between the A_2 and A_3 terms, which may be traced back to the results of the picture-changing in equations (4.23-4.26). The poles in the last two terms cancel when we go on-shell, yielding the finite result

$$\mathcal{A}_2+\mathcal{A}_3 = \left(1-m^2\right)\int_0^\infty \frac{\mathrm{d}t}{t} f(t)\, g(t) \sum_{\alpha\beta} \delta_{\alpha\beta}\vartheta_{\alpha\beta}(0)^4\,. \tag{4.145}$$

Comparison of (4.145) with the partition function (4.133) and Yukawa normalization (4.134) then shows that

$$f(t) = t^{-2}\mathrm{e}^{\pi t}\frac{1}{1-m^2}\mathcal{Y}_{\mathrm{qu}}\prod_{i=1}^{3}\left[\frac{\Gamma\left(1-\theta_1^i\right)\Gamma\left(1-\theta_2^i\right)\Gamma\left(1-\theta_3^i\right)}{8\pi^2}\right]^{-\frac{1}{2}}. \tag{4.146}$$

In a compact space, $\mathcal{Z}_{\mathrm{qu}}$ is modified by a power of $t^{\frac{3}{2}}$ as $t\to\infty$, since the Kaluza-Klein modes are quenched in this limit and ought to be resummed (c.f eq. 3.8). In this case one should also include a power of $t^{\frac{3}{2}}$ in (4.145) coming from the resummation (4.104), so there is no net effect upon $f(t)$.

As a check, one may wish to verify that the same power of t is obtained when the term A_1 is factored onto the partition function. It is then necessary to consider the term $\Phi(z_1,z_2,z_3)$ which is present in A_1 (displayed explicitly in figure 4.5). Note that by (4.66),

$$\lim_{w\to z} F_3(w,z) = 1 \tag{4.147}$$

so that the first term in Φ becomes θ_3. The second term in Φ vanishes by $\theta_1+\theta_2+\theta_3=$

1, and hence one finds that

$$\lim_{z_1 \to z_2 \to z_3} \sum_{i=1}^{3} \Phi^i(z_1, z_2, z_3) = m^2 + 1 . \tag{4.148}$$

Comparing (4.71) and (4.75), we see that the rest of A_1 is of the same form as A_3 in the factorization limit; therefore, the correct power of t will be obtained.

4.6.2 The running coupling: logarithmic and power-law regimes

At last, we have manufactured all the ingredients necessary to evaluate Yukawa coupling renormalization. We begin by considering the case of an $\mathcal{N} = 1$ supersymmetric set-up, where the amplitude comes purely from the term A_3, and again work with pinching limit 3 of figure 4.2.

It is now necessary to include the effects of the spin-dependent theta functions $\vartheta_{\alpha\beta}$, which is most easily done by working with A_3 in the post-Riemann-identity form (4.76). Fixing $y_1 = 0$, making the replacement (4.135), using the result (C.40) for $\det W$ in the limit $y_2 \to 0$ and taking the limit $y_2 \to 0$ in the full expression leads to the following explicit form for A_3:

$$\begin{aligned} A_3 = -\overline{u}_1 u_2 \mathrm{e}^{-S_{\mathrm{cl}}} k_2 \cdot k_3 y_2^{k_1 \cdot k_2 - \frac{3}{2}} \sinh(y_3)^{k_1 \cdot k_3 + \frac{1}{2}\left(\theta_1^1 + \theta_1^2 + \theta_1^3\right) - 1} \sinh(y_{23})^{k_2 \cdot k_3 + \frac{1}{2}\left(\theta_2^1 + \theta_2^2 + \theta_2^3\right) - 3} \\ \left[\prod_{i=1}^{3} \left(\frac{\Gamma(1-\theta_1)\Gamma(1-\theta_2)\Gamma(1-\theta_3)}{4\pi}\right)^{\frac{1}{2}} \left((2\pi y_2)^{1-\theta_3}(t-y_3)\right)^{-\frac{1}{2}} \sinh\left(\left(\theta_3^i - 1\right) y_3\right)^{\frac{1}{2}} y_2^{\frac{1}{2}}\right] \\ \mathrm{e}^{-\pi t} \sinh\left(\left(1 + \theta_3^1 + \theta_3^2 + \theta_3^3\right) y_3\right) \sinh\left(\left(1 + \theta_3^1 - \theta_3^2 - \theta_3^3\right) y_3\right) \\ \sinh\left(\left(1 - \theta_3^1 + \theta_3^2 - \theta_3^3\right) y_3\right) \sinh\left(\left(1 - \theta_3^1 - \theta_3^2 + \theta_3^3\right) y_3\right) . \end{aligned} \tag{4.149}$$

To cast (4.149) into a form that may be integrated, we note that it is dominated by large y_3, y_{23} and so we may approximate the sinh functions as exponentials, leading to the rather more pleasant result

$$A_3 \simeq \mathrm{e}^{-S_{\mathrm{cl}}} k_2 \cdot k_3 h(t) \mathrm{e}^{\left(k_1 \cdot k_3 + k_2 \cdot k_3 - m^2\right)\pi y_3} (t - y_3)^{-\frac{3}{2}} y_2^{-1 + k_1 \cdot k_2 + \frac{1}{2}m^2} , \tag{4.150}$$

where

$$h(t) = \mathrm{e}^{-\pi t} (2\pi)^{\frac{1}{2} - k_1 \cdot k_3 - k_2 \cdot k_3 + m^2} \prod_{i=1}^{3} \left[\frac{\Gamma(1-\theta_1^i)\Gamma(1-\theta_2^i)\Gamma(1-\theta_3^i)}{4\pi}\right]^{\frac{1}{2}} \tag{4.151}$$

with an overall phase dropped. The effect of $\mathrm{e}^{-S_{\mathrm{cl}}}$ needs to be taken into account; specifically, one must decide whether or not to perform the Poisson resummation (4.131). The condition for the resummation to be valid is that $2\pi\alpha'\Delta t \gg L$, so that the integral depends upon the value of $\Delta t = t - y_3$; ergo, the result obtained will depend upon the energy scale under consideration.

As $\Delta t \to \infty$, resummation of the Kaluza-Klein modes is appropriate. Then, the classical action (4.131) contributes a factor

$$\frac{(t-y_3)^{\frac{3}{2}}}{L_1 L_2 L_3} \tag{4.152}$$

to A_3 (we have set $\alpha' = \frac{1}{2}$ here). Choosing to make the change of variables (4.137), the amplitude integral reads

$$\mathcal{A}_3 = -\mathrm{i}\int_{1/\Lambda^2}^{1/\mu^2} \frac{\mathrm{d}t}{t} f(t)\, t^3 \int_0^1 \mathrm{d}\rho \int_{1/t\Lambda'^2}^1 \mathrm{d}\lambda\, A_3 \tag{4.153}$$

At this point we should say something about the cut-offs on the integrals. Firstly, note that we will require a UV cutoff Λ on our t-integral, despite the UV-finite nature of string theory. This cutoff is an artefact of making the large-t approximation, equivalent to sending $\alpha' \to 0$; if we were able to perform the appropriate elliptic integrals *without* making this approximation, we ought to find a UV-regular result. Secondly, we have placed a lower cut-off of $1/t\Lambda'^2$ on the λ integral. This may be viewed as a UV cutoff, since it removes the region where $y_3 \to t$. With a suitable choice for Λ', it also enforces the requirement that $2\pi\alpha'\Delta t \gg L$ for the Kaluza-Klein resummation to be valid.

With our change of variables, we have

$$\begin{aligned}\mathcal{A}_3 = &-\int_{1/\Lambda^2}^{1/\mu^2} \frac{\mathrm{d}t}{t} f(t)\, h(t)\, t^{2+k_1\cdot k_2+\frac{1}{2}m^2} (L_1 L_2 L_3)^{-1}\, k_2\cdot k_3 \\ &\int_0^1 \mathrm{d}\rho\, \rho^{-1+k_1\cdot k_2+\frac{1}{2}m^2} \int_{1/t\Lambda'^2}^1 \mathrm{d}\lambda\, \mathrm{e}^{\left(k_1\cdot k_3+k_2\cdot k_3-m^2\right)\pi t(1-\lambda)} (1-\lambda)^{k_1\cdot k_2+\frac{1}{2}m^2} .\end{aligned} \tag{4.154}$$

As in the previous section, the function of the ρ integral is to supply a pole corresponding to the internal propagator in figure 4.2. The λ integral contains no poles when taken on-shell, so we may impose the on-shell conditions (4.142) here *before*

performing the integral. Sending the cutoff $\Lambda' \to \infty$,

$$\begin{aligned}\mathcal{A}_3 &= -\left(L_1L_2L_3\right)^{-1}\frac{k_2\cdot k_3}{k_1\cdot k_2+\frac{1}{2}m^2}\int_{1/\Lambda^2}^{1/\mu^2}\frac{\mathrm{d}t}{t}f\left(t\right)h\left(t\right)t^{2+k_1\cdot k_2+\frac{1}{2}m^2}\\ &= \mathcal{Y}_{\mathrm{qu}}\left(2\pi\right)^{-1}\left(L_1L_2L_3\right)^{-1}\int_{1/\Lambda^2}^{1/\mu^2}\frac{\mathrm{d}t}{t}\\ &\propto \log\left(\frac{\mu}{\Lambda}\right).\end{aligned} \tag{4.155}$$

Where in the second line we have set $m^2 = 0$ and cancelled the poles before taking everything on-shell. As one would expect, the string calculation reproduces the usual logarithmic running of couplings at low energy.

At higher energy scales, t can become sufficiently small that resummation of the Kaluza-Klein modes is no longer appropriate: $2\pi\alpha'\Delta t \ll L_i$ for all L_i. The classical action then contributes no powers of Δt to the integral, which now reads

$$\begin{aligned}\mathcal{A}_3 = &-\int_{1/\Lambda^2}^{1/\mu^2}\frac{\mathrm{d}t}{t}f\left(t\right)h\left(t\right)t^{\frac{1}{2}+k_1\cdot k_2+\frac{1}{2}m^2}\\ &k_2\cdot k_3\int_0^1\mathrm{d}\rho\,\rho^{-1+k_1\cdot k_2+\frac{1}{2}m^2}\int_{1/t\Lambda'^2}^1\mathrm{d}\lambda\,\mathrm{e}^{\left(k_1\cdot k_3+k_2\cdot k_3-m^2\right)\pi t(1-\lambda)}\left(1-\lambda\right)^{k_1\cdot k_2+\frac{1}{2}m^2}\lambda^{-\frac{3}{2}}.\end{aligned} \tag{4.156}$$

Notice that this differs from (4.154) by a power of $t^{-\frac{3}{2}}$. Also, the λ integral now has a pole as $\lambda \to 0$ (*i.e.* $y_3 \to t$), so that after performing the ρ integral, cancelling poles and taking everything on-shell,

$$\mathcal{A}_3 = \mathcal{Y}_{\mathrm{qu}}\left(2\pi\right)^{-1}\int_{1/\Lambda^2}^{1/\mu^2}\mathrm{d}t\,t^{-\frac{5}{2}}\int_{1/t\Lambda'^2}^1\mathrm{d}\lambda\,\lambda^{-\frac{3}{2}}. \tag{4.157}$$

The IR and UV cutoffs in the two integrals should be associated with each other, so that

$$\mathcal{A}_3 \propto \mu^3 + \frac{3}{2}\Lambda^2\Lambda'. \tag{4.158}$$

We have obtained μ^3 running, as one would expect for D6-branes where three extra dimensions are present.

If the wrapping lengths L_i are of mixed sizes, the amplitude may be an admixture of the two regimes, with the power of μ in (4.158) dropping by one for each dimension which is not resummed. One may then envisage a situation where the power-law behaviour changes as the energy scale μ increases, beginning first with logarithmic running and then switching to power-law behaviour, with the power increasing as

a greater number of extra dimensions open up (*i.e.* as $2\pi\alpha'\Delta t$ exceeds the brane wrapping lengths L_i in the various tori).

In a non-supersymmetric model, the above results are modified in two ways. Firstly, the terms A_1 and A_2 no longer vanish via the Riemann identity; therefore we have a vertex renormalization term plus an additional source of field renormalization. We will not evaluate the vertex renormalization here (although we point out that sections 4.2-4.4 contain all of the necessary ingredients to do so), but instead examine how the field renormalization is modified. The function $f(t)$ which was determined in sec. 4.6.1 is not modified in a nonsupersymmetric model; the only difference is that we can no longer set m^2 there, so that the amplitudes A_2 and A_3 will now have a factor of $1 - m^2$ on the bottom.

Evaluation of the term A_3 proceeds exactly as above. The cancellation of poles in 4.155 and 4.157 appears now no longer valid, since we have $m^2 \neq 0$. However, including the term A_2 (which may be calculated in an analogous manner to A_3, save for an intermediate expansion in m^2) leads to an extra contribution which conspires to produce a cancellation of the same form as that in (4.144). This extra contribution cancels with the factor of $1-m^2$ in $f(t)$, so that the field renormalization behaviour in non-supersymmetric models is the same as that in supersymmetric models.

In the case where one of the branes goes through an orbifold fixed point, or we have O-planes in our model, the comments at the end of section 4.3 apply – the spin-dependent portions of the A_i are modified. $f(t)$ should then be determined by factoring onto a *twisted* partition function, in which the modifications of the spin-dependent terms must be identical to those in the A_i. Up to an overall normalization, then, $f(t)$ will be unchanged. The field renormalization may then be evaluated by the procedure above, except that those portions of A_3 which come from spin-dependent terms (explicitly, the last two lines of 4.149) must be appropriately modified.

4.7 Summary and discussion

In this work, we have performed the first one-loop string calculation of Yukawa couplings on intersecting branes. We began by developing the necessary technology for the calculation, in particular enumerating the selection rules on string states, describing the effects of picture-changing on the vertex operators and developing open-string correlators for the spin and twist fields. We then applied this technology to demonstrate the supersymmetric non-renormalization theorem, and identified the

vertex and field renormalization contributions to the amplitude.

Following this, we derived an expression for the classical instanton part of the twist fields, before examining them in the various field-theory pinching limits of figure 4.2. In each limit, the classical action could be correctly factorized onto the appropriate tree-level Yukawa coupling(s) and partition function piece. The origin of Kaluza-Klein modes in those limits which contain bosons in the loop was identified. Finally we showed how Yukawa beta functions in intersecting brane models may be extracted from the calculation, finding that in the field-theory limit both logarithmic and power-law runnings are recovered depending upon the energy scale under consideration.

One point that we did not address is the quantum normalization of the various limits. Note that the normalization which enters the amplitude from the twist operators (via the $|\det W|^{-\frac{1}{2}}$ term) does not have the correct form (4.134), and that this must be inserted into the normalization function $f(t)$ manually. Even so, one might expect that it ought to be possible to recover the correct normalization factor by comparing the limits 2 and 3, which should contain factors of $\mathcal{Y}^3$ and $\mathcal{Y}$ respectively. Sadly, this is not the case: the problem is that limit 2 of figure 4.2 contains only twisted states in the loop, and thus ought to be factored onto a twisted partition function (a partition function between two branes at an angle). Strictly speaking, the $f(t)$ obtained is now *different*. It is then necessary to include manually a $\mathcal{Y}^3$ factor, and our reasoning becomes circular. We conclude that our three-point calculation cannot be used to extract the quantum normalization factor (4.134) – this is exactly the situation at tree-level, where the normalization must be obtained by factorization of a four-point correlator onto a three-point correlator [50,51,85,91–95].

As a final remark, we note that much of the conformal field theory framework developed in this chapter is applicable to one-loop calculations on intersecting branes in general (and also in fact to orbifold models, providing an alternative to the calculations presented in [72]). In particular it would be interesting to apply our results to a four-point correlator at one-loop, which contains information about the one-loop Kähler potential [95]. Furthermore, factorization of this four-point amplitude onto a three-point amplitude should explicitly reproduce the Yukawa normalization factor (4.134).

Chapter 5

Overall Summary

String theory is widely recognized as the leading candidate for the 'ultimate theory' which is presumed to lie somewhere beyond the Standard Model. From a phenomenologist's point of view, the key issue with the theory is its requirement that spacetime be ten-dimensional, and that no top-down principle which selects the Standard Model vacuum currently exists. String phenomenology, being the construction and investigation of models which embed our four-dimensional world in the higher-dimensional space, is then an important area of research.

It is often the case that amplitude calculations in these models are performed in extra-dimensional field theories, which is not always an entirely appropriate tool. A general comment about this thesis is that we have shown that it is quite viable, and not overly cumbersome, to use one-loop string technology for phenomenological purposes. Furthermore, we have demonstrated that it is possible to implement such calculations directly through the Polyakov path-integral, without resorting to the 'background field' methods previously used in string phenomenology at one loop [48, 49].

We began in chapter 1 by motivating and introducing the subject of string compactifications in general terms, finally introducing the brane-based models to which our calculations are relevant. Chapter 2 then gave a pedagogical introduction to string theory – in particular, quantization of the classical string, string perturbation theory and an introduction to branes. We also introduced the one-loop partition function, a primary element in our later calculations, and discussed the effect of branes at a relative angle.

In chapter 3 we showed that the hidden-sector branes which occur in certain brane models can communicate with the visible sector through a novel effect known as Kinetic Mixing, in which $U(1)$'s from two sectors mix together. In a brane

model, Kinetic Mixing occurs via a one-loop annulus diagram between a brane and antibrane, with two open-string boson vertex operator insertions on the boundary. To evaluate this diagram, we first explored the behaviour of the one-loop partition function in a compact space and showed how to isolate the physically meaningful contribution. We then introduced appropriate vertex operators and calculated their correlation in terms of Jacobi ϑ-functions.

Using experimental limits on milli-charged particles, we demonstrated that in intermediate-scale string constructions with $M_S \sim 10^{11}$ GeV one must either have the antibranes situated on orientifold planes so that $\mathrm{Tr}\,(\lambda_{\mathrm{visible}})\,\mathrm{Tr}\,(\lambda_{\mathrm{hidden}}) = 0$, require that have extra dimensions which are massively antisymmetric in size (and predict milli-charged particles), accept a string scale of $M_s \lesssim 10^8\,\mathrm{GeV}$ (and again, predict milli-charged particles), or ask that all $U(1)$'s on the antibrane are broken. However, in the latter case, supersymmetry-breaking communication then once again constrains $M_s \lesssim 10^8\,\mathrm{GeV}$.

We then turned to models based on intersecting branes in chapter 4, where we calculated the one-loop renormalization of Yukawa couplings. Again, this involved the computation of a three-point diagram, this time with three vertex operator insertions on the boundary. This time, the vertex operators represented strings localized at brane intersections. To ensure that the overall amplitude had the correct ϕ-charge, it was necessary to perform picture-changing operations on these operators. It was also necessary to ensure that the amplitude obeyed conservation of fermion number (H-charge conservation).

Evaluation of the amplitude required knowledge of the correlation functions of the various fields appearing in the picture-changed vertex operators. In particular, we had to develop correlators for spin fields on the annulus (section 4.2.4), twist fields on the annulus (section 4.2.6, based upon work in ref. [84]) and excited twist fields on the annulus (section 4.2.7). Using this technology we identifed the vertex and field-renormalization contributions to the amplitude, demonstrating that the vertex renormalization contribution vanishes in $\mathcal{N} = 1$ supersymmetric models.

We then discussed the classical contribution to the amplitude (*i.e.* the area of the string worldsheet), and demonstrated that it behaved correctly in the various field-theory limits which occur as vertices are pinched together on the worldsheet. Finally, we picked a particular field theory limit corresponding to a field renormalization, and evaluated the amplitude explicitly. We found that at low energies the Yukawa coupling runs logarithmically, but at higher energies switches to a power-law behaviour as Kaluza-Klein modes open up. This confirms the field-theory calculations presented in refs. [62, 63].

As we mentioned in the conclusion to the previous chapter, a prime contribution made in this thesis is the wide applicability of the material in chapter 4 to one-loop computations in all string models, both heterotic and brane-based. Some possible extensions were mentioned in section 4.7: a more general exercise would be to extend the results given to an N-point coupling on intersecting branes. In particular, it ought to be possible to generalize the discussion of H-charge conservation and picture-changing to specfic classes of amplitudes involving fermions and bosons, and also to explicitly evaluate the N-point W-integrals as two vertices coaelesce. We leave this generalization for a future researcher.

Appendix A

The Jacobi ϑ-functions

We make extensive use of the Jacobi ϑ-functions, for which we take the usual definition [10, 47],

$$\begin{aligned}
\vartheta_{00}(z,\mathrm{i}t) =& \vartheta_3(z|\mathrm{i}t) \\
=& \sum_{n=-\infty}^{\infty} \mathrm{e}^{-\pi n^2 t}\mathrm{e}^{2\mathrm{i}\pi n z} && \text{(A.1)} \\
=& 1 + 2\mathrm{e}^{-\pi t}\cos(2\pi z) + 2\mathrm{e}^{-4\pi t}\cos(4\pi z) + \cdots && \text{(A.2)} \\
\vartheta_{01}(z,\mathrm{i}t) =& \vartheta_4(z|\mathrm{i}t) \\
=& \sum_{n=-\infty}^{\infty} (-1)^n \mathrm{e}^{-\pi n^2 t}\mathrm{e}^{2\mathrm{i}\pi n z} && \text{(A.3)} \\
=& 1 - 2\mathrm{e}^{-\pi t}\cos(2\pi z) + 2\mathrm{e}^{-4\pi t}\cos(4\pi z) - \cdots && \text{(A.4)} \\
\vartheta_{10}(z,\mathrm{i}t) =& \vartheta_2(z|\mathrm{i}t) \\
=& \sum_{n=-\infty}^{\infty} \mathrm{e}^{-\pi\left(n-\frac{1}{2}\right)^2 t}\mathrm{e}^{2\mathrm{i}\pi\left(n-\frac{1}{2}\right)z} && \text{(A.5)} \\
=& 2\mathrm{e}^{-\pi t/4}\cos(\pi z) + 2\mathrm{e}^{-9\pi t/4}\cos(3\pi z) + \cdots && \text{(A.6)} \\
\vartheta_{11}(z,\mathrm{i}t) =& -\vartheta_1(z|\mathrm{i}t) \\
=& \sum_{n=-\infty}^{\infty} (-1)^{n-\frac{1}{2}} \mathrm{e}^{-\pi\left(n-\frac{1}{2}\right)^2 t}\mathrm{e}^{2\mathrm{i}\pi\left(n-\frac{1}{2}\right)z} && \text{(A.7)} \\
=& -2\mathrm{e}^{-\pi t/4}\sin(\pi z) + 2\mathrm{e}^{-9\pi t/4}\sin(3\pi z) + \cdots && \text{(A.8)}
\end{aligned}$$

We also define the Dedekind η-function as

$$\eta(\mathrm{i}t) = \mathrm{e}^{-\pi t/12}\prod_{n=1}^{\infty}\left(1 - \mathrm{e}^{-2\pi n t}\right) .$$

A useful expansion involving this function is

$$\eta\,(\mathrm{i}t)^{-m} = \mathrm{e}^{m\pi t/12} + m\mathrm{e}^{(m-24)\pi/12t} + \cdots$$

The ϑ and η functions possess a defined behaviour under the transformation $t \to 1/t$ (which is a special case of the modular transformation),

$$\vartheta_{\alpha\beta}\,(\mathrm{i}x, \mathrm{i}t) = \mathrm{i}^{\alpha\beta} t^{-1/2} \mathrm{e}^{\pi x^2/t} \vartheta_{\beta\alpha}\,(x/t, \mathrm{i}/t) \tag{A.9}$$

$$\eta(\mathrm{i}t) = t^{-1/2}\eta(\mathrm{i}/t)\,, \tag{A.10}$$

which allows their expansions to be written in terms of $1/t$. Also, the ϑ-functions obey a handy 'Riemann' identity,

$$\sum_{\alpha\beta} \delta_{\alpha\beta}\vartheta_{\alpha\beta}\,(x)\,\vartheta_{\alpha\beta}\,(y)\,\vartheta_{\alpha\beta}\,(u)\,\vartheta_{\alpha\beta}\,(v) = 2\vartheta_1\,(x')\,\vartheta_1\,(y')\,\vartheta_1\,(u')\,\vartheta_1\,(v')\,, \tag{A.11}$$

where $\delta_{00} = \delta_{11} = +1$, $\delta_{01} = \delta_{10} = -1$ and

$$\begin{aligned} x' &= \tfrac{1}{2}\,(x+y+u+v) & u' &= \tfrac{1}{2}\,(x+y-u-v) \\ y' &= \tfrac{1}{2}\,(x-y+u-v) & v' &= \tfrac{1}{2}\,(x-y-u+v)\,. \end{aligned} \tag{A.12}$$

Appendix B

Contractions between X fields

The operator calculations of chapters 3 and 4 require correlators between operators of the form X, $\dot{X}$ and $e^{ik\cdot X}$. The contractions between these operators (in particular, between two $\dot{X}$ operators) are most easily evaluated in a path-integral formalism.

Start with a generating functional

$$W[J] = \left\langle \exp\left[i \int d^2z\, J(z) \cdot X(z) \right] \right\rangle \tag{B.1}$$

where $J^\mu(z)$ is some current. Expanding X^μ in terms of a complete set of functions and completing the square as usual gives [10]

$$W[J] = \mathcal{Z}_X \exp\left[-\frac{1}{2} \int d^2z\, d^2w\, J^\mu(z)\, J_\mu(w)\, G(z-w) \right] . \tag{B.2}$$

Setting $J^\mu(z) = 0$ will give us the path integral with no vertex operators, which is just the partition function $\mathcal{Z}_X$. $G(z-w)$ is the Green's-function propagator for bosonic fields on the worldsheet, with the property $G(0) = 0$.

We will need the expectation value of n exponentials and m time derivatives of X^μ. Following ref. [96], we note that functionally differentiating (B.1) gives

$$-i\frac{\delta W}{\delta J_\mu(w)} = \left\langle X^\mu(w) \exp\left[i \int d^2z\, J(z) \cdot X(z) \right] \right\rangle . \tag{B.3}$$

Making the convenient choice $J_0^\mu(z) = \sum_{i=1}^n k_i^\mu \delta^2(z - z_i)$,

$$\left\langle \prod_{j=1}^m \dot{X}^{\mu_j}(z_j) \prod_{i=1}^n e^{ik_i\cdot X(z_i)} \right\rangle = \left[\prod_{j=1}^m -i\frac{\partial}{\partial y_j} \frac{\delta}{\delta J_{\mu_j}(z_j)} \right] W[J] \Bigg|_{J^\mu = J_0^\mu} \tag{B.4}$$

Here, we have used mixed notations as convenient; $\dot{X}^\mu \equiv \partial_y X^\mu$.

Using the representation (B.2) for $W[J]$, we find for the case of interest in chapter 3,

$$\left\langle \dot{X}^{\mu_1}(z_1)\, \mathrm{e}^{\mathrm{i}k_1\cdot X(z_1)} \dot{X}^{\mu_2}(z_2)\, \mathrm{e}^{\mathrm{i}k_2\cdot X(z_2)} \right\rangle = (-\mathrm{i})^2 \frac{\partial^2}{\partial y_1 \partial y_2} \frac{\delta^2 W[J]}{\delta J_{\mu_1}(z_1)\, J_{\mu_2}(z_2)}\bigg|_{J^\mu = J_o^\mu}$$
$$= -\mathcal{Z}_X \mathrm{e}^{-k_1\cdot k_2 G(z_1-z_2)} \left[k_1^{\mu_2} k_2^{\mu_1} \frac{\partial G(z_1-z_2)}{\partial y_1} \frac{\partial G(z_1-z_2)}{\partial y_2} + \eta^{\mu_1\mu_2} \frac{\partial^2 G(z_1-z_2)}{\partial y_1 \partial y_2} \right]. \quad \text{(B.5)}$$

From an operator point of view, the first term in square brackets comes from a product of two $\dot{X} \leftrightarrow$ exp contractions, and the second from a product of an $\dot{X} \leftrightarrow \dot{X}$ and an exp $\leftrightarrow$ exp contraction. In the actual calculation, we will need to integrate the right-hand side of (B.5) over y_1 and y_2. We may therefore integrate by parts, with the result

$$\int \mathrm{d}y_1 \mathrm{d}y_2 \left\langle \dot{X}^{\mu_1}(z_1)\, \mathrm{e}^{\mathrm{i}k_1\cdot X(z_1)} \dot{X}^{\mu_2}(z_2)\, \mathrm{e}^{\mathrm{i}k_2\cdot X(z_2)} \right\rangle$$
$$= -\mathcal{Z}_X \mathrm{e}^{-k_1\cdot k_2 G(z_1-z_2)} \left[k_1^{\mu_2} k_2^{\mu_1} - \eta^{\mu_1\mu_2}(k_1\cdot k_2) \right] \frac{\partial G(z_1-z_2)}{\partial y_1} \frac{\partial G(z_1-z_2)}{\partial y_2}, \quad \text{(B.6)}$$

which has the correct tensor structure for a vacuum polarization diagram.

The correlators of interest in chapter 4 are simpler, containing at most one $\dot{X}$ operator:

$$\left\langle \dot{X}^\mu(z_k) \prod_{i=1}^{n} \mathrm{e}^{\mathrm{i}k_i\cdot X(z_i)} \right\rangle = \mathcal{Z}_X \prod_{\substack{i<j \\ i\neq k}} \mathrm{i}k_j^\mu \mathrm{e}^{-k_1\cdot k_2 G(z_1-z_2)} \frac{\partial G(z_j-z_k)}{\partial y_k}. \quad \text{(B.7)}$$

Appendix C

W integrals in various limits

Information about the geometry of the problem is contained in the W-integrals (4.58), which we examine in the $t \to \infty$ limit. Begin with integrals around γ_1, which we take to be along the imaginary axis $z = \mathrm{i}q$. Using the expansion (A.8) together with the result $\theta_1 + \theta_2 + \theta_3 = 1$, one can write the integrals up to exponentially suppressed terms as

$$W_1^1 = \mathrm{i}\int_{(y_3-t)/2}^{(y_3+t)/2} \mathrm{d}q \; (\mathrm{i}\sinh \pi q)^{\theta_1 - 1} \left(\mathrm{i}\sinh \pi \left(q - y_2\right)\right)^{\theta_2} \left(\mathrm{i}\sinh \pi \left(q - y_3\right)\right)^{\theta_3 - 1} \\ \mathrm{i}\sinh \pi \left(q + \theta_2 y_2 + \left(\theta_3 - 1\right) y_3\right) \quad \text{(C.1)}$$

$$W_1^2 = \mathrm{i}\int_{(y_3-t)/2}^{(y_3+t)/2} \mathrm{d}q \; (\mathrm{i}\sinh \pi q)^{\theta_1} \left(\mathrm{i}\sinh \pi \left(q - y_2\right)\right)^{\theta_2 - 1} \left(\mathrm{i}\sinh \pi \left(q - y_3\right)\right)^{\theta_3 - 1} \\ \mathrm{i}\sinh \pi \left(q + \left(\theta_2 - 1\right) y_2 + \left(\theta_3 - 1\right) y_3\right) \quad \text{(C.2)}$$

$$W_1^3 = -\mathrm{i}\int_{-(y_3+t)/2}^{-(y_3-t)/2} \mathrm{d}q \; \overline{\left(-\mathrm{i}\sinh \pi q\right)^{-\theta_1} \left(-\mathrm{i}\sinh \pi \left(q + y_2\right)\right)^{-\theta_2} \left(-\mathrm{i}\sinh \pi \left(q + y_3\right)\right)^{-\theta_3}} \\ \overline{-\mathrm{i}\sinh \pi \left(q + \theta_2 y_2 + \theta_3 y_3\right)}, \quad \text{(C.3)}$$

where the translational invariance of the problem has been used to set $y_1 = 0$ (in what follows we always assume $0 < y_1 < y_2 < t$). Our approximation has lost the periodicity of ϑ_1 in the imaginary direction; therefore, we have chosen limits on the integrals so as to keep the branch cuts in the centre of the worldsheet, ensuring that we integrate over one complete period.

Integrals around around γ_2 are simpler. Using the same approximation, one finds

integrals of sine functions rather than sinh functions, taken along the real axis. In this case, we always find $W_2^i = 1$. Finally, integrals around γ_3 are of the same form as those around γ_1 but with the limits taken as 0 and y_2, and the overall result multiplied by a phase factor

$$P = 4e^{i\pi(\theta_2-\theta_1)} \sin(\pi\theta_2) \sin(\pi\theta_1) , \tag{C.4}$$

which comes from the Pochhammer loop [51].

C.1 Limit 0: $t \to \infty$, $y_1 \to y_2 \to y_3$

In this limit, we may expand (C.3) in y_1 and y_2 under the integrals, with the results

$$W_1^1 = W_1^2 = it + \mathcal{O}(y_i) \qquad W_1^3 = -it + \mathcal{O}(y_i) , \tag{C.5}$$

which give W the form

$$W \simeq \begin{pmatrix} it & it & -it \\ 1 & 1 & 1 \\ W_3^1 & W_3^2 & W_3^3 \end{pmatrix} \tag{C.6}$$

and hence

$$|\det W| = 2t\left(W_3^1 - W_3^2\right) . \tag{C.7}$$

Trigonometric identities simplify this combination to

$$W_3^1 - W_3^2 = iP \sinh(\pi y_2) \sinh(\pi(y_2\theta_2 + y_3(\theta_3 - 1))) \int_0^{y_2} dq\ (i\sinh\pi q)^{\theta_1-1} (i\sinh\pi(q-y_2))^{\theta_2-1} (i\sinh\pi(q-y_3))^{\theta_3-1} , \tag{C.8}$$

and in the limit of small y_i the integral reduces to one which may be evaluated using the Gauss hypergeometric function ${}_2F_1$,

$$\int_0^{y_2} dq\ q^{\theta_1-1}(q-y_2)^{\theta_2-1}(q-y_3)^{\theta_3-1} = \frac{\Gamma(\theta_1)\Gamma(\theta_2)}{\Gamma(\theta_1+\theta_2)} {}_2F_1\left(\theta_1, 1-\theta_3, \theta_1+\theta_2; \frac{y_2}{y_3}\right) y_2^{\theta_1+\theta_2-1} y_3^{\theta_3-1} . \tag{C.9}$$

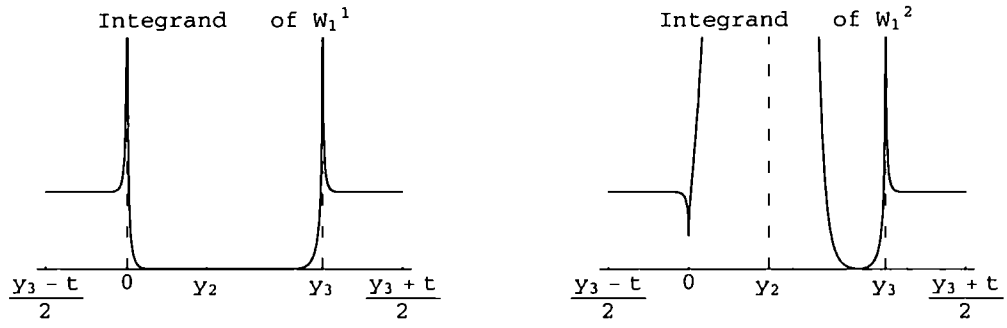

Figure C.1: Absolute value of the W_1^i integrands, for arbitrarily chosen angles $0 < \theta_j < \frac{1}{2}$ and generic y_i. Not shown is W_1^3, which is simply a reflection of W_1^1 in the y-axis.

Including the phase factor P and using the condition $\theta_1 + \theta_2 + \theta_3 = 1$, plus the identity ${}_2F_1(a, b, b; z) = (1 - z)^{-a}$, we end up with

$$|\det W| = \frac{8\pi^2 t}{\Gamma(1-\theta_1)\,\Gamma(1-\theta_2)\,\Gamma(1-\theta_3)} y_2^{-\theta_3} y_3^{-\theta_2} (y_3 - y_2)^{-\theta_1}\, y_2\,(\theta_2 y_2 - (1-\theta_3)\, y_3)\,. \tag{C.10}$$

If desired, we may reinstate y_1 by requiring that $\det W$ be translationally invariant; the result is shown in equation (4.136). We will also make use of W_3^3, which may be evaluated through use of hypergeometric functions as

$$W_3^3 = \frac{4\pi^2 y_{12}^{\theta_3} y_{13}^{\theta_2} y_{23}^{\theta_1}}{\Gamma(1-\theta_1)\Gamma(1-\theta_2)\Gamma(1-\theta_3)}\,. \tag{C.11}$$

C.2 Limit 1: $(t - y_3) \to \infty$, generic y_i

The structure of our integrands in this case is shown in figure C.1. The integrands of W_1^1 and W_3^1 both contain poles at $q = 0$ and $q = y_3$, but are regular elsewhere. Let us first consider integrals about γ_1. One may expand the W_1^1 integrand about the $q = 0$ pole as follows:

$$\begin{aligned} W_1^1\big|_0 &= \mathrm{i}\left(-\frac{1}{2}\right)^{1-\theta_1} \int_{(y_3-t)/2}^{\infty} \mathrm{d}q\ (\sinh \pi q)^{\theta_1 - 1}\, e^{\pi q(\theta_1 - 1)} \\ &= \mathrm{i}\frac{(-1)^{1-\theta_1}}{2\pi} B\left(\mathrm{e}^{\pi(t-y_3)}; 1-\theta_1, \theta_1\right) + 1\,, \end{aligned} \tag{C.12}$$

where $B(z; a, b)$ is the incomplete Euler Beta function. Expanding around the $q = y_3$ pole gives a similar result,

$$\begin{aligned} W_1^1\big|_{y_3} &= \mathrm{i}\left(\frac{1}{2}\right)^{1-\theta_3} \int_{-\infty}^{(y_3+t)/2} \mathrm{d}q \ (\sinh \pi (q - y_3))^{\theta_3 - 1} \, e^{\pi(q-y_3)(\theta_3-1)} \\ &= \mathrm{i}\left(\frac{1}{2}\right)^{1-\theta_3} \int_{-\infty}^{(t-y_3)/2} \mathrm{d}q' \ (\sinh \pi q')^{\theta_3 - 1} \, e^{\pi q'(\theta_3-1)} \\ &= \mathrm{i}\frac{(-1)^{1-\theta_3}}{2\pi} B\left(\mathrm{e}^{\pi(t-y_3)}; 1 - \theta_3, \theta_3\right) . \end{aligned} \tag{C.13}$$

The full W_1^1 is then found as the sum of these two,

$$W_1^1 = \frac{\mathrm{i}}{2\pi}\left[(-1)^{1-\theta_1} B\left(\mathrm{e}^{\pi(t-y_3)}; 1 - \theta_1, \theta_1\right) + (-1)^{1-\theta_3} B\left(\mathrm{e}^{\pi(t-y_3)}; 1 - \theta_3, \theta_3\right)\right] + 1 . \tag{C.14}$$

Since we are interested in the limit where $t - y_3 \to \infty$, we may apply the large-z expansion of the incomplete Euler Beta function,

$$B(z; a, b) = (-1)^{-a}\left(\mathrm{i}\pi + \log z - \psi(a) - \gamma_E\right) + \mathcal{O}\left(z^{-1}\right) \qquad (|z| \to \infty, \ a + b = 1) , \tag{C.15}$$

with the result

$$W_1^1 = \mathrm{i}(t - y_3) - \frac{\mathrm{i}}{2\pi}\left(2\gamma_E + \psi(1 - \theta_1) + \psi(1 - \theta_3)\right) + \mathcal{O}\left(t^{-1}\right) . \tag{C.16}$$

Now consider the W_1^3 integral, which is similar. An analogous expansion about the poles at $q = 0$ and $q = -y_3$ leads to

$$W_1^3 = -\frac{\mathrm{i}}{2\pi}\left[(-1)^{\theta_1} B\left(\mathrm{e}^{\pi(t-y_3)}; \theta_1, 1 - \theta_1\right) + (-1)^{\theta_3} B\left(\mathrm{e}^{\pi(t-y_3)}; \theta_3, 1 - \theta_3\right)\right] - 1 \tag{C.17}$$

and using the large-z expansion (C.15),

$$W_1^3 = -\mathrm{i}(t - y_3) + \frac{\mathrm{i}}{2\pi}\left(2\gamma_E + \psi(\theta_1) + \psi(\theta_3)\right) + \mathcal{O}\left(t^{-1}\right) . \tag{C.18}$$

The integrands for W_1^2 have poles at $q = y_2$ and $q = y_3$; however, the pole at y_2 is exponentially dominant for generic y_2. Therefore, the leading term in W_1^2 for generic y_2 is

$$W_1^2\big|_{y_2} = \mathrm{i}\,(-1)^{\theta_3}\,2^{\theta_2-1}\mathrm{e}^{\pi y_2(1-\theta_2)}\int_{-\infty}^{\infty}\mathrm{d}q\;\left(\sinh\pi\,(q-y_2)\right)^{\theta_2-1}\,\mathrm{e}^{\pi q(\theta_1-\theta_3)}$$
$$= \frac{\mathrm{i}\mathrm{e}^{2\pi y_2\theta_1}\Gamma\,(\theta_1)\,\Gamma\,(\theta_3)}{2\pi\Gamma\,(1-\theta_2)}\,. \tag{C.19}$$

We could also extract the sub-leading behaviour, which we expect to be of a similar form to the result in W_1^1, but as we will see below it is unnecessary for our calculation.

Integrals around the Pochhammer cycle γ_3 may be found using the same technique of expanding about poles in q, but keeping only the portion of the integral which corresponds to the region $0 < q < y_2$. For instance, W_3^1 is found from the positive portion of the expansion around the first pole multiplied by the Pochhammer factor (C.4),

$$W_3^1 = \mathrm{i}P\,W_1^1\big|_{0,q>0}$$
$$= -\mathrm{i}P\frac{(-1)^{\theta_1}}{2\,\sin(\pi\theta_1)}$$
$$= -2\mathrm{i}\mathrm{e}^{\mathrm{i}\pi\theta_2}\sin\,(\pi\theta_2)\,. \tag{C.20}$$

(The integrals W_1^i are along the principal branch, and so $(-1) = \mathrm{e}^{\mathrm{i}\pi}$.) Repeating the procedure for W_3^3 leads to an identical result,

$$W_3^3 = -2\mathrm{i}\mathrm{e}^{\mathrm{i}\pi\theta_2}\sin\,(\pi\theta_2)\,. \tag{C.21}$$

For generic y_2, the leading term in the W_3^2 integral is the portion of the $W_1^2\big|_{y_2}$ integral which is below the pole at $q = y_2$, multiplied by the Pochhammer factor,

$$W_3^2 \simeq \mathrm{i}P\,W_1^2\big|_{y_2,q<y_2}$$
$$= \mathrm{i}P\frac{(-1)^{\theta_1}\,\mathrm{e}^{2\pi y_2\theta_1}\Gamma\,(\theta_1)\,\Gamma\,(\theta_2)}{2\pi\Gamma\,(1-\theta_3)}$$
$$= \frac{2\mathrm{i}\pi\mathrm{e}^{\mathrm{i}\pi\theta_2}\mathrm{e}^{2\pi y_2\theta_1}}{\Gamma\,(1-\theta_1)\,\Gamma\,(1-\theta_2)\,\Gamma\,(1-\theta_3)}\,. \tag{C.22}$$

Going from the second line to the third makes use of the reflection identity $\Gamma\,(\theta)\,\Gamma\,(1-\theta) = \pi\,\csc\,(\pi\theta)$.

It proves convenient to define a set of functions as follows,

$$\begin{aligned} A &= -\frac{\mathrm{i}}{2}\left[\cot(\pi\theta_1) + \cot(\pi\theta_3)\right] = -\frac{i}{2}\left(\frac{\sin(\pi\theta_2)}{\sin(\pi\theta_1)\sin(\pi\theta_3)}\right) \\ B &= -2\mathrm{i}e^{i\pi\theta_2}\sin(\pi\theta_2) \\ C &= -\frac{\Gamma(\theta_2)}{\Gamma(1-\theta_1)\Gamma(1-\theta_3)}e^{2\pi y_2\theta_1}, \\ D &= -\frac{\mathrm{i}}{2\pi}\left[2\gamma_E + \psi(1-\theta_1) + \psi(1-\theta_3)\right] \end{aligned} \tag{C.23}$$

in terms of which the W matrix may be expressed as

$$W = \begin{pmatrix} \mathrm{i}\Delta t + D & AC & -\mathrm{i}\Delta t + D + A \\ 1 & 1 & 1 \\ B & BC & B \end{pmatrix}, \tag{C.24}$$

where $\Delta t = t - y_3$, we have dropped terms of order t^{-1} and also used the relation

$$\psi(\theta) = \psi(1-\theta) - \pi\cot(\pi\theta)\ .$$

When we take the determinant, the dependence on $W_1^2 = AC$ drops out, leaving

$$\begin{aligned} |\det W| &= |B(1-C)(A + 2D - 2\mathrm{i}\Delta t)| \\ &\simeq 2|BC|\,\Delta t\,. \end{aligned} \tag{C.25}$$

Explicitly, the leading term is

$$|\det W| \simeq \frac{4\mathrm{e}^{2\pi y_2\theta_1}(t - y_3)}{\Gamma(1-\theta_1)\,\Gamma(1-\theta_2)\,\Gamma(1-\theta_3)}\,. \tag{C.26}$$

The angular factor in front of this expression is identical to that found in (C.10).

C.3 Limit 2: $(t - y_3) \to 0$, generic y_i

As far as the W-integrals are concerned, the difference between this case and the first lies in only the integrals about γ_1. The expressions (C.14) and (C.17) for W_1^1 and W_1^3 are still valid in this limit, and their final form is obtained by using the expansion of the incomplete Euler beta function about $z = 1$,

$$B(z; a, b) = B(a, b) + \mathcal{O}\left(z^a(1-z)^b\right), \tag{C.27}$$

with $B(a,b) = \Gamma(a)\Gamma(b)/\Gamma(a+b)$ the ordinary Euler beta function. We find

$$W_1^1 = -\frac{\mathrm{i}}{2}\left[\cot(\pi\theta_1) + \cot(\pi\theta_3)\right] + \frac{\mathrm{i}}{2}\left[\frac{\pi^{\theta_1-1}}{\theta_1}(t-y_3)^{\theta_1} + \frac{\pi^{\theta_3-1}}{\theta_3}(t-y_3)^{\theta_3}\right] + \mathcal{O}\left((t-y_3)^{1+\theta_i}\right), \quad \text{(C.28)}$$

and,

$$W_1^3 = -\frac{\mathrm{i}}{2}\left[\cot(\pi\theta_1) + \cot(\pi\theta_3)\right] - \frac{\mathrm{i}}{2}\left[\frac{\pi^{-\theta_1}}{1-\theta_1}(t-y_3)^{1-\theta_1} + \frac{\pi^{-\theta_3}}{1-\theta_3}(t-y_3)^{1-\theta_3}\right] + \mathcal{O}\left((t-y_3)^{2-\theta_i}\right). \quad \text{(C.29)}$$

The integral W_1^2 is unchanged from before, as are all integrals around γ_2 and γ_3. Writing

$$\begin{aligned}\Delta t_1' &= \frac{\mathrm{i}}{2}\left[\frac{\pi^{\theta_1-1}}{\theta_1}(t-y_3)^{\theta_1} + \frac{\pi^{\theta_3-1}}{\theta_3}(t-y_3)^{\theta_3}\right] \\ \Delta t_3' &= \frac{\mathrm{i}}{2}\left[\frac{\pi^{-\theta_1}}{1-\theta_1}(t-y_3)^{1-\theta_1} + \frac{\pi^{-\theta_3}}{1-\theta_3}(t-y_3)^{1-\theta_3}\right],\end{aligned} \quad \text{(C.30)}$$

and using the definitions (C.23), the W matrix is

$$W = \begin{pmatrix} A + i\Delta t_1' & AC & A - i\Delta t_3' \\ 1 & 1 & 1 \\ B & BC & B \end{pmatrix}. \quad \text{(C.31)}$$

Note that the t-independent terms in W_1^1 and W_1^3 now have the *same* sign, whereas in the previous section their signs were different. This means that they drop out of the determinant to leave

$$|\det W| \simeq \frac{4\mathrm{e}^{2\pi y_2\theta_1}(\Delta t_1' + \Delta t_3')}{\Gamma(1-\theta_1)\Gamma(1-\theta_2)\Gamma(1-\theta_3)}. \quad \text{(C.32)}$$

C.4 Limit 3: $(t - y_3) \to \infty$, $y_2 \to y_1$

In this limit, an appropriate approach is to expand in y_2 under each integral and keep the leading term. For W_1^1, this gives

$$W_1^1 \simeq \mathrm{i} \int_{(y_3-t)/2}^{(y_3+t)/2} \mathrm{d}q \; (\mathrm{i} \sinh \pi q)^{-\theta_3} \left(\mathrm{i} \sinh \pi \left(q - y_3\right)\right)^{\theta_3 - 1} \mathrm{i} \sinh \pi \left(q + (\theta_3 - 1)\, y_3\right) , \tag{C.33}$$

which has poles at $q = 0$ and $q = y_3$. As before, one may expand about these poles, integrate and use the expansion (C.15), leading to

$$W_1^1 = \mathrm{i}\,(t - y_3) - \frac{\mathrm{i}}{2\pi} \left(2\gamma_E + \psi\left(\theta_3\right) + \psi\left(1 - \theta_3\right)\right) + \mathcal{O}\left(t^{-1}\right) . \tag{C.34}$$

Other integrals about γ_1 are found in a similar fashion, with the result $W_1^1 = W_1^2 = -W_1^3$. Accordingly,

$$W = \begin{pmatrix} W_1^1 & W_1^1 & -W_1^1 \\ 1 & 1 & 1 \\ W_3^1 & W_3^2 & W_3^3 \end{pmatrix} , \tag{C.35}$$

and so

$$|\det W| = 2W_1^1 \left(W_3^1 - W_3^2\right) . \tag{C.36}$$

The integrals about γ_3 may performed by approximating them as, for instance,

$$\begin{aligned} W_3^1 &= \mathrm{i}P\,(-1)^{\theta_1 - 1} \left(2\pi\right)^{-\theta_3} \int_0^{y_2} \mathrm{d}q \; \mathrm{e}^{-\pi\theta_3(y_2 - q)} q^{\theta_1 - 1} \left(y_2 - q\right)^{\theta_2} \\ &= \mathrm{i}P\,(-1)^{\theta_1 - 1} \left(-2\pi\right)^{-\theta_3} y_2^{1-\theta_3} \mathrm{e}^{-\pi\theta_3 y_2} \int_0^1 \mathrm{d}\lambda \; \mathrm{e}^{\pi\theta_3 y_2 \lambda} \lambda^{\theta_1 - 1} \left(1 - \lambda\right)^{\theta_2} , \end{aligned} \tag{C.37}$$

and using the integral

$$\int_0^1 \mathrm{d}\lambda \; \mathrm{e}^{z\lambda} \lambda^{a-1} \left(1 - \lambda\right)^{-a+b-1} = \frac{\Gamma\left(a\right)\Gamma\left(b - a\right)}{\Gamma\left(b\right)} + \mathcal{O}\left(z\right) , \tag{C.38}$$

which may be found via the Kummer hypergeometric function ${}_1F_1$. The final results are

$$
\begin{aligned}
W_3^1 &= \frac{2\pi i e^{i\pi\theta_2}}{\Gamma(1-\theta_1)\Gamma(1-\theta_2)\Gamma(1-\theta_3)} \left(\frac{\theta_2}{1-\theta_3}\right) (2\pi y_2)^{1-\theta_3} \\
W_3^2 &= -\frac{2\pi i e^{i\pi\theta_2}}{\Gamma(1-\theta_1)\Gamma(1-\theta_2)\Gamma(1-\theta_3)} \left(\frac{\theta_1}{1-\theta_3}\right) (2\pi y_2)^{1-\theta_3} \\
W_3^3 &= \frac{2\pi i e^{i\pi(\theta_2-2\theta_1)}}{\Gamma(\theta_1)\Gamma(\theta_2)\Gamma(\theta_3)} \left(\frac{1}{\theta_3}\right) (2\pi y_2)^{\theta_3} ,
\end{aligned}
\tag{C.39}
$$

and the determinant therefore has the leading term

$$
|\det W| \simeq \frac{4\pi (2\pi y_2)^{1-\theta_3}}{\Gamma(1-\theta_1)\Gamma(1-\theta_2)\Gamma(1-\theta_3)} (t - y_3) . \tag{C.40}
$$

Bibliography

[1] S. P. Martin, *A supersymmetry primer*, hep-ph/9709356.

[2] G. Aldazabal, L. E. Ibanez, F. Quevedo, and A. M. Uranga, *D-branes at singularities: A bottom-up approach to the string embedding of the standard model*, *JHEP* **08** (2000) 002, [hep-th/0005067].

[3] A. M. Uranga, *Chiral four-dimensional string compactifications with intersecting D-branes*, *Class. Quant. Grav.* **20** (2003) S373–S394, [hep-th/0301032].

[4] E. Kiritsis, *D-branes in standard model building, gravity and cosmology*, *Fortsch. Phys.* **52** (2004) 200–263, [hep-th/0310001].

[5] D. Lust, *Intersecting brane worlds: A path to the standard model?*, *Class. Quant. Grav.* **21** (2004) S1399–1424, [hep-th/0401156].

[6] R. Blumenhagen, *Recent progress in intersecting D-brane models*, hep-th/0412025.

[7] M. B. Green, J. H. Schwarz, and E. Witten, *Superstring Theory. vol. 2: Loop amplitudes, anomalies and phenomenology.* 1987. CUP.

[8] M. B. Green, J. H. Schwarz, and E. Witten, *Superstring Theory. vol. 1: Introduction.* 1987. CUP.

[9] D. Bailin and A. Love, *Supersymmetric gauge field theory and string theory.* Bristol, UK: IOP (1994) 322 p. (Graduate student series in physics).

[10] J. Polchinski, *String Theory. Vol. 1: An introduction to the bosonic string.* CUP, 1998.

[11] J. Polchinski, *String Theory. Vol. 2: Superstring theory and beyond.* CUP, 1998.

[12] R. J. Szabo, *BUSSTEPP lectures on string theory: An introduction to string theory and D-brane dynamics*, hep-th/0207142.

[13] M. E. Peskin, *Introduction to string and superstring theory, Lectures presented at the 1986 Theoretical Advanced Study Institute in Particle Physics, Santa Cruz, Calif., Jun 23 - Jul 19, 1986.*

[14] J. Polchinski, *Evaluation of the one loop string path integral, Commun. Math. Phys.* **104** (1986) 37.

[15] M. Berkooz, M. R. Douglas, and R. G. Leigh, *Branes intersecting at angles, Nucl. Phys.* **B480** (1996) 265–278, [hep-th/9606139].

[16] L. J. Dixon, D. Friedan, E. J. Martinec, and S. H. Shenker, *The conformal field theory of orbifolds, Nucl. Phys.* **B282** (1987) 13–73.

[17] S. Hamidi and C. Vafa, *Interactions on orbifolds, Nucl. Phys.* **B279** (1987) 465.

[18] M. E. Angulo, D. Bailin, and H.-X. Yang, *Tadpole and anomaly cancellation conditions in d-brane orbifold models, Int. J. Mod. Phys.* **A18** (2003) 3637–3694, [hep-th/0210150].

[19] B. Holdom, *Two $U(1)$'s and ϵ charge shifts, Phys. Lett.* **B166** (1986) 196.

[20] K. R. Dienes, C. F. Kolda, and J. March-Russell, *Kinetic mixing and the supersymmetric gauge hierarchy, Nucl. Phys.* **B492** (1997) 104–118, [hep-ph/9610479].

[21] L. E. Ibanez, C. Munoz, and S. Rigolin, *Aspects of type I string phenomenology, Nucl. Phys.* **B553** (1999) 43–80, [hep-ph/9812397].

[22] S. Davidson, S. Hannestad, and G. Raffelt, *Updated bounds on milli-charged particles, JHEP* **05** (2000) 003, [hep-ph/0001179].

[23] K. Benakli, *Phenomenology of low quantum gravity scale models, Phys. Rev.* **D60** (1999) 104002, [hep-ph/9809582].

[24] C. P. Burgess, L. E. Ibanez, and F. Quevedo, *Strings at the intermediate scale or is the Fermi scale dual to the Planck scale?, Phys. Lett.* **B447** (1999) 257–265, [hep-ph/9810535].

[25] G. K. Leontaris and N. D. Tracas, *String unification at intermediate energies: Phenomenological viability and implications*, *Phys. Lett.* **B454** (1999) 53–58, [hep-ph/9902368].

[26] I. Antoniadis, E. Dudas, and A. Sagnotti, *Brane supersymmetry breaking*, *Phys. Lett.* **B464** (1999) 38–45, [hep-th/9908023].

[27] G. Aldazabal, L. E. Ibanez, and F. Quevedo, *A D-brane alternative to the MSSM*, *JHEP* **02** (2000) 015, [hep-ph/0001083].

[28] S. A. Abel, B. C. Allanach, F. Quevedo, L. Ibanez, and M. Klein, *Soft SUSY breaking, dilaton domination and intermediate scale string models*, *JHEP* **12** (2000) 026, [hep-ph/0005260].

[29] C. Angelantonj, R. Blumenhagen, and M. R. Gaberdiel, *Asymmetric orientifolds, brane supersymmetry breaking and non-BPS branes*, *Nucl. Phys.* **B589** (2000) 545–576, [hep-th/0006033].

[30] R. Rabadan and A. M. Uranga, *Type IIB orientifolds without untwisted tadpoles, and non- BPS D-branes*, *JHEP* **01** (2001) 029, [hep-th/0009135].

[31] D. Bailin, G. V. Kraniotis, and A. Love, *Supersymmetric standard models on D-branes*, *Phys. Lett.* **B502** (2001) 209–215, [hep-th/0011289].

[32] D. Bailin, G. V. Kraniotis, and A. Love, *Searching for string theories of the standard model*, *In proceedings: Cairo 2001, High energy physics.*

[33] D. G. Cerdeno *et. al.*, *Determination of the string scale in D-brane scenarios and dark matter implications*, *Nucl. Phys.* **B603** (2001) 231–258, [hep-ph/0102270].

[34] B. C. Allanach, D. Grellscheid, and F. Quevedo, *Selecting supersymmetric string scenarios from sparticle spectra*, *JHEP* **05** (2002) 048, [hep-ph/0111057].

[35] C. P. Burgess, P. Martineau, F. Quevedo, G. Rajesh, and R. J. Zhang, *Brane antibrane inflation in orbifold and orientifold models*, *JHEP* **03** (2002) 052, [hep-th/0111025].

[36] H.-X. Yang, *Standard-like model from $D = 4$ type IIB orbifolds*, hep-th/0112259.

[37] L. F. Alday and G. Aldazabal, *In quest of 'just' the standard model on D-branes at a singularity*, *JHEP* **05** (2002) 022, [hep-th/0203129].

[38] S. A. Abel and A. W. Owen, *CP violation and CKM predictions from discrete torsion*, *Nucl. Phys.* **B651** (2003) 191–210, [hep-th/0205031].

[39] J. Polchinski, *Dirichlet-Branes and Ramond-Ramond Charges*, *Phys. Rev. Lett.* **75** (1995) 4724–4727, [hep-th/9510017].

[40] T. Banks and L. Susskind, *Brane - Antibrane forces*, hep-th/9511194.

[41] W. Fischler and L. Susskind, *Dilaton tadpoles, string condensates and scale invariance*, *Phys. Lett.* **B171** (1986) 383.

[42] W. Fischler and L. Susskind, *Dilaton tadpoles, string condensates and scale invariance. 2*, *Phys. Lett.* **B173** (1986) 262.

[43] E. Dudas and J. Mourad, *Brane solutions in strings with broken supersymmetry and dilaton tadpoles*, *Phys. Lett.* **B486** (2000) 172–178, [hep-th/0004165].

[44] C. P. Burgess and T. R. Morris, *Open and unoriented strings á la Polyakov*, *Nucl. Phys.* **B291** (1987) 256.

[45] C. P. Burgess and T. R. Morris, *Open superstrings á la Polyakov*, *Nucl. Phys.* **B291** (1987) 285.

[46] E. Kiritsis, *Introduction to Superstring Theory, Lectures presented at the Catholic University of Leuven and University of Padova.*

[47] D. Mumford, *Tata Lectures on Theta I.* Birkhäuser, 1982.

[48] V. S. Kaplunovsky, *One loop threshold effects in string unification*, *Nucl. Phys.* **B307** (1988) 145, [hep-th/9205068].

[49] V. S. Kaplunovsky, *One loop threshold effects in string unification*, hep-th/9205070.

[50] M. Cvetic and I. Papadimitriou, *Conformal field theory couplings for intersecting D-branes on orientifolds*, *Phys. Rev.* **D68** (2003) 046001, [hep-th/0303083].

[51] S. A. Abel and A. W. Owen, *Interactions in intersecting brane models*, *Nucl. Phys.* **B663** (2003) 197–214, [hep-th/0303124].

[52] S. A. Abel, M. Masip, and J. Santiago, *Flavour changing neutral currents in intersecting brane models*, *JHEP* **04** (2003) 057, [hep-ph/0303087].

[53] S. A. Abel and A. W. Owen, *N-point amplitudes in intersecting brane models*, *Nucl. Phys.* **B682** (2004) 183–216, [hep-th/0310257].

[54] D. M. Ghilencea, L. E. Ibanez, N. Irges, and F. Quevedo, *TeV-scale Z' bosons from D-branes*, *JHEP* **08** (2002) 016, [hep-ph/0205083].

[55] D. Cremades, L. E. Ibanez, and F. Marchesano, *Yukawa couplings in intersecting D-brane models*, *JHEP* **07** (2003) 038, [hep-th/0302105].

[56] D. Cremades, L. E. Ibanez, and F. Marchesano, *Computing Yukawa couplings from magnetized extra dimensions*, *JHEP* **05** (2004) 079, [hep-th/0404229].

[57] J. A. Casas, F. Gomez, and C. Munoz, *Complete structure of $Z(N)$ Yukawa couplings*, *Int. J. Mod. Phys.* **A8** (1993) 455–506, [hep-th/9110060].

[58] S. A. Abel and C. Munoz, *Quark and lepton masses and mixing angles from superstring constructions*, *JHEP* **02** (2003) 010, [hep-ph/0212258].

[59] T. Kobayashi and O. Lebedev, *Heterotic Yukawa couplings and continuous Wilson lines*, *Phys. Lett.* **B566** (2003) 164–170, [hep-th/0303009].

[60] P. Ko, T. Kobayashi, and J.-h. Park, *Quark masses and mixing angles in heterotic orbifold models*, *Phys. Lett.* **B598** (2004) 263–272, [hep-ph/0406041].

[61] J. Erdmenger, Z. Guralnik, R. Helling, and I. Kirsch, *A world-volume perspective on the recombination of intersecting branes*, *JHEP* **04** (2004) 064, [hep-th/0309043].

[62] K. R. Dienes, E. Dudas, and T. Gherghetta, *Grand unification at intermediate mass scales through extra dimensions*, *Nucl. Phys.* **B537** (1999) 47–108, [hep-ph/9806292].

[63] K. R. Dienes, E. Dudas, and T. Gherghetta, *Extra spacetime dimensions and unification*, *Phys. Lett.* **B436** (1998) 55–65, [hep-ph/9803466].

[64] S. A. Abel and S. F. King, *On fixed points and fermion mass structure from large extra dimensions*, *Phys. Rev.* **D59** (1999) 095010, [hep-ph/9809467].

[65] D. M. Ghilencea, H. P. Nilles, and S. Stieberger, *Divergences in Kaluza-Klein models and their string regularization*, *New J. Phys.* **4** (2002) 15, [hep-th/0108183].

[66] D. M. Ghilencea, *Higher derivative operators as loop counterterms in one-dimensional field theory orbifolds*, hep-ph/0409214.

[67] T. R. Taylor and G. Veneziano, *Strings and $D = 4$*, *Phys. Lett.* **B212** (1988) 147.

[68] I. Antoniadis, C. Bachas, and E. Dudas, *Gauge couplings in four-dimensional type I string orbifolds*, *Nucl. Phys.* **B560** (1999) 93–134, [hep-th/9906039].

[69] S. A. Abel, O. Lebedev, and J. Santiago, *Flavour in intersecting brane models and bounds on the string scale*, *Nucl. Phys.* **B696** (2004) 141–173, [hep-ph/0312157].

[70] G. Mandal and S. R. Wadia, *Nonrenormalization of Yukawa couplings on orbifolds*, *Phys. Lett.* **B195** (1987) 547.

[71] O. Lechtenfeld and W. Lerche, *On nonrenormalization theorems for four-dimensional superstrings*, *Phys. Lett.* **B227** (1989) 373.

[72] J. A. Minahan, *One loop amplitudes on orbifolds and the renormalization of coupling constants*, *Nucl. Phys.* **B298** (1988) 36.

[73] M. Cvetic, *Blown - up orbifolds*, http://www.slac.stanford.edu/cgi-wrap/getdoc/slac-pub-4325.pdf.

[74] M. Cvetic, *Phenomenological implications of the blownup orbifolds*, http://www.slac.stanford.edu/cgi-wrap/getdoc/slac-pub-4324.pdf.

[75] M. Cvetic, *Suppression of nonrenormalizable terms in the effective superpotential for (blownup) orbifold compactification*, *Phys. Rev. Lett.* **59** (1987) 1795.

[76] A. Font, L. E. Ibanez, H. P. Nilles, and F. Quevedo, *Yukawa couplings in degenerate orbifolds: Towards a realistic $SU(3) \times SU(2) \times U(1)$ superstring*, *Phys. Lett.* **210B** (1988) 101.

[77] A. Font, L. E. Ibanez, H. P. Nilles, and F. Quevedo, *On the concept of naturalness in string theories*, *Phys. Lett.* **B213** (1988) 274.

[78] A. Font, L. E. Ibanez, H. P. Nilles, and F. Quevedo, *Degenerate orbifolds*, *Nucl. Phys.* **B307** (1988) 109.

[79] T. Kobayashi, *Selection rules for nonrenormalizable couplings in superstring theories*, *Phys. Lett.* **B354** (1995) 264–270, [hep-ph/9504371].

[80] J. J. Atick and A. Sen, *Spin field correlators on an arbitrary genus Riemann surface and nonrenormalization theorems in string theories*, *Phys. Lett.* **B186** (1987) 339.

[81] J. J. Atick and A. Sen, *Covariant one loop fermion emission amplitudes in closed string theories*, *Nucl. Phys.* **B293** (1987) 317.

[82] J. J. Atick and A. Sen, *Correlation functions of spin operators on a torus*, *Nucl. Phys.* **B286** (1987) 189.

[83] J. J. Atick, L. J. Dixon, and A. Sen, *String calculation of Fayet-Iliopoulos D terms in arbitrary supersymmetric compactifications*, *Nucl. Phys.* **B292** (1987) 109–149.

[84] J. J. Atick, L. J. Dixon, P. A. Griffin, and D. Nemeschansky, *Multiloop twist field correlation functions for $Z(N)$ orbifolds*, *Nucl. Phys.* **B298** (1988) 1–35.

[85] D. Bailin, A. Love, and W. A. Sabra, *Yukawa couplings involving excited twisted sector states for $Z(N)$ and $Z(M) \times Z(N)$ orbifolds*, *Nucl. Phys.* **B416** (1994) 539–562, [hep-th/9307172].

[86] D. Bailin, A. Love, and W. A. Sabra, *Yukawa couplings involving excited twisted sector states for $Z(M) \times Z(N)$ orbifolds*, *Phys. Lett.* **B311** (1993) 110–116, [hep-th/9304066].

[87] G. Aldazabal, S. Franco, L. E. Ibanez, R. Rabadan, and A. M. Uranga, *$D = 4$ chiral string compactifications from intersecting branes*, *J. Math. Phys.* **42** (2001) 3103–3126, [hep-th/0011073].

[88] I. R. Klebanov and E. Witten, *Proton decay in intersecting D-brane models*, *Nucl. Phys.* **B664** (2003) 3–20, [hep-th/0304079].

[89] D. Friedan, E. J. Martinec, and S. H. Shenker, *Conformal invariance, supersymmetry and string theory*, *Nucl. Phys.* **B271** (1986) 93.

[90] D. Polyakov, *Picture changing operators and space-time supersymmetry*, *Nucl. Phys.* **B449** (1995) 159–182, [hep-th/9502124].

[91] T. T. Burwick, R. K. Kaiser, and H. F. Muller, *General Yukawa couplings of strings on $Z(N)$ orbifolds*, *Nucl. Phys.* **B355** (1991) 689–711.

[92] S. Stieberger, D. Jungnickel, J. Lauer, and M. Spalinski, *Yukawa couplings for bosonic $Z(N)$ orbifolds: Their moduli and twisted sector dependence*, *Mod. Phys. Lett.* **A7** (1992) 3059–3070, [hep-th/9204037].

[93] J. Erler, D. Jungnickel, M. Spalinski, and S. Stieberger, *Higher twisted sector couplings of $Z(N)$ orbifolds*, *Nucl. Phys.* **B397** (1993) 379–416, [hep-th/9207049].

[94] S. Stieberger, *Moduli and twisted sector dependence on $Z(N) \times Z(M)$ orbifold couplings*, *Phys. Lett.* **B300** (1993) 347–353, [hep-th/9211027].

[95] D. Lust, P. Mayr, R. Richter, and S. Stieberger, *Scattering of gauge, matter, and moduli fields from intersecting branes*, *Nucl. Phys.* **B696** (2004) 205–250, [hep-th/0404134].

[96] M. Headrick, *Solutions to selected problems from Polchinski's String Theory*, http://www2.lns.mit.edu/ headrick/physics/polchinski/chapter7.ps.